Understanding the effects of growth and size-at-age variation on the dynamics of fish populations

Christine Stawitz

A dissertation

submitted in partial fulfillment of the

requirements for the degree of

Doctor of Philosophy

University of Washington

2017

Reading Committee:

Timothy Essington, Chair

Trevor Branch

Melissa Haltuch

Program Authorized to Offer Degree:

Quantitative Ecology and Resource Management

University of Washington

Abstract

Understanding the effects of growth and size-at-age variation on the dynamics of fish populations

Christine Stawitz

Chair of the Supervisory Committee:
Professor Timothy E. Essington
School of Aquatic and Fishery Sciences

Understanding drivers of populations is of tantamount importance across a broad scale of researchers, from theoretical ecologists to tactical resource managers. Drivers may be internal feedbacks (density-dependent) or external (density-independent) processes, such as changes in prey, predator, or competitor populations, or environmental stochasticity. In a closed population, these drivers affect populations by altering demographic rates (i.e. mortality, reproduction, somatic growth). Although there is increasing evidence that no demographic rates are static, at least in patchy and stochastic aquatic environments, it is an ongoing question to identify the most important types and scale of variation for population dynamics models. In this dissertation, I seek to quantify the magnitude and effect of growth and size-at-age variation on fish population dynamics using a variety of different modeling techniques. In the first chapter, I use a state-space

statistical model to quantify the magnitude and type of temporal size-at-age variation experienced by a number of Pacific groundfish populations. In the second chapter, I use these estimates of growth variation, along with parameters taken from fisheries stock assessment models, to illustrate how both growth and recruitment variation may introduce fluctuations into simulated populations with otherwise static demographic rates. In the third chapter, I use an integrated analysis model to simulate and estimate patterns of growth variation in Petrale sole (*Eopsetta jordani*) to examine the effect of growth misspecification on estimates of population status. In the final chapter, I adapt a size-structured ecosystem model to Tonlé Sap Lake, Cambodia, and explore ways to validate model accuracy in a species-rich, data-poor ecosystem. This work highlights the importance of accounting for multiple types of demographic stochasticity across life history type and how appropriate model complexity scales with data quality and quantity.

TABLE OF CONTENTS

List of Figures v

List of Tables viii

Introduction 1

Chapter 1. A state-space approach for detecting growth variation and application to North Pacific groundfish 4

1.1 Introduction 5

1.2 Methods 9

1.2.1 Growth model framework 9

1.2.2 Simulation study 12

1.2.3 Bayesian methods 13

1.2.4 Model application 14

1.3 Results 17

1.3.1 Simulation study 17

1.3.2 Estimated growth mode and pattern 18

1.3.3 Effect of survey data 19

1.3.4 Growth anomaly magnitude 20

1.4 Discussion 20

Chapter 2. Somatic growth contributes to population variation in marine fishes 38

2.1 Introduction 39

2.2 Methods 41

2.2.1 Species selection and life history traits 42
2.2.2 Population model 43
2.2.3 Early life history 43
2.2.4 Growth 45
2.2.5 Scaling of growth deviations 46
2.2.6 Simulation 47
2.3 Results 48
2.3.1 Empirical and simulated demographic variability 48
2.3.2 Importance of growth or recruitment variability 49
2.3.3 Interaction effect with age truncation 50
2.3.4 Comparison to alternative population models 51
2.3.5 Relation to life history characteristics 51
2.4 Discussion 52

Chapter 3. How does growth misspecification affect management advice derived from integrated fisheries stock assessment models? 65

3.1 Introduction 66
3.2 Methods 69
3.2.1 Model adaptation 70
3.2.2 Specification of operation model growth parameters 71
3.2.3 Simulation framework 73
3.2.4 Response metrics and convergence criteria 74
3.3 Results 75
3.3.1 Bias in management quantities in data-rich case 76

3.3.2 Increase in uncertainty in data-rich case 78
3.3.3 Effect of data limitation 78
3.3.4 Convergence 79
3.4 Discussion 79
Chapter 4. Testing the applicability of size-spectrum food models to a species-rich tropical lake 91
Abstract 91
4.1 Introduction 93
4.2 Methods 96
4.2.1 Ecosystem model 96
4.2.2 Dynamics 97
4.2.3 Consumption 98
4.2.4 Energy allocation and mortality 99
4.2.5 Relative biomass comparison 100
4.2.6 Trophic level comparison 101
4.2.7 Weight composition 102
4.2.8 Sensitivity analyses 103
4.3 Results 104
4.3.1 Relative biomass comparison 105
4.3.2 Trophic level 106
4.3.3 Weight composition 106
4.4 Discussion 107

Synthesis 120

Works Cited 125

Appendix A 134

Appendix B 142

LIST OF FIGURES

Figure 1.1 - Average percentage of DIC weight attributed to the four alternative estimation models for four underlying "true" growth models: A) constant operating model, B) annual operating model, C) cohort operating model and D) initial size operating model. Results represent aggregated DIC weight over 50 iterations..... 33

Figure 1.2 - Deviance information criterion (DIC) weights across tested models for A) all stocks across ecosystems, B) all stocks in the California Current ecosystem, C) all stocks in the Bering Sea/Aleutian Islands ecosystem, and D) all stocks in the Gulf of Alaska ecosystem. 34

Figure 1.3 - Growth anomaly estimates for 6 stocks. The x-axis represents anomaly year for panel A and birth year for panels B and C. A) The annual growth anomaly model was chosen for Gulf of Alaska Pacific halibut and California Current petrale sole. These are examples of stocks which experienced highly variable growth anomalies. B) The initial size effect model was chosen for Bering Sea/Aleutian Islands Walleye pollock and California Current Pacific hake. C) The cohort growth anomaly model was chosen for California Current chilipepper rockfish and Gulf of Alaska Pacific cod. 35

Figure 1.4 - Median predicted sizes (line) and prediction intervals (shaded area) for a A) Pacific halibut born in 1995 (light gray, solid line) and 2004 (dark gray, dashed line), B) petrale sole born in 1971 (light gray, solid line) and 1982 (dark gray, dashed line), C) walleye pollock born in 1973 (light gray, solid line) and 1964 (dark gray, dashed line), D) Pacific hake born in 1959 (light gray, solid line) and 1990 (dark gray, dashed line), E) chilipepper rockfish born in 1965 (light gray, solid line) and 1982 (dark gray, dashed line), and F) Pacific cod born in 1986 (light gray, solid line) and 1996 (dark gray, dashed line). Annual, initial size, and cohort growth anomalies were used to generate trajectories A & B, C & D, and E & F, respectively. 36

Figure 2.1 - Schematic for population model. Superscript numbers in parentheses refer to the equation used to model the associated process. Items denoted in green represent processes

which become variable as a result of introduced growth variation. Items in blue represent processes which become variable as a result of introduced recruitment variation. .. 58
Figure 2.2 - Empirical estimates of recruitment (a,c,e) and growth (b.d.f) scenarios for petrale sole, Pacific hake, and widow rockfish. 59
Figure 2.3 - Comparison of simulated recruitment deviations (gray) to empirical recruitment estimates (blue). 60
Figure 2.4 - CV of simulated length-at-age for each species modeled. Color represents species, where each line is one simulation. 61
Figure 2.5 - 95% quantiles (lines) and medians (points) of mature biomass CV across three levels of age truncation. “Growth” denotes scenarios with growth variation only, “Rec” denotes scenarios with recruitment variation only, and “Both” denotes scenarios with both types of variation. 62
Figure 2.6 – 95% quantiles (lines) and medians (points) of the coefficient of variation of annual production from output scenarios. “Growth” denotes scenarios with growth variation only, “Rec” denotes scenarios with recruitment variation only, and “Both” denotes scenarios with both types of variation. 63
Figure 2.7 - Colors and bubble size indicate relative dominance of growth (purple) or recruitment (red) variation (as measured by the difference of the median output CVs of annual production), against (a) the catabolic coefficient (A) compared with mortality rate (M) and (b) the standard deviation of recruitment deviations compared with autocorrelation of growth deviations. 64
Figure 3.1 - Comparison of trajectory in spawning stock biomass as model simplification occurred (from top to bottom). Dark blue represents the assessment model used for the 2015 update assessment; red model represents the final simulation model. Shaded areas represent 95% confidence interval..... 86
Figure 3.2 - Illustration of data used in base estimation model by year and type. 87
Figure 3.3 - Input growth parameter variation across four EM and OM configurations. Gray dashed line represents starting parameter value, and black line represents simulated patterns under alternative growth scenarios for male and female fish. 88

Figure 3.4 - Median (point) and 95% quantiles (lines) of relative error in estimates of depletion in the final model year (left), spawning stock biomass at maximum sustainable yield (middle), and unfished biomass (right). Operating model configurations (OM) and estimation model configurations (EM) for each scenario are on the left. 89

Figure 3.5 - Time series of relative error in estimated spawning stock biomass over time. Gray shaded area represents the 95% quantile, while black line represents the median. The straight black line represents no error over the time series. Each scenario is presented on the same scale, with the maximum pictured error of +0.5 and -0.5. Operating model configurations (OM) and estimation model configurations (EM) for each scenario are on the left. 90

Figure 4.1 - Size spectra across scenarios. Gray dashed lines represent the two resource spectra. Gray is *Rasbora*, pink is *Henicorhynchus*, green is *Channa*, blue is *Boesemania*, and orange is *Pangasius*. Black is the community (total) size spectrum. Size spectrum and resource spectra from base case plotted on species-specific plots to facilitate comparison.. 117

Figure 4.2 - Comparison of calculated trophic level (rounded to nearest integer value) from empirical measurements of $\delta 15N$ (yellow, orange, red points) and model-predicted trophic level (gray region) across sensitivity ranges. 118

Figure 4.3 - Comparison of empirical weight distribution (black line) and median weight (black dashed line) with model output weight composition (gray) and mean weight (blue shaded area) ranges across sensitivity ranges. 119

Figure A.1 - Growth anomaly estimates for stocks with significant annual growth anomalies that are not shown in Figure 1.3..... 139

Figure A.2 - Growth anomaly estimates for stocks with significant initial size anomalies that are not shown in Figure 1.3. The x-axis represents year of birth of the cohort. 140

LIST OF TABLES

Table 1.1 - Stocks used for model application, listed by scientific name, common name, and source (Northwest Fisheries Science Center [NWFSC]; Alaska Fisheries Science Center [AFSC]; International Pacific Halibut Commission [IPHC]) and type of data (scientific survey [S]; commercial catch port-sampled [C]) used..... 27

Table 1.2 - Process and observation model components of the state-space model. 28

Table 1.3 - Parameter values used to generate data in simulation study. 29

Table 1.4 - Variable notation, description, and Bayesian prior distribution (when applicable) for all data and parameters used. 30

Table 1.5 - Model selection results, aggregated by ecosystem and stock, with stocks grouped into families or similar morphologies; “mixed evidence” indicates that DIC weight was nearly evenly split between two or more alternative models, thus we could not distinguish which was more highly supported by model selection. 31

Table 1.6 - Comparison between model runs using both survey and commercial data and runs using commercial data only for BSAI stocks for which the annual model was not selected; all other model components (i.e. using gear and/or season as separate observations) are the same. 32

Table 2.1 - Species life-history parameters: female natural mortality (M), length-weight coefficient (α), length-weight exponent (β), stock-recruit model (SR) (BH denotes Beverton-Holt, R denotes Ricker, and C denotes constant mean recruitment), parameters of the S-R relationship: for Beverton-Holt: steepness (h), log of unfished recruitment ($\ln(R_0)$), a and b if Ricker or standard Beverton-Holt is used, recruitment deviation autocorrelation (ρ_r) and variance (σ_r^2) estimate for each species. 56

Table 2.2 – Equations used in modeling 57

Table 3.1 - Scenarios tested span 15 permutations of operating and estimation model growth specifications, and each scenario is run for both the data-rich and data-poor case. . 84

Table 3.2 – Time blocks evaluated for periods of growth variation. Negative log likelihoods are derived from the simplified assessment model fit to available data. Asterisk(*) denotes selected block time periods. 85

Table 4.1 - Equations governing the size-spectrum model, where i denotes species groups, R_x denotes resource spectra, m denotes predator weight, m_p denotes prey weight, and j denotes prey fish. 112

Table 4.2 - Parameter values used in the model. General model parameters taken from Jacobsen et al. (2013), except where specified. When five values are provided, parameters are species-specific. In matrices, columns denote prey/resources and rows denote predator species groups. 114

Table 4.3 - Parameter values for evaluated sensitivity cases. Values in bold denote those used in the base model configuration. 115

Table 4.4 - Relative biomass from each of the data sources (Sopha & van Zalinge 2001; Hortle, K.G., Lieng, S., Valbo-Jorgensen 2004; MRC 2010) and model estimates under different sources of uncertainty (κ ratio [c], diet composition of predators, and fishing [F].)116

Table A.1 - Ages and years included in our analysis for stocks in the Gulf of Alaska ecosystem. 134

Table A.2 - Ages and years included in our analysis for stocks in the Bering Sea & Aleutian Islands ecosystem. 135

Table A.3 - Ages and years included in our analysis for stocks in the California Current ecosystem. 136

Table A.4 - Results of comparisons of estimated annual growth anomalies to estimated fishing mortality (F) from stock assessments; only stocks with estimated F values in the RAM legacy database were compared. 137

Table B.1 - Maturity (M) and selectivity (S) parameters used. Blank values at ages < Amax denote values of 1; selectivity values are not included for species with length-based selectivity. 142

ACKNOWLEDGEMENTS

Many people and organizations contributed to this dissertation. First, my advisor, Tim Essington, deserves many thanks for being an invaluable mentor as I entered the world of scientific research. Tim is an excellent teacher, a fantastic diplomat, and an awe-inspiring scientist, and I'm extremely grateful to have had him to model both scientific and character excellence. Graduate school is a long and taxing endeavor, but Tim's dedication to his mentees and trust in their opinions, and support of their career goals and work-life balance, made it also a very pleasant six years.

I am also extremely grateful to the rest of my committee! Melissa Haltuch mentored me in the world of stock assessment science, patiently helped me debug code and improve my writing, and became a friend. Anne Hollowed is the most fantastic advocate for her mentees, in addition to always examining the bigger picture and connections of research topics. Trevor Branch's encyclopedic knowledge of fisheries research improved my chapters immensely, and following his reading suggestions has made me a much more thoughtful and well-rounded fisheries scientist. His commitment to creating the most beautiful figures has also inspired me. I had two GSRs throughout this process – thank you Parker MacCready for keeping me honest about correlation vs. causation, and Nives Dolsak for her thoughtful questions, even though she was a late-comer.

Thank you to my funding sources: the Quantitative Ecology and Resource Management program, NOAA's Fisheries and the Environment program, the IGERT Program on Ocean Change funded by the National Science Foundation, and the National Marine Fisheries Service and Washington Sea Grant's Population Dynamics Fellowship. I'm fortunate in that all of these funding sources came with groups of amazing researchers, who have become lifelong friends.

Beyond my committee: Paul Spencer co-authored Chapter 1, and his considerable wisdom on fish life history has influenced other chapters. Ken Haste Andersen and Nis Sand Jacobsen took me under their wing to teach me size-structured modeling. Gordon Holtgrieve and Thomas Pool shared their data and expert knowledge, without which Chapter 4 would have been impossible. I'm also indebted to Steve Martell for sharing Pacific Halibut length data, Kelli Johnson, Cole Monnahan, and Ian Taylor for providing endless assistance with SS3 software, Allan Hicks and Ian Stewart for modeling feedback, Nate Mantua for helping develop the question I addressed in Chapter 1, Megan Stachura for recruitment data used in Chapter 2, and Miriam Doyle, Owen Hamel, Jim Ianelli, Tom Helser, Aaron Berger, and Kelli Johnson for text edits.

I'd like to thank the QERM administrators, Joanne Besch and Erica Owens, for all of their support. QERMies got me through the hardest professional year of my life and have continued to be the best sounding boards and some of my dearest friends. My labmates are my other greatest mentors and supporters. You are all true inspirations not only as scientists, but as karaoke stars, mountain climbers, fashion icons, bird rescuers, gluten-free bakers, ecosystem modelers, dancers, and wonderful people. I feel privileged to have basked in your greatness M-F for the last five years.

Finally, as a parent I now understand the tightrope my parents walked raising me, between providing unconditional love while pushing me to be my best. I'm so grateful for your support. Thank you to my dog Oakley for being the most steadfast companion. Thank you to my son, for bringing so much joy into my life. To my husband Daniel, thank you for supporting me when I didn't believe in myself. Thank you for standing by my choices, even when their consequences were more responsibility shifted on to you. You're my biggest inspiration.

INTRODUCTION

Understanding why populations fluctuate is a central goal of population ecology. Animal populations have been shown to experience dramatic fluctuations, caused by variation in key demographic rates governing processes of reproduction, somatic growth, and mortality (Sæther and Bakke 2000). Variation may be caused by density-dependent processes, like competition for food inducing variation in somatic growth (Hairston et al. 1960, Bjorndal et al. 2000) or mortality rates (Hixon and Jones 2005), or competition for space limiting reproductive success (Ricker 1954, Travis et al. 1999). Populations may also experience temporal variation in natural mortality due to changing predator biomass (Baum and Worm 2009) or temporal variation in growth due to changing prey biomass (Hansen et al. 1993). Finally, stochastic environmental variation can make conditions more or less favorable for a population, inducing temporal variation into their reproductive success (Warner and Chesson 1985), mortality (Sæther 1997), or somatic growth rate (Hurst et al. 2010).

However, incorporating all sources of variation in population models used to answer tactical or strategic management questions is typically infeasible or undesirable. Such a complex model is likely overfit to the available ecological data and therefore has limited predictive power (Caswell 1988). Therefore, deciding how (i.e. deterministically or stochastically) and when different types of variability should be included are core considerations when ensuring population models and the question they are meant to answer align in scope (Clark 2004). If models are too complex or too simplistic, management decisions based on their predictions may be misguided (Maunder and Punt 2013), leading to negative impacts on ecosystems and human populations.

The question of how to accurately specify demographic variability is perhaps nowhere more pertinent than in models applied to fish populations, because they are highly temporally variable and immensely commercially important. Dramatic fluctuations in catches have been observed since the earliest recordings (Hjort 1914). Because this unpredictability has substantial consequences for fishermen depending on fish resources, fisheries science has sought to understand and predict these fluctuations for over a century. However, only recently have advances in modeling tools, computing power, and data sharing made it feasible to include multiple sources of demographic variation in fish population models (Hilborn and Mangel 1997).

The introduction of the "critical period hypothesis" (Hjort 1914) led to recruitment variability being considered the most influential source of demographic variability resulting in fluctuations in fish population productivity. Substantial efforts followed to develop a mechanistic understanding for recruitment variability, for example the "match-mismatch hypothesis" (Cushing 1982), the "stable ocean hypothesis" (Lasker 1981), and the "stable retention" hypothesis (Sinclair 1987, Iles and Sinclair 1989). Recently, however, fishery scientists are increasingly identifying that natural mortality and somatic growth variation also contribute to fluctuations in biomass of fish populations (Lorenzen and Enberg 2002, Baum and Worm 2009, Gaichas et al. 2010). The shift towards ecosystem-based management strategies (Hollowed et al. 2000, Pikitch et al. 2004), which explicitly consider varying natural mortality and somatic growth rates, and temporal variation in size structure, is further evidence that scientists increasingly see value in considering multiple sources of demographic variability in fisheries population models applied to management.

Despite this recognition, somatic growth and size-structure variation are incorporated infrequently into fisheries models, partly because the magnitude of this variation and its potential

to influence population dynamics relative to recruitment variation are less well-studied. Density-dependent effects in growth have been shown to regulate some fish species more than recruitment (Lorenzen and Enberg 2002, Lorenzen 2008). Reference points can be biased when density-dependent growth is not accounted for, potentially leading managers to more optimistic outlooks for fish stocks (Helser and Brodziak 1998, Gårdmark et al. 2006). Density-independent growth variation not included in management models can also bias management advice (Kuriyama et al. 2016) and increase extinction risk when productivity is low (Rideout et al. 2014). A particular challenge in understanding the magnitude of growth variation in fish is imperfect measurement, as growth and size structure are estimated imperfectly from length-at-age data subject to sampling bias (Ricker 1969, Lin Lai and Gunderson 1987).

In this dissertation, I present four research chapters that seek to advance our understanding of how growth and size dynamics influence fish population models and management. In the first chapter, I present a method to estimate the magnitude and type of growth variation in fish populations from multiple data sources, which I then apply to several groundfish populations. The second and third chapter use simulation techniques to identify the potential effects of growth variation on populations using respectively a simple age-structured population model and a realistic integrated assessment model. In the final chapter, I examine if an ecosystem model parameterized based on assumptions of how life history processes scale allometrically with size can capture the dynamics of a data-poor tropical lake system.

Chapter 1. A state-space approach for detecting growth variation and application to North Pacific groundfish

ABSTRACT

Understanding demographic variation in recruitment and somatic growth is key to improving our understanding of population dynamics and forecasting ability. Although recruitment variability has been extensively studied, somatic growth variation has received less attention, in part because of difficulties in modeling growth from individual size-at-age estimates. Here we develop a Bayesian state-space approach to test for the prevalence of alternative forms of growth rate variability (e.g. annual, cohort-level, or in the first year recruited to the fishery) in size-at-age data. We apply this technique to twenty-nine Pacific groundfish species across the California Current, Gulf of Alaska, and Bering Sea/Aleutian Islands marine ecosystems. About 40% of modeled stocks were estimated to exhibit temporal growth variation. In the majority of stocks, growth trends fluctuated annually across ages in a single year, suggesting that either there are shared environmental features that dictate growth across multiple ages, or the presence of some systematic (within year) observation errors. This method represents a novel way to use size-at-age data from fishery or other sources to test hypotheses about growth dynamics variability.

1.1 INTRODUCTION

Marine fish productivity varies due to fluctuations in demographic processes such as recruitment, mortality and somatic growth. Therefore, quantifying causes of variability in these processes and corresponding effects on production can help us understand and predict changes in marine populations. Much research has sought to quantify and predict effects of recruitment variation (Hjort 1914, Cushing 1982) and natural mortality (Hixon and Jones 2005, Baum and Worm 2009) on productivity. However, dominant patterns in and magnitudes of somatic growth variation over long time scales are not quantified for many commercially important fish stocks, despite substantial evidence that growth is variable (Quinn and Deriso 1999, Black et al. 2008) and also regulates productivity (Lorenzen and Enberg 2002) . Quantifying the magnitude and characteristics of this variation is a necessary first step towards measuring and predicting growth responses to density-dependent and -independent factors. Methods to describe growth rate changes across marine fish populations, which can help establish relationships between growth rates, environmental conditions, and stock productivity, are limited.

One method of modeling growth is to fit population size-at-age data to a model that describes individual or cohort growth rates. For example, the von Bertalanffy growth function (VBGF), relates individual size-at-age based on the difference between anabolic and catabolic processes of an animal's metabolism (Bertalanffy 1957). Thus, unobserved changes in consumption and catabolism of fish may be modeled via variation in the asymptotic maximum length (L_∞) or rate parameter (k), respectively, along the axis (i.e. temporal, spatial, year-class, etc.) on which growth is assumed to be changing. However, individual growth models are poorly suited to describe population-level patterns (Chapman 1961, Kirkwood 1983), because individual-level

variation can bias estimates of size-at-age statistics (Sainsbury 1980). The standard VBGF parameters of L_∞ and k are difficult to interpret and highly correlated, making it difficult to simultaneously estimate changes in both (Schnute and Fournier 1980). Although alternative parameterizations of the VBGF have been proposed (Schnute 1981), the majority of studies which estimate growth variation do so using the standard VBGF with variation in one parameter (Cloern and Nichols 1978, Millar et al. 1999, Baudron et al. 2014) . Consequently, models include either only catabolic variation (if k varies), or both anabolic and catabolic variation (if L_∞ varies), which is more biologically plausible, but can cause difficulties in fitting the growth curve as target maximum size is non-constant.

Once a growth framework is chosen, the next challenge is identifying whether growth rate fluctuations are more highly correlated within cohorts (cohort-scale), across ages in a population within a year (annual-scale), or among juveniles within cohorts. These alternative growth variation patterns may be driven by environmental and/or competitive processes. For example, annual growth patterns are related to upwelling indices and sea surface temperature, across mature (Kreuz et al. 1982, Black et al. 2008) and juvenile (Hagen and Quinn 1991) life stages of rockfish and flatfish. Density-dependent growth anomalies, in which increases in stock biomass lead to reduced size-at-age, may differ among cohorts or length classes (Rijnsdorp and van Leeuwen 1992, Walters and Wilderbuer 2000), or be shared across cohorts that are close in age (Whitten et al. 2013). Intra-cohort competition in juvenile life stages can result in reduced or enhanced size of fish entering adulthood (Jones 1987), which might lead to reduced or enhanced individual adult size within a cohort throughout its life. However, few studies have quantitatively distinguished whether annual-scale, cohort-scale, or stage-structured growth anomalies are more pronounced in fisheries size-at-age data.

Biases and imprecision in age estimates are common and increase with fish age, complicating estimates of growth variation. These include negative bias due to surface otolith ageing (Beamish 1979a, Campana 2001) and reader bias when more accurate break-and-burn ages are used (Kimura and Lyons 1991). Treating age as a random effect may account for the effects of ageing error (Cope and Punt 2007), but requires the ability to validate fish age and ageing error bias (Campana 2001, Hamel et al. 2008, Haltuch et al. 2013a), which is not always possible. An alternative framework is to consider age as the dependent variable (Kirkwood 1983, Taylor et al. 2005), but this approach makes it difficult to compare across stocks with different longevities and life history characteristics.

A final issue is differentiating trends in size-at-age data caused by annual changes in size-selective sampling (i.e. location, date, fishing pressure, or gear selectivity) from trends caused by annual growth variation. For example, some stocks exhibit spatial variation in size-at-age (Campana et al. 1995, Olsen et al. 2005, Gertseva et al. 2010); therefore, samples collected in non-standardized locations through time may exhibit spurious temporal patterns. Spurious annual trends may also be caused by annual fishing season changes, which lead to unbalanced sampling across months of the growing season. Temporal changes in selectivity due to changes in fishing gear is common (Myers and Hoenig 1997) and can confound detection of simultaneous temporal changes in growth rate (Thorson and Simpfendorfer 2009, Thorson and Prager 2011). Size-selectivity of gear used in surveys and commercial fishing can introduce sampling bias (Goodyear 1995) by disproportionally selecting larger individuals and faster-growing young fish that are larger than slower-growing older fish (Schnute and Fournier 1980, Hagen and Quinn 1991). Therefore, when changes in growth rate trends are estimated from sample mean size-at-

age, it is crucial to consider the potential biasing effect of gear selectivity and heterogeneous sampling.

Here we develop a novel analytic framework to estimate growth variability in marine populations using an autoregressive state-space framework that permits comparison of different modes of variation (e.g. annual, cohort) and can explicitly account for ageing error and changes in sampling. State-space models are increasingly used to model population dynamics (Millar and Meyer 2000, de Valpine and Hastings 2002, Buckland et al. 2004), because they consist of a series of unobserved values (true size-at-age), and a set of observations (estimated size-at-age), which are dependent upon the unobserved values. Observations can be biased, but may be used to infer relevant properties of the unobserved system state (Durbin and Koopman 2012). The unobserved values are modeled as a time series with inherent autocorrelation, frequently referred to as the process equation, while a parallel observation equation relates the observed states to the unobserved values.

In this study, we present a state-space approach that employs a simple autoregressive process model to estimate and compare variation modes in size-at-age data, from which inferences about growth rate variation can be made. The objective of this study is to develop a modeling framework that can extract growth trends from size-at-age data across species and ecosystems and apply it across large marine ecosystems to better understand growth variability patterns. Our approach has three main benefits over traditional growth model approaches that incorporate only constant process error: (1) our framework does not assume that population size-at-age follows any particular mechanistic growth model, while capturing the inherent autocorrelation in size-at-age that these models predict, (2) three different modes of growth variation (annual, cohort, and initial size) are

modeled and compared using model selection, and (3) the effects of ageing and sampling error are considered explicitly while population growth anomalies are estimated. We first validate our model's ability to estimate growth variation from a simulated population and then demonstrate our method's applicability using survey and commercial catch time series of size-at-age data for twenty-nine North Pacific groundfish species (Table 1.1).

1.2 METHODS

We developed a state-space model for growth variation, tested the model on simulated data, and then applied the model to a large number of commercially harvested groundfish stocks in the Northeast Pacific. The state-space model framework captured three modes of growth variation and these were contrasted with a no trend (null) model. Next, we tested our model's ability to correctly estimate the true pattern of growth variation from data generated using a VBGF with annual, cohort, or initial size variation on parameters. We then used Bayesian methods to fit our state-space model to time series of mean length-at-age from 29 fish species for which California Current, Gulf of Alaska, and Bering Sea/Aleutian Islands survey and commercial catch monitoring data was available. We evaluated whether changes in sampling and fishing rate were responsible for our estimated growth trends through sensitivity testing and post hoc comparisons.

1.2.1 *Growth model framework*

1.2.1.1 Process model

State-space models simultaneously estimate parameters in two equations – a process and an observation equation – where the ecological state can be described by an autoregressive process equation, and the observed data points are a function of the ecological state and observation error. Throughout the course of this paper, to differentiate between process and observation equation

variables, we refer to changes in the process component of the equation as growth anomalies, while variation in observation data is referred to as observation error. If the state-space framework is ineffective at correctly distinguishing the true growth rate change from observation error, some fraction of observation error may be attributed to growth anomalies. However, we accept this limitation and assume these growth anomalies are a reasonable proxy for true growth rate change. Growth anomalies are modeled as an autoregressive process, which allows for compounding of these anomalies throughout time. This attribute is important, as growth models predict future body size as a function of present body size. Conversely, the observation model includes factors that affect measurement of true states at given points in time, but do not affect observations in subsequent years. As a result, we modeled hypothesized growth variation modes (i.e. inter-annual, inter-cohort) within the process component of the model and factors affecting sampled size-at-age (i.e. age method, latitude) within the observation component.

All four alternative process models were developed using the same structure: an auto-regressive model with lag 1 on normalized length data (constant model: Table 1.2, Equation 2). Throughout this paper, "normalized length" refers to the standardized residual of mean length-at-age in a given year from mean length-at-age across pooled samples from a standardized 15-year reference period (1995-2010). A reference period is used to increase comparability across stocks by ensuring sample mean size-at-age is calculated from a period of standard ocean and fishing conditions. Normalized length is calculated as in Table 1.2, Equation 1. Throughout this paper, the "first modeled age" refers to the first age which is selected at 40% or greater by the fishery, which is unique and consistent for each stock. Process error, a parameter that estimates the amount of natural variability in population growth rate, was included in all models and assumed to be normally distributed with constant variance across time, sex, and cohort. Male and female fish

were simultaneously modeled using two process equations to account for sexually dimorphic growth, with the process error and autoregressive parameters shared between the two sexes. Although males and females can differ in growth parameters due to the increased energetic needs of reproductive females (Olsen et al. 2005), we did not have reason to believe population-level growth variation patterns significantly differed between sexes.

To the process model without trend (constant) described above, we added parameters to capture three alternative growth variation patterns: anomalies shared across years (annual), cohorts (cohort), or size at first modeled age (initial size) (Table 1.2). The annual growth anomaly model assumes all fish in a given year experience a constant year deviation from their "average" normalized length (Table 1.2, Equation 3), while the cohort anomaly model assumes fish within a cohort share the same deviation from "average" normalized length in all years of the cohort members' life (Table 1.2, Equation 4). The initial size variation model assumes variability is primarily manifest in the cohort's normalized length at the first modeled age, e.g. due to juvenile competition (Table 1.2, Equation 5).

1.2.1.2 Observation model

We constructed a unique observation equation for each data source, each of which combines the fitted process model values with the effect of sampling changes and additional measurement error. We modeled survey and commercial data for each sex as unique observations of the two (male & female) length-at-age processes (Table 1.2, Equations 6 and 7). To account for changes in sampling due to shifts in fishing season or gear type used, size-at-age data from summer and winter fisheries and the two most commonly-used gear types were modeled using different observation equations. In each observation equation, we estimated coefficients for time-varying covariates that might influence observed size-at-age: sampling latitude, depth and age method of the catch. Latitude and

depth were measured as continuous covariates, while age method was measured as the percentage of fish in a given age-year sample that were aged using break-and-burn methods. We assumed that the coefficients of these covariates in each observation equation were constant across sex, data source, season, and gear type. However, we assumed that commercial data might have different observation errors than survey data due to sampling changes driven by fishing regulations, so observation error parameters were data-source specific, though still shared between sexes.

1.2.2 *Simulation study*

We tested if the correct process model was chosen by model selection when fit to simulated data generated from a deterministic growth model with parameter variation. All parameters used to simulate data are outlined in Table 1.3. We used a von Bertalanffy growth model as our operating model to simulate length-at-age for a hypothetical fish population under our four hypothesized scenarios – one with constant VBGF parameters (constant), one with annual variation in the VBGF L_∞ parameter (annual anomaly), one with cohort variation in the VBGF L_∞ parameter (cohort anomaly), and one with cohort variation in the VBGF L_0 parameter (initial size variation). To all of these simulated "true" lengths-at-age, we added normally distributed process error. We used a negative coefficient on latitude to simulate a decline in mean size-at-age of samples with decreasing temperature. Depth is a major axis of population structure in groundfish, with fish typically moving deeper as they grow and mature (Gunderson and Vetter 2006), therefore we used positive coefficients on depth. Surface ageing techniques are known to underestimate fish age (Beamish 1979a, Beamish 1979b), so we simulated a negative effect on size-at-age in years when a higher percentage of fish were aged using break-and-burn techniques. We used female survey data and life history parameters from Gulf of Alaska Pacific halibut stock assessments to ensure covariate data and generated sizes were realistic and tuned error standard deviations (s.d.s) to

match true data variability patterns. We added normally distributed observation errors to the generated process data points described above. Process and observation errors were set to be much larger than the values estimated from the data to ensure the conclusions of our simulation analysis were conservative. Finally, we fit our four alternative process models to the simulated data to determine if the statistical model chosen by model selection matched the operating model used to generate them. Fifty different data sets were generated for each growth variation mode, and all models were fit as described in the "Bayesian methods" section below.

1.2.3 *Bayesian methods*

We used Bayesian numerical methods (Markov Chain Monte Carlo [MCMC] simulations), because the model could not be easily fit using maximum likelihood approximation. Uninformative priors and hyperpriors were used for all parameters (Table 1.4), except for the priors of the autoregressive β coefficient on the previous years' normalized length and the η_x coefficients on covariate mean values, which were constrained to be normal with a mean of zero and a standard deviation of one. Very high values of these coefficients would indicate that normalized length was increasing at rates that were not biologically reasonable, so constraints on the prior for the variance of these parameters were warranted. The prior on year anomaly standard deviation (σ_γ) was constrained to be between zero and one, because larger values would indicate changes in size-at-age of multiple sample standard deviations of observed length from year to year. We used the deviance information criterion (DIC) for model selection using the "effective number of parameters" (pD) penalty function (Spiegelhalter et al. 1998, Plummer et al. 2006). Convergence was evaluated using visual examination of trace plots and posterior density plots and the Gelman-Rubin convergence statistic (Gelman and Rubin 1992). For the simulation study and model fitting, 3 chains were run for 150,000 iterations, thinning every 200th iteration, with a burn-in period of

30,000 iterations. All runs were performed using Just Another Gibbs Sampler (JAGS) version 3.2.0, the rjags R package (Plummer 2013) was used to calculate the DIC, and convergence was checked using the R coda package (Plummer et al. 2006).

1.2.4 *Model application*

1.2.4.1 Data

Length-at-age data time series were provided by the US National Marine Fisheries Service's Northwest Fisheries Science Center (NWFSC) and Alaska Fisheries Science Center (AFSC), and the International Pacific Halibut Commission (IPHC). A total of 29 groundfish species from the Bering Sea, Aleutian Islands, and California Current ecosystems were included in this study (Table 1). Commercial port-sampled data from the Pacific Fisheries Information Network (PacFIN) retrieval dated 6/09/2014, Pacific States Marine Fisheries Commission, Portland, Oregon (www.psmfc.org) were provided for the California Current ecosystem through the NWFSC, and commercial Resource Assessment and Conservation Engineering (RACE) observer and survey data were provided by the AFSC. The IPHC provided Pacific halibut survey data. Non-sexed fish and samples with unreasonable length measurements (e.g. negative, 0, or larger than maximum species length) were removed. Commercial data labeled by observers or port samplers as non-random or non-commercial were also removed. We did not model periods of the time series missing more than three consecutive years of data, as our model's ability to extrapolate is limited. Stocks with fewer than 10 years of data were excluded, as biological changes are difficult to detect on such short time scales for long-lived groundfish species.

Additional filtering was needed to minimize the potential for sampling error, fishery gear selectivity, and ageing error to bias our estimates of growth rate changes. To account for sampling error in estimates of mean length-at-age, it was necessary to determine a threshold

level of precision to deem estimates usable in our analysis. We used the coefficient of variation (CV) as a threshold metric, and we modeled years and fish ages in which the CV of the observed lengths-at-age was less than 0.25. If calculated length anomalies for a given age did not meet the CV threshold in more than 90% of years with data, we removed these ages from the analysis. Estimates of ageing error derived from stock assessments were used to exclude the oldest subset of fish based on a maximum tolerable ageing error threshold. This threshold depended on the species, as ageing error can potentially affect length estimates for shorter lived fish more than longer lived species. To account for the influence of selectivity, we used stock assessment selectivity curves to remove ages of fish that were selected at <40% from our analysis. In cases where stock assessment selectivity curves were very peaked (i.e. walleye Pollock, Pacific cod), this resulted in removal of the youngest-aged fish (Table A.1, Table A.2, Table A.3). A more conservatively filtered data set, where only fish selected at greater than 80% were modeled, was also tested to ensure estimates were robust to our selectivity assumptions.

Different data types were used for stocks in each ecosystem because of data availability. Stocks in the Gulf of Alaska and Bering Sea/Aleutian Islands ecosystems were modeled using both survey and commercial data or survey data only if commercial data were not available. In the California Current, commercial data were more extensive and had longer time series, thus only commercial data were used (Table A.1, Table A.2, Table A.3). Groundfish summer fisheries harvest in April through October while winter fisheries operate from November to March. If there was any change in the percentage of fish caught in each season or using each gear type throughout the studied time period, fish caught in the summer and winter fishery and using the two most common gear types were modeled using unique observation equations, as described in the Growth model framework section above. In all cases, data were only separated

by gear and season if the separated data met our minimum sample size requirements, otherwise data were kept aggregated. For the stocks with both data sources, four different data observations were fit using four observation model equations (Table 1.2). Ecosystems for which only one data type was available were modeled using two observation processes, one for each sex. We also modeled a subset of Bering Sea/Aleutian Islands stocks using commercial data only as an analysis of model sensitivity to the addition of survey data. Age method and latitude were used as predictors for the ecosystems in Alaska, but only port sampling location was available for the California Current data. Therefore, we did not include location as a covariate for this ecosystem. Data were aggregated for one pair of stocks (northern and southern rock sole) in some years, so we assumed these stocks' data could be grouped based on physical and demographic similarity in order to keep them in the analysis. Northern Pacific halibut are thought to be a single stock centered in the Gulf of Alaska with ontogenetic migration patterns (Clark et al. 1999), therefore we only modeled halibut in the Gulf of Alaska ecosystem.

1.2.4.2 Magnitude of growth anomalies

To assess if estimated growth anomalies were large enough to substantially impact fish size, we translated our fitted growth anomalies back into fish length. To do this, we chose two periods for each stock in which substantial growth anomalies were estimated, during which estimated growth anomalies showed different patterns (i.e. one period net positive, the other net negative). We then projected mean size-at-age patterns for two cohorts, one born at the start of each period, under the growth variation mode chosen by model selection. For annual growth anomalies, the sample mean was used as a starting length for the initial age to ensure fish started at the same size at the first modeled age, and then the estimated annual anomaly was used to predict size at each subsequent age. Initial size effects dictated the estimated starting size for stocks experiencing this variability

pattern, after which growth was modeled using identical parameter estimates for the two simulated trajectories. For stocks with the cohort anomaly pattern selected, the starting length was standardized for the two trajectories, as described for the annual anomaly model, and then the estimated cohort anomaly dictated two growth curves for the two trajectories. We then compared the size-at-age trajectories graphically to determine if credible intervals for the trajectories overlapped.

1.3 RESULTS

1.3.1 *Simulation study*

The state-space model accurately identified the true type of growth variation in nearly all scenarios. When initial size variation, cohort growth anomalies, and annual growth anomalies were used to simulate data, the correct process model was chosen by DIC in all cases (Figure 1.1). When no process variation was simulated (i.e. constant model), over half of the DIC weight was attributed correctly to the constant model, but some weight was also attributed to the annual and cohort anomaly models. DIC has been known to prefer overly parameterized models (Ando 2007), so the incorrect attribution of some DIC weight to more highly parameterized models (Figure 1.1) is expected and should be considered when applying this method of model selection. For all process models, the most DIC weight was given to the models that included age method. We found the estimation models had poor convergence when all covariates were included. Examination of covariance matrices from cases which did converge revealed this was likely due to high correlation (>.8) between depth and latitude covariates. All selected models included either age method only or age method and latitude as observation covariates. As such, in our final model, we removed depth as a covariate.

1.3.2 *Estimated growth mode and pattern*

Out of the 37 stocks tested, 13 showed evidence of substantial growth variation (Table 1.5), as defined as greater than four years during which the estimated growth anomaly credible interval did not overlap zero and a ΔDIC exceeding 5 between the chosen growth anomaly and the constant model. When growth variation was detected, annual and initial size anomalies were the dominant modes of variation. The annual growth anomaly model including age method as a covariate was given the majority of DIC weight in the California Current and Gulf of Alaska ecosystems, while the initial size effect model was given the majority of DIC weight in the Bering Sea/Aleutian Island ecosystem (Figure 1.2). The annual growth anomaly model was selected for 10 out of 17 stocks modeled in the California Current ecosystem, 6 out of 11 stocks modeled in the Gulf of Alaska ecosystem, and 2 out of 9 stocks in the Bering Sea/Aleutian Islands ecosystem. The initial size variation model was selected for 7 stocks in total (2 stocks in the California Current, 1 stock in the Gulf of Alaska, and 4 stocks in the Bering Sea/Aleutian Islands), and the cohort anomaly model was selected for 3 stocks in total (1 stock in the California Current and 2 stocks in the Gulf of Alaska). A sizable number of stocks (7/37) had DIC weight split between the constant and other anomaly models (ΔDIC ≤5), therefore there is not sufficient statistical evidence to conclude growth variation is observed in these stocks (Table 1.5). Model selection for species present in multiple ecosystems was generally inconsistent across ecosystems, with the exception of Pacific ocean perch and northern rockfish, for which annual anomalies were observed across ecosystems (Table 1.5). On average, growth anomalies were most substantial when the annual or initial size model was selected, while cohort anomalies were generally smaller in magnitude with fewer inter-annual changes in the direction of estimated growth anomalies.

Estimated anomaly patterns took one of three predominant forms: (1) substantial variability with no sustained trend (trendless), (2) sustained trends (3) near-zero (Figure 1.3), although some stocks exhibited combinations of these three patterns. Patterns characterized as lacking a sustained trend consisted of substantial positive or negative growth anomalies, but were centered on the zero line for the entirety of the time series (Figure 1.3: CC petrale sole, BSAI walleye pollock, and GOA Pacific cod; Figure A.1: CC yellowtail, widow, darkblotched and canary rockfish, GOA walleye pollock; Figure A.2: BSAI rock sole). Sustained trends consisted of monotonically increasing or decreasing growth anomaly estimates, or growth anomalies which exhibited a step change from negative to positive or vice versa (Figure 1.3: GOA Pacific halibut, CC Pacific hake; Figure A.1: CC sablefish and Dover sole). Growth anomalies close to zero were defined as those for which the credible interval of the growth anomaly overlapped zero for a minimum of all but four or fewer time series years (Figure 1.3: CC chilipepper; Figure A.2: BSAI yellowfin sole and Atka mackerel). Stocks with trendless variability in estimated growth anomalies sometimes corresponded to those that were modeled using only one data source or had fewer observations in each year. It is important to note that most BSAI species are primarily located uniquely in either the Bering Sea (BS) or Aleutian Islands (AI). However, patterns observed in the combined BSAI ecosystem were identical to those observed when the finer-scale BS and AI ecosystems were used and they are therefore aggregated in the results section for clarity.

1.3.3 *Effect of survey data*

When the annual model was not selected in the BSAI ecosystem, we found that removing survey data from the analysis resulted in a larger number of stocks (5/7) being classified as experiencing annual variation in growth (Table 1.6). Whether or not adding commercial data changed the outcome did not depend on the relative proportion of survey and commercial data. This suggests

including even a small amount of survey data can assist in correctly classifying the mode of growth variation and that annual growth anomalies estimated using only commercial data may be spurious.

1.3.4 *Growth anomaly magnitude*

Growth anomalies caused notable differences in predicted size-at-age for some stocks, but for others the anomalies translated into relatively small changes. For example, Gulf of Alaska Pacific halibut born in earlier years are predicted to be larger than halibut in later years throughout their life (Figure 1.4A), which is consistent with the estimated downward trend in annual growth anomalies in this stock. Petrale sole, which have estimated trendless anomalies, are predicted to be substantially different in size for cohorts that are out-of-phase with each other (Figure 1.4B). However, for petrale sole, the predicted trajectory includes negative growth from one year to the next outside of the prediction interval. This may be due to strong sensitivity to annual variation in environmental conditions, or because there is annually-fluctuating observation error that could not be removed from the estimated true anomalies for this stock. Walleye pollock and Pacific hake born in earlier years are predicted to be smaller when they enter the fishery, which led to small predicted differences in size until later years of life in pollock (Figure 1.4C) and Pacific hake (Figure 1.4D). Note that our model of anomalies creates a tendency for size-at-age to revert to the mean, so this creates a growth pattern (e.g. in pollock) that resembles compensatory growth. In contrast, chilipepper rockfish and Pacific cod, which were shown to experience cohort growth anomalies of smaller magnitude, showed smaller differences between cohorts (Figure 1.4 E,F).

1.4 DISCUSSION

In this study, we demonstrated the ability of a state-space model to identify growth variation patterns from size-at-age data and then applied this model to Pacific groundfish stocks. Our

simulation study results suggest that state-space autoregressive models are able to capture population-level size-at-age patterns produced by annual, cohort or initial size growth anomalies. In our application, we found the most common form of growth variation differed among ecosystems, with annual growth anomalies most common in the California Current and Gulf of Alaska groundfish stocks and initial size effects most common in the Bering Sea/Aleutian Island stocks. Estimated annual and initial size anomalies were characterized by variation centered on zero for most California Current and Bering Sea/Aleutian Island stocks. With the exception of Gulf of Alaska halibut, the Gulf of Alaska ecosystem was characterized by small growth anomalies. This analysis framework can be extended to other stocks with sufficient time series of survey and/or commercial catch monitoring length-at-age data.

We hypothesized that a time series model would be sufficient to detect different variation modes in biologically-derived growth model parameters, and this hypothesis was borne out in our simulation study. This implies that a correct specification of the mechanistic growth model is not necessary to correctly infer the dominant mode and scale of growth variation caused by changes in growth parameters. A substantial majority of DIC weight was attributed to the correct variation mode in our tested scenarios, suggesting that the analytic framework is robust. However, given that we randomly sampled from our simulated population, our simulation study results do not imply that our model can successfully differentiate trends due to changes in sampling from those due to biology. Thus, our simulation study results could be advanced by incorporating realistic selectivity patterns for individuals or directly incorporating selectivity into the estimation framework as in Cope and Punt (2007).

The primary strength of this method is its flexibility: the model accounts for different types of growth variability and is robust to the measurement and sampling error inherent in common size-

at-age data sources. This approach is also easier to integrate into fishery stock assessments than previous methods of growth estimation for two main reasons. The first is our method's use of the fishery-independent and –dependent data used in assessments. Many studies which have characterized growth variation patterns rely on otolith dendrochronology (Hagen and Quinn 1991, Zhao et al. 1997, Black et al. 2008) or isolated hatchery populations of freshwater fish with highly accurate age information (He et al. 2011) to minimize the effect of heterogeneous sampling and ageing error on growth estimates. However, dendrochronology analysis is costly and time-consuming to conduct. Therefore, this approach allows for estimation of growth rate variability at broad scales from existing databases when additional data collection is infeasible or undesirable. The second advantage of our state-space approach is that it separates estimates of growth process and observation error. Historically, growth curves incorporate only process error, with the result that observation error is also captured in the process error estimate. In a stock assessment, growth process error is propagated through the model and contributes to uncertainty in management reference point estimates. Therefore, isolating process from observation error in growth could improve the precision of management reference points in fishery stock assessment.

Important caveats to consider when applying this method were revealed through simulation testing and application of various iterations of the model. In simulation testing, we found substantial DIC weight was attributed to the alternative growth variation models when data were simulated using constant growth parameters. DIC has been known to prefer overly complex models (Ando 2007), therefore, when applying this method of model selection to data it is important to consider the potential for overfitting. Another important consideration when applying a state-space approach is that use of multiple sources of data greatly improves the model's ability to differentiate between changes in sampling and true population growth variation. In our

sensitivity analysis, we found using commercial data only to model growth of stocks in the BSAI ecosystem led in an increase in the number of stocks with estimated annual effects. Additionally, in a prior iteration of the model, gear types and fishery seasons were not modeled as independent observation processes with a similar outcome. This suggests the model is likely to attribute changes in fishing, including shifts in fishery season and/or gear types, to annual biological growth changes when true growth is constant or varies by cohort. As such, it is important to use a unique observation process for each data set that has substantial sampling differences. If only one data source is available and inter-annual anomaly estimates exceed biologically plausible growth shifts, we found using more informative priors on the standard deviation of the annual growth anomaly can also yield more realistic trends and/or shift model selection preference away from annual anomalies.

Differences in the dominant mode and trend in growth variation across ecosystems (i.e. primarily trendless annual growth anomalies in the California Current, trendless initial size variation in the Bering Sea/Aleutian Islands, and insubstantial annual anomalies in the Gulf of Alaska) could indicate growth responses to unique ecosystem processes. The California Current is an upwelling-driven, highly variable system (McGowan et al. 1998), while Alaskan ecosystems experience climate forcing on longer time scales (Hollowed et al. 2001). Therefore, climate forcing on growth in the California Current may take a more dominant role, while in the Bering Sea/Aleutian Islands density-dependent effects on growth may be stronger. However, some estimated growth anomaly patterns in the California Current experienced interannual shifts that may surpass biologically plausible ranges (i.e. negative growth in petrale sole, Figure 1.4). This, taken with the results of our sensitivity analysis, likely indicates some annual trends are spurious and due to a limitation of the model's utility when using only fishery-dependent data. The generally

small estimated annual anomalies for a majority of stocks in the Gulf of Alaska may be due to data limitations, because survey sampling is more limited in this system compared to the Bering Sea/Aleutian Islands.

Our finding that growth rate variation was most pronounced at annual scales (i.e., annual growth anomalies) provides support for the hypothesis that time-varying factors (including one or more of climate, fishing, or sampling changes) are an important driver of fish growth. This finding is consistent with the hypothesis that broad scale controlling factors such as temperature (Fry 1971) govern growth variation of fish, but we lack sufficient evidence to draw inferences about mechanisms. Synchronous annual growth trends across species might indicate shared responses to basin scale climatic conditions, as has been found in studies on recruitment (Hollowed et al. 2001, Mueter et al. 2007, Stachura et al. 2014). However, annual trends across stocks within an ecosystem were not highly correlated in our results, suggesting that basin-scale climate variability is not the primary driver of these effects. In the California Current ecosystem, annual growth anomalies potentially capture sampling changes in commercial time series. Alternatively, in the Gulf of Alaska ecosystem, annual anomalies may represent a response to either local-scale ocean conditions and productivity or the combined effect of species-specific factors, such as density, fishing, and inter-species competition, on growth.

We observed significant cohort growth anomalies in only one stock (Gulf of Alaska Pacific cod). This is surprising as cohort growth anomalies are presumed to represent density-dependent growth effects that are commonly documented in marine fish populations (Helser and Almeida 1997, Walters and Wilderbuer 2000, Rogers et al. 2011). We interpret this as evidence that intraspecific competition for food occurs not only within a cohort, but across multiple cohorts as observed in Whitten et al. (2013), in which case the observed significant annual growth anomalies

may be caused by density-dependence and not ocean productivity. Additionally, the cohort anomaly model contains more parameters than the annual anomaly model and as a result is penalized in our model selection framework. Therefore, if both types of anomalies are represented in equal magnitude in the data, the annual model will be chosen. Accounting for the simultaneous presence of both cohort and annual anomalies could increase the number of observed significant cohort anomalies and improve our estimates of variation, especially in cases (7/37) when DIC weight was split across multiple models.

Anthropogenic factors may affect estimated growth trends, either through actual changes to population size-at-age via the selection of larger individuals by the fishery or by changes in sampling that creates the appearance of growth trend. None of our annual growth trends exhibited a constant decline corresponding to increased or sustained fishing pressure. Fishing pressure in California Current and Alaskan ecosystems did not ramp up until the 1950's (Miller et al. 2014) and 1970's (Melnychuk et al. 2013) respectively. Taken with our results, this short time-scale of fishing suggests fisheries-induced evolution is not primarily responsible for detected size-at-age changes in these stocks. A more likely anthropogenic effect is a decrease in mean size-at-age due to skewed gear selection of larger, faster-growing individuals by fisheries (Hilborn and Minte-Vera 2008). A minority (4/19) of modeled stocks were observed to have a significant negative Pearson's correlation between fishing rate and annual growth anomaly (Table A.4), which does not provide very clear evidence that fishery removal of faster-growing individuals is related to detected growth anomalies. Finally, although we accounted for the impacts of temporal changes in sampling, including gear type and fishing season, some residual effects of temporal sampling changes could be influencing our results. A significant effect of catch latitude on growth was not detected in most stocks; however, spatial effects could be more strongly correlated with longitude

in the Bering Sea/Aleutian Islands ecosystem or not detected for California Current stocks due to the coarser resolution of available location data.

In summary, we have demonstrated that a time series model may be used to isolate modes of growth variation from length-at-age data. The model we constructed represents a more robust way to model population size-at-age variability for two reasons. It allows for a quantitative comparison between alternative growth variation types and appropriately accounts for biological process error and inaccurate measurements of size-at-age. Our application allows us to infer that annual growth patterns dominate across California Current and Gulf of Alaska groundfish species, but these patterns are not highly synchronous within large marine ecosystems. In the Bering Sea and Aleutian Islands ecosystem, initial size effects were shown to be more prevalent. This method represents a substantial step towards quantifying the magnitude and mode of growth variation quickly and robustly across species with existing high-quality fisheries data. After these trends are quantified, they may be used in future studies to assess the likelihood of a mechanistic relationship between these patterns and potential abiotic, biotic, and anthropogenic drivers.

TABLES

Table 1.1 - Stocks used for model application, listed by scientific name, common name, and source (Northwest Fisheries Science Center [NWFSC]; Alaska Fisheries Science Center [AFSC]; International Pacific Halibut Commission [IPHC]) and type of data (scientific survey [S]; commercial catch port-sampled [C]) used.

Scientific name	Common Name	Source	Type
Anoplopoma fimbria	sablefish	NWFSC	C
		AFSC	C, S
Eopsetta jordani	petrale sole	NWFSC	C
Merluccius productus	Pacific hake	NWFSC	C
Ophiodon elongatus	lingcod	NWFSC	C
Parophyrus vetulus	english sole	NWFSC	C
Atheresthes stomias	arrowtooth flounder	AFSC	S
		NWFSC	C
Gadus macrocephalus	Pacific cod	AFSC	C
Glyptocephalus zachirus	rex sole	AFSC	S
Hippoglossoides elassodon	flathead sole	AFSC	C, S
Hippoglossus stenolepis	Pacific halibut	IPHC	S
Lepidopsetta bilineata	southern rock sole	AFSC	C, S
Lepidopsetta polyxystra	northern rock sole	AFSC	C, S
Limanda aspera	yellowfin sole	AFSC	C, S
Microstomus pacificus	Dover sole	AFSC	C, S
		NWFSC	C
Pleurogrammus monopterygius	Atka mackerel	AFSC	C, S
Sebastes alutus	Pacific ocean perch	AFSC	C, S
		NWFSC	C
Sebastes ciliatus	dusky rockfish	AFSC	C, S
Sebastes crameri	darkblotched rockfish	NWFSC	C
Sebastes entomelas	widow rockfish	NWFSC	C
Sebastes flavidus	yellowtail rockfish	NWFSC	C
Sebastes goodei	chilipepper	NWFSC	C
Sebastes melanops	black rockfish	NWFSC	C
Sebastes melanostomus	blackgill rockfish	NWFSC	C
Sebastes miniatus	yelloweye rockfish	NWFSC	C
Sebastes pinniger	canary rockfish	NWFSC	C
Sebastes polyspinis	northern rockfish	AFSC	C, S
Sebastes rufus	bank rockfish	NWFSC	C
Theragra chalcogramma	walleye pollock	AFSC	C, S

Table 1.2 - Process and observation model components of the state-space model.

Equation number	Description	Equation	
1	Normalized length	$x_{a,t,g} = \frac{\overline{L_{a,t,g}} - \overline{L_{a,g}}}{s_{a,g}}$	
Equation number	**Process model**	**Equation**	**Initial size**
2	Constant model	$X_{a,g,t} = \beta X_{a-1,g,t-1} + \epsilon_{a,g,t}$	$X_{g,1} \sim N(0, {\sigma_{x0}}^2)$
3	Annual anomalies	$X_{a,g,t} = \beta X_{a-1,g,t-1} + \gamma_t + \epsilon_{a,g,t}$	$X_{g,1} \sim N(0, {\sigma_{x0}}^2)$
4	Cohort anomalies	$X_{a,g,t} = \beta X_{a-1,g,t-1} + \delta_c + \epsilon_{a,g,t}$	$X_{g,1} \sim N(0, {\sigma_{x0}}^2)$
5	Initial size variation	$X_{a,g,t} = \beta X_{a-1,g,t-1} + \epsilon_{a,g,t}$	$X_{g,1,c} \sim N(0, {\sigma_{x0}}^2)$
Equation number	**Observation model**	**Equation**	
6	Age method and latitude	$Y_{a,g,t,o} = X_{a,g,t} + \eta_1 a_{a,g,t} + \eta_2 l_{a,g,t} + \xi_{a,t,o}$	
7	Age method only	$Y_{a,g,t,o} = X_{a,g,t} + \eta_1 a_{a,g,t} + \xi_{a,t,o}$	

Table 1.3 - Parameter values used to generate data in simulation study.

Parameter	Description	Value
$\boldsymbol{\sigma_p}$	Process error	5
$\boldsymbol{\sigma_o}$	Observation error	2
$\boldsymbol{\eta_1}$	Coefficient on mean age method of length observation	-.5
$\boldsymbol{\eta_2}$	Coefficient on mean latitude of length observation	-.01
$\boldsymbol{\eta_3}$	Coefficient on mean depth of length observation	-.01
$\boldsymbol{\sigma_{L_0}}$	Variation in L_0 parameter	5
$\boldsymbol{\sigma_{L_\infty}}$	Variation in L_∞ parameter	10
$\boldsymbol{\sigma_k}$	Variation in k parameter	.05
$\boldsymbol{L_\infty}$	VBGF parameter	910mm
$\boldsymbol{L_0}$	VBGF parameter	390mm
$\boldsymbol{k}$	VBGF parameter	.3
$\boldsymbol{n}$	Number of years	37y.
$\boldsymbol{a}$	Age range	7y.-12y.

Table 1.4 - Variable notation, description, and Bayesian prior distribution (when applicable) for all data and parameters used.

Parameter	Description	Distribution
$X_{a,g,t}$	normalized length of fish at age a of sex g at time t	-
γ_t	annual anomaly on all cohorts in year t	-
δ_c	cohort anomaly on cohort c, the cohort to which fish of age a born in year t belong	-
$X_{g,1}$	mean normalized length for a fish of sex g upon >40% selection by the fishery	-
$X_{1,g,c}$	mean normalized length for a fish of recruitment age in cohort c >40% selection by the fishery	-
$Y_{a,g,t,o}$	observed normalized length of fish at age a of sex g at time t from data source o	-
β	coefficient of the previous years' length on the current year	N(0,1)
η_2	coefficient of mean age method on the normalized length	N(0,1)
η_3	coefficient of mean latitude on the normalized length	N(0,1)
$a_{a,g,t,o}$	mean age method for fish of age a in year t of sex g from data origin o	N($\mu_{a,g,o}, \sigma^2_{a,g,o}$)
$l_{a,g,t,o}$	mean latitude for fish of age a of sex g in year t from data origin o	N($\mu_{l,g,o}, \sigma^2_{l,g,o}$)
$\mu_{a,g,o}$	mean age method for fish of age a and sex g from data origin o	U(0,2)
$\sigma_{a,g,o}$	s.d. of age method for fish of age a and sex g from data origin o	U(0,1)
$\mu_{l,g,o}$	mean latitude for fish of age a and sex g from data origin o	N(0,1000)
$\sigma_{l,g,o}$	s.d. of latitude for fish of age a and sex g from data origin o	U(0,10)
$\epsilon_{a,g,t}$	process error	-
$\xi_{a,t,o}$	observation error	-
σ_γ	standard deviation on year anomaly	U(0,1)
σ_δ	standard deviation on cohort anomaly	U(0,10)
σ_p	process error standard deviation	U(0,10)
σ_o	observation error standard deviation	U(0,10)
σ_{X0}	initial size variation standard deviation	U(0,10)

Table 1.5 - Model selection results, aggregated by ecosystem and stock, with stocks grouped into families or similar morphologies; “mixed evidence” indicates that DIC weight was nearly evenly split between two or more alternative models, thus we could not distinguish which was more highly supported by model selection.

Stock	CC	BSAI	GOA
bank rockfish	Constant†‡§		
black rockfish	Annual†‡§		
blackgill rockfish	Mixed evidence†‡§		
canary rockfish	Annual†‡§‖		
chilipepper	Cohort†‡§		
darkblotched rockfish	Annual†‡§‖		
dusky rockfish			Annual
northern rockfish		Annual	Annual§
Pacific ocean perch	Annual†§	Mixed evidence§	Annual§
widow rockfish	Annual†§‖		
yelloweye rockfish	Initial size†‡§		
yellowtail rockfish	Annual†§‖		
Atka mackerel		Initial size§	Annual
lingcod	Mixed evidence†‡§		
Pacific cod		Annual	Cohort‖¶
Pacific hake	Initial size†§‖		
sablefish	Annual†‡§‖	Initial size‡	Initial size§¶
walleye pollock		Initial size§‖	Annual§‖
arrowtooth flounder	Annual†§		Cohort*
dover sole	Annual†§‖		
english sole	Mixed evidence†§		
flathead sole		Mixed evidence	Mixed evidence
Pacific halibut			Annual*‖
petrale sole	Annual†§‖		
rex sole			Constant*
rock sole		Initial size§‖	
yellowfin sole		Initial size§	

***** denotes stocks modeled using survey data only.
† denotes stocks modeled using commercial data only.
‡ denotes stocks modeled using the two most common gear types as unique observation processes.
§ denotes stocks modeled with summer and winter fisheries as unique observation processes.
‖ denotes stocks that have significant growth anomalies.
¶ denotes stocks with a DIC-chosen model that included a latitude covariate.

Table 1.6 - Comparison between model runs using both survey and commercial data and runs using commercial data only for BSAI stocks for which the annual model was not selected; all other model components (i.e. using gear and/or season as separate observations) are the same.

Stock	Commercial and Survey	Commercial only	Percentage commercial data
Pacific ocean perch	Mixed evidence	Annual	35%
Atka mackerel	Initial size	Annual	73%
sablefish	Initial size	Annual	83%
walleye pollock	Initial size	Annual	24%
flathead sole	Mixed evidence	Mixed evidence	37%
rock sole	Initial size	Initial size	39%
yellowfin sole	Initial size	Annual	31%

FIGURES

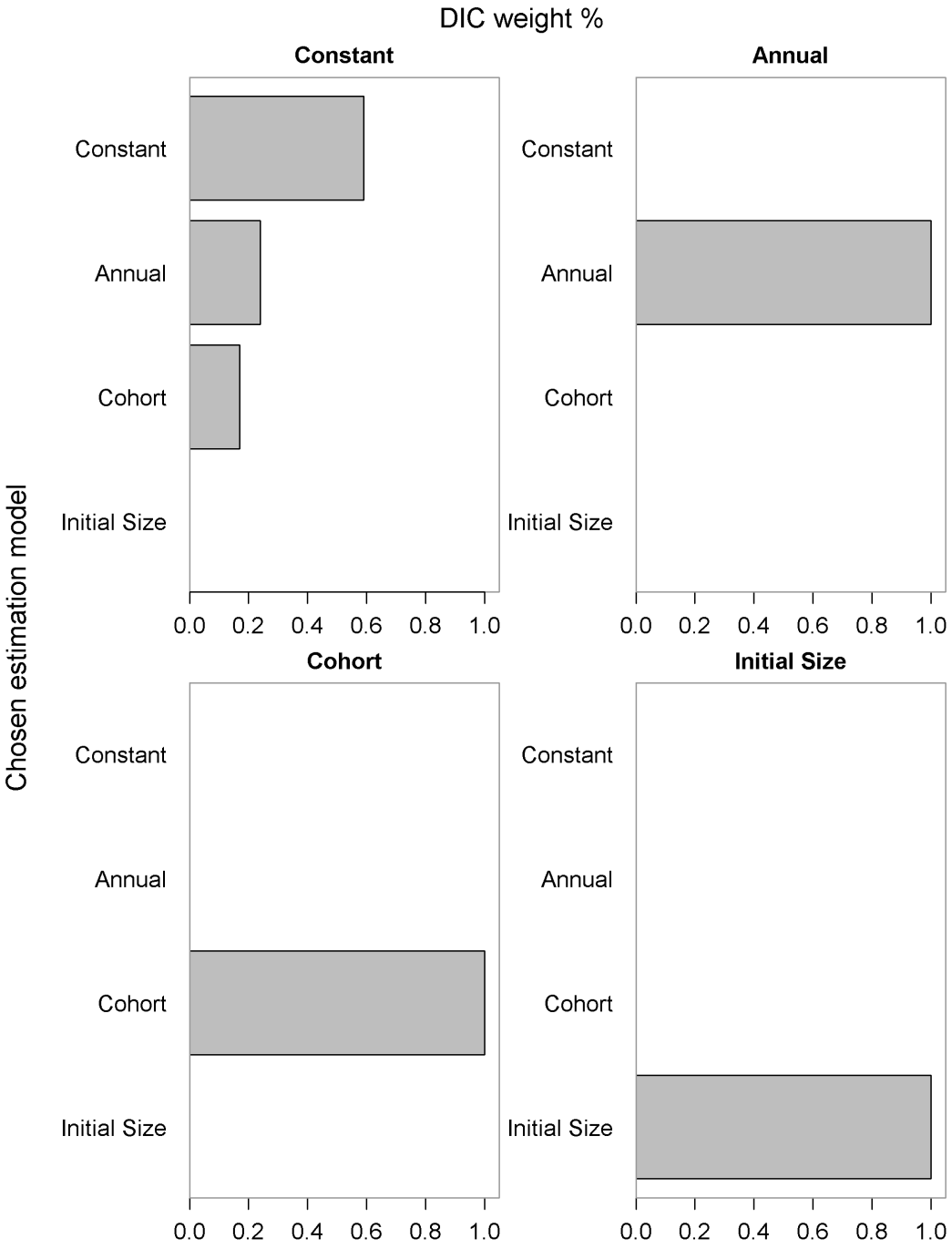

Figure 1.1 - Average percentage of DIC weight attributed to the four alternative estimation models for four underlying "true" growth models: A) constant operating model, B) annual operating model, C) cohort operating model and D) initial size operating model. Results represent aggregated DIC weight over 50 iterations.

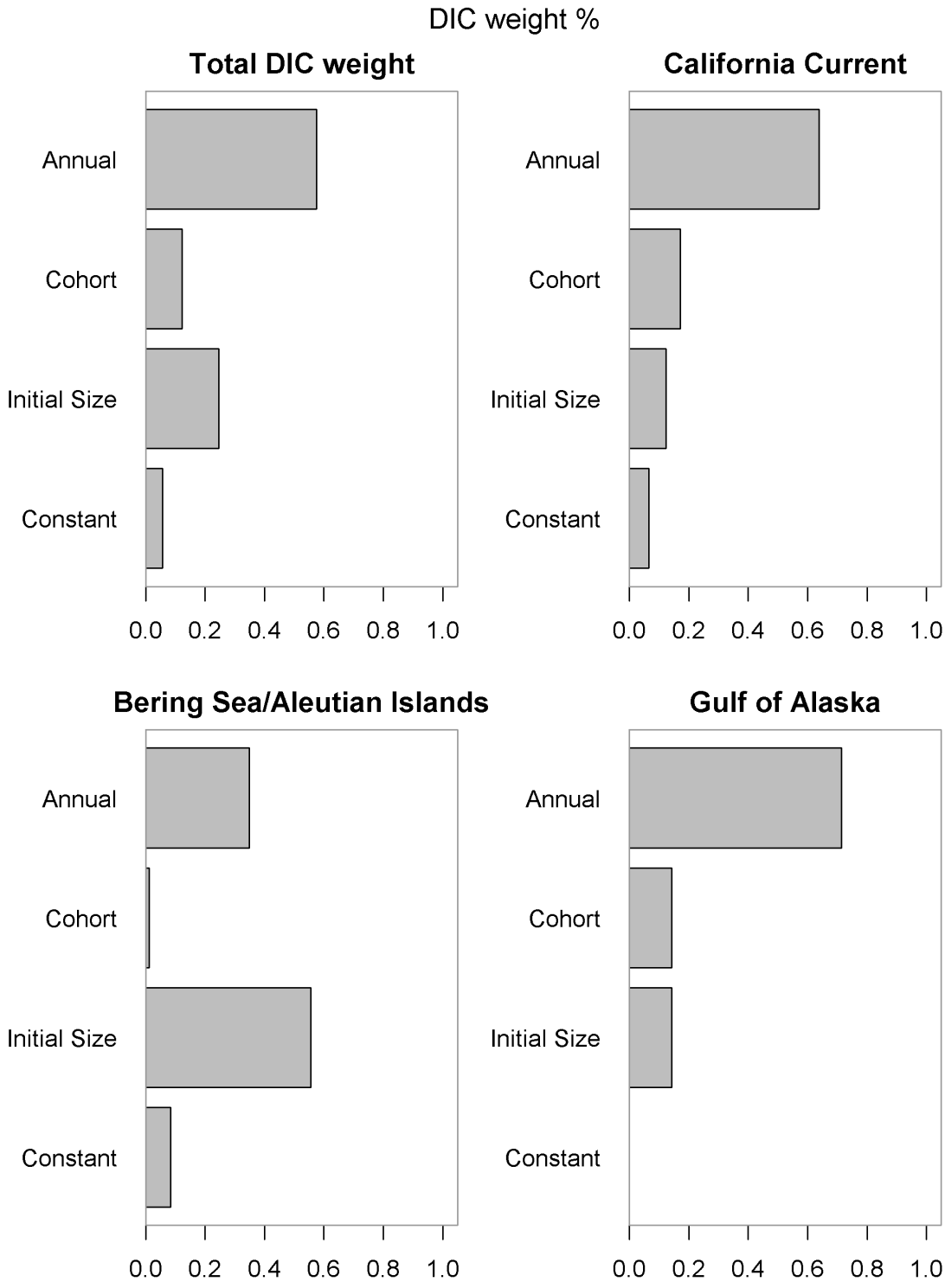

Figure 1.2 - Deviance information criterion (DIC) weights across tested models for A) all stocks across ecosystems, B) all stocks in the California Current ecosystem, C) all stocks in the Bering Sea/Aleutian Islands ecosystem, and D) all stocks in the Gulf of Alaska ecosystem.

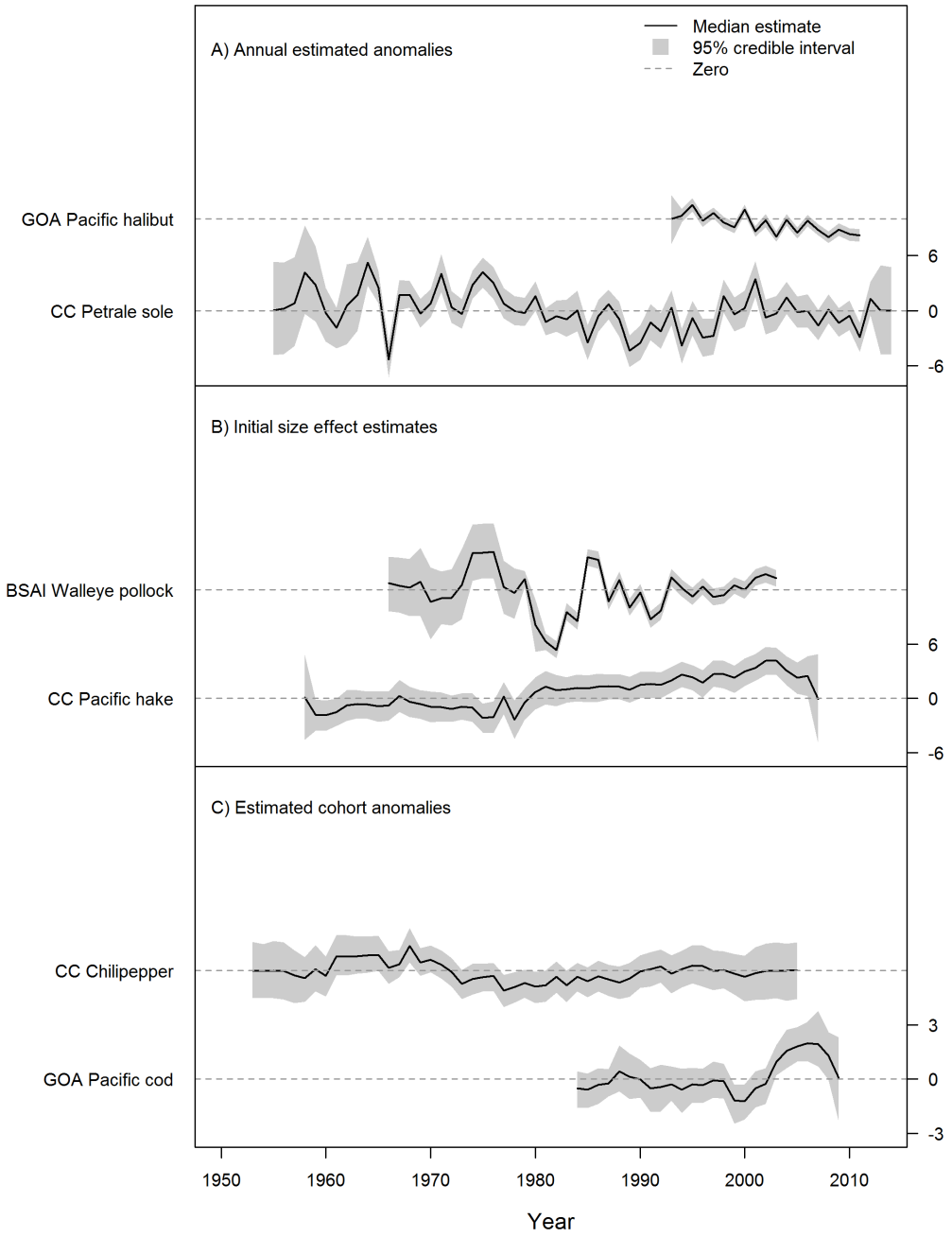

Figure 1.3 - Growth anomaly estimates for 6 stocks. The x-axis represents anomaly year for panel A and birth year for panels B and C. A) The annual growth anomaly model was chosen for Gulf of Alaska Pacific halibut and California Current petrale sole. These are examples of stocks which experienced highly variable growth anomalies. B) The initial size effect model was chosen for Bering Sea/Aleutian Islands Walleye pollock and California Current Pacific hake. C) The

cohort growth anomaly model was chosen for California Current chilipepper rockfish and Gulf of Alaska Pacific cod.

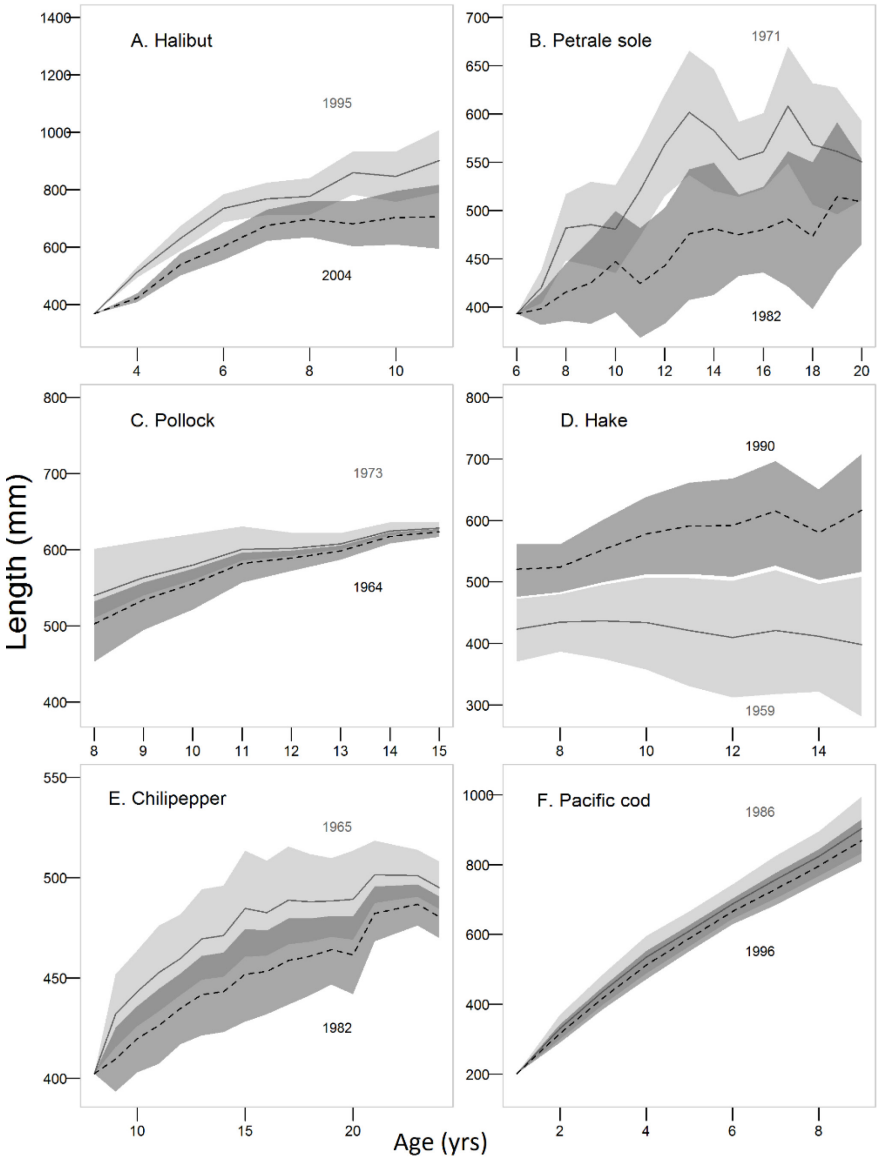

Figure 1.4 - Median predicted sizes (line) and prediction intervals (shaded area) for a A) Pacific halibut born in 1995 (light gray, solid line) and 2004 (dark gray, dashed line), B) petrale sole born in 1971 (light gray, solid line) and 1982 (dark gray, dashed line), C) walleye pollock born in 1973 (light gray, solid line) and 1964 (dark gray, dashed line), D) Pacific hake born in 1959 (light gray, solid line) and 1990 (dark gray, dashed line), E) chilipepper rockfish born in

1965 (light gray, solid line) and 1982 (dark gray, dashed line), and F) Pacific cod born in 1986 (light gray, solid line) and 1996 (dark gray, dashed line). Annual, initial size, and cohort growth anomalies were used to generate trajectories A & B, C & D, and E & F, respectively.

Chapter 2. Somatic growth contributes to population variation in marine fishes

ABSTRACT

Understanding population fluctuations is a major goal of population ecology. Fluctuations can be caused by internal feedbacks or through environmentally-driven variation in vital rates. In unpredictable environments, such as marine systems, variation in survival rate during a critical juvenile stage (recruitment) is common and thought to be the most important cause of population variation. However, somatic growth rates also vary in response to both internal and external drivers. There is increasing evidence that this induced growth variation contributes to population fluctuations, particularly in animals experiencing indeterminate growth. In this study, we examine the relative effects of empirical variation in somatic growth and recruitment on population production and variability across eight different life history archetypes of marine fish. We used empirical estimates of reproductive success and somatic growth rate variation, coupled with an age-structured population model, to simulate the relative role of both types of variation in population variability. The effects of this variation on population production and biomass were examined across three variation scenarios, in which somatic growth only, reproduction only, or both processes varied temporally. We also examined three levels of age truncation to explore if modified population age structure altered these dynamics. The contribution of somatic growth to biomass variability exceeded that of recruitment for some species (2/8 species), while in others (5/8 species), recruitment variation was more influential. When population production was examined, growth variability was more influential, having a minimal effect for only three species. The relative importance of the two processes was not clearly correlated with key life history traits (i.e. growth and mortality rates), but instead was determined by the extent that vital

rates varied. These results were consistent across age truncation levels, although increasing age truncation slightly increased the relative effect of recruitment variation on biomass variation for three species. These results suggest somatic growth variation can be as important as early life history survival in driving population fluctuations in species that experience indeterminate growth. This analysis provides a counterexample to the commonly-held assumption of many marine population dynamics models: that population variability is induced primarily through variation in reproductive success.

2.1 INTRODUCTION

Animal populations across taxa experience dramatic fluctuations, even in the absence of habitat modification, harvest, or migration (Costantino et al. 1997, Doney and Sailley 2013). Understanding why populations fluctuate is a central goal of population ecology. In a closed population, this variability is caused by variation in the key demographic processes of reproduction, somatic growth, and mortality. This variation may be introduced internally via density-dependent processes like competition (Hairston et al. 1960, Bjorndal et al. 2000), or through density-independent drivers, such as environmental conditions and interspecies interactions (Henson and Cushing 1997, Sæther 1997, Wilson 2011) . Which demographic rate is most variable and is the primary driver of population fluctuations is often not well understood.

The relative importance of different types of demographic variation on populations depends upon, as well as shapes, the life history strategies of animals. Long-lived species may be less sensitive to variation in reproductive success rates due to the impact of the storage effect on this life history type (Warner and Chesson 1985). Species with indeterminate growth may be more strongly affected by growth rate variation, either through maternal effects on reproduction (Sæther 1997, Hendry et al. 2001) or by its direct effect on population biomass (Lorenzen 1996).

At the same time, environmental variation which drives changes in demographic rates can drive selection for life history traits. For example, species whose offspring face unpredictable and variable survivorship, may adopt a bet-hedging strategy (i.e. low parental investment, high fecundity) (Mitchell 1988) or an opportunistic strategy (i.e. short lifespan, early age-at-maturity).

Marine teleost fish demonstrate this interplay between life history strategy and demographic variability and its consequences for population variability. The dominant paradigm in marine fish population dynamics is that environmental forcing drives changes in population production in marine fish (Hollowed et al. 2001), due to environmentally-induced variation in survivorship through key early life history stages (recruitment). However, a growing body of evidence suggests adult somatic growth rates also vary considerably, either temporally across entire populations in response to environmental shifts, or between birth years due to density-dependent effects (Baudron et al. 2014, Stawitz et al. 2015a, Thorson and Minte-Vera 2016). Although it is suspected that adult somatic growth variation also drives population production (Lorenzen 2008) in marine fish, few studies have directly examined the relative influence of somatic growth and recruitment variability to population fluctuations. We expect the relative importance of the two to vary depending on species life history traits. Specifically, opportunistic species, which have a small maximum size, early age-at-maturation, and short life spans (Winemiller and Rose 1992), are likely to be sensitive to variation in reproductive success. Larger, longer-lived species are more likely to be sensitive to somatic growth variation. However, these sensitivities may ultimately depend on the magnitudes of somatic growth and reproductive variation.

Alteration of population age structure may govern how population dynamics respond to changes in vital rates (Caswell et al. 1997). This is particularly relevant for marine fish, which

experience size-selective mortality through fishing. This mortality in turn truncates age structure by removing older, larger individuals, resulting in population biomass tracking recruitment variability more closely (Hsieh et al. 2009). In contrast, populations with a complete age structure are expected to be more resilient to fluctuations in reproductive success. However, the growth of adult individuals comprises a significant portion of population production when age structure is intact, particularly in long-lived species. Therefore, populations with a complete age structure could show a stronger response to somatic growth rate variation.

Here, we collated life history information with empirical time series of growth and recruitment variability across a variety of marine fish species to judge the relative importance of the two processes in inducing population variability. Our approach was to use using a common population model coupled with empirical recruitment and growth variation trends, applied to species with diverse life history traits. In this way, we assessed population variability with both rates varying or with only a single vital rate varying. We repeated this under different levels of age-truncation. Our hypothesis is that growth variability will be more important for long-lived species with indeterminate growth, while recruitment variability will be more important for shorter-lived species which mature earlier to maximize their lifetime reproductive output. The relative impact of recruitment variability is expected to increase as age truncation is more pronounced.

2.2 METHODS

We tested population responses to realistic fluctuations in growth and early life history for eight fish species spanning a gradient of life history traits (Table 2.). Deviation time series and population trajectories long enough to capture lagged effects of demographic variation on populations, as well as ensure an equivalent number of lifespans were simulated across species.

Specifically, we compiled time series characteristics (i.e. autocorrelation, variance) of recruitment (Stachura et al. 2014) and somatic growth (Stawitz et al. 2015a), and used these to simulate growth and recruitment time series with similar characteristics. We then combined these trajectories with a standard stage-structured population model to evaluate how variability in each rate was transmitted as variability in population biomass and production. By alternatively stabilizing each process, we quantified the relative contribution of each to population productivity.

2.2.1 *Species selection and life history traits*

We compiled life history parameters from a collection of Northeast Pacific teleosts for which empirical time series of growth and recruitment were available. Species were chosen across a gradient of life history invariants to determine if life history traits dictated how populations responded to variability. Long-lived canary rockfish (*Sebastes pinniger*) and widow rockfish (*Sebastes entomelas*) were chosen based on their unique strategy of high early growth rate and resulting large size-at-maturity (Beverton 1992). Gadids, including California Current Pacific hake (*Merluccius productus*), Eastern Bering Sea walleye pollock (*Gadus chalcogrammus*), and Gulf of Alaska Pacific cod (*Gadus macrocephalus*), were chosen as they are a similar size to rockfish, but reach maturity at relatively smaller sizes. Flatfish, including California Current petrale sole (*Eopsetta jordani*) and Northern rock sole (*Lepidopsetta polyxystra*), and Gulf of Alaska Pacific Halibut (*Hippoglossus stenolepis*), in contrast, exhibit slower early growth rates and increased growth later in life, as compared to rockfish (Beverton 1992). Life history parameter values (Table 2.1, Table B.1) were taken from population model estimates for female fish (Hare 2010, He et al. 2011, Stewart et al. 2011, Haltuch et al. 2013b, Wallace and Cope 2013, A'mar and Palsson 2014, Ianelli et al. 2014, Wilderbuer and Nichol 2014).

2.2.2 *Population model*

A standard stage-structured population model for female fish was used to simulate populations. Maturation was assumed to be age-dependent, with egg production proportional to body weight. Though body size affects maturity (Stearns and Koella 1986), the full age-length reaction norm for maturity is not known for all species. Because growth rate time series are more commonly expressed in terms of body length, an allometric length-weight relationship (Quinn and Deriso 1999) was used for each species to translate length into somatic mass. Note that this presumes that the length-weight relationship was constant, regardless of growth rate. This is consistent with the findings of empirical studies (Thorson and Minte-Vera 2016), though this assumption may introduce bias compared with models which do not convert length to weight (Kuriyama et al. 2016). All demographic rates other than growth and recruitment were constant in this model to permit comparison of known reproduction and growth rate variability on these populations.

2.2.3 *Early life history*

Early life history survivorship was simulated using one of three production functions ($f(B)$) that relate the mean number of individuals surviving the egg, larval, and early juvenile stage (termed "recruits": R) to biomass of reproductively mature fish (B) (Eq. 2.1: asymptotic: Beverton Holt; Eq. 2.2. knife-edged),

$$\text{a. } R = \frac{.8hR_0B}{.2\phi_0R_0(1-h)+(h-.2)B} \text{ or } R = \frac{\alpha B}{1+\beta B} \tag{2.1}$$

$$\text{b. } R = \begin{cases} \bar{R}; & B > .1\bar{R} \\ 0; & B \leq .1\bar{R} \end{cases} \tag{2.2}$$

where h, R_0, φ_0 are the parameters of the Beverton-Holt function under the Mace and Doonan (1988) parameterization and α and β are the parameters of the Beverton-Holt function under the

Beverton and Holt (1957) parameterization, and $\bar{R}$ is the biomass of the mean numbers of recruits.

Functions were chosen based on which provided the best fit (AIC) to the observed pattern of biomass and recruitment. We assumed that there was lognormal, auto-correlated variability around these mean levels owing to environmental conditions, therefore juvenile survivorship was simulated as in Equation 2.3,

$$R = f(B)\gamma_t, \qquad \gamma_t = \rho_r \gamma_{t-1} + \sqrt{1-\rho_r^2}\epsilon_t, \qquad \epsilon_t \sim N\left(\log\left(-\frac{\sigma_r^2}{2}\right), \sigma_r^2\right) \tag{2.3}$$

where γ_t represents the recruitment deviation, and ρ_r and σ_r^2 represent the estimated autocorrelation and variance in recruitment deviations, respectively.

We used recruitment parameters estimated or compiled by Stachura et al. (2014) from empirical estimates of recruitment deviations. We simulated deviations from mean recruitment using estimated parameters of auto-regressive (AR) models fit to estimated recruitment deviations. Simulation was used to create growth and recruitment deviation time series that were of equivalent length and long enough to reliably generate variability statistics of population response. First, we fit two AR models to each species' recruitment deviation time series using the forecast package in R (Hyndman and Khandakar 2007): one that included an auto-regressive term (ρ_r) and one that did not ($\rho_r=0$), and compared using AIC (Shibata 1976). Second, we simulated recruitment deviations using the chosen auto-regressive term ($\Delta AIC \leq 2$). We compared the simulated and empirical time series to ensure that the magnitude and frequency of simulated variations were plausible.

2.2.4 *Growth*

We simulated growth by adding deviations based on empirical estimates to the simulated mean lengths-at-age ($\overline{L_a}$) and length increments ($\overline{\Delta L_{a,a+1}}$) calculated from the Schnute (1981) parameterization of the von Bertalanffy growth curve (Bertalanffy 1938) (Equations 2.4, 2.5). This parameterization was used as it was used to estimate growth parameters in the population models from which life history parameter values were taken.

$$\overline{L_a} = \begin{cases} L_{min} + ba, & a < a_{min} \\ L_\infty + (L_{amin} - L_\infty)\exp\left(-k(a - a_{min})\right), & A_c \geq a \geq a_{min} \\ \dfrac{\sum_{a=A}^{2A}\exp(-0.2(a-A+1))(L_{Ac} + (\frac{a-Ac}{Ac})(L_\infty - L_{Ac})}{\sum_{a=A_c}^{2A_c}\exp(-0.2(a-A_c+1))}, & a \geq A_c \end{cases} \tag{2.4}$$

$$L_\infty = L_{amin} + \frac{L_A - L_{amin}}{1 - \exp(-k(A - a_3))} \tag{2.5}$$

where a_{min} and A denote the youngest and oldest sampled fish, respectively, L_{amin} denotes the length of fish at age a_{min}, L_A denotes the length of fish at age A_c, L_∞ denotes the mean length at maximum age, and k represents the relative growth rate. Mean growth curve parameter estimates (L_{amin}, L_A, k) were taken from population model estimates, unless a single growth curve in the Schnute (1981) form was not estimated in previous analyses. In these cases, for consistency, the Schnute growth curve with a normal error structure was fit to length-at-age data from scientific surveys to obtain simulation growth parameters (Table 2.1) using maximum likelihood estimation.

Two alternative types of variation were simulated, depending on which growth variation mode was selected by model selection for each species in Stawitz et al. (2015a). Annual variation refers to a deviation from mean length-at-age on fish of all ages in the same year, while

inter-cohort variation refers to a positive or negative deviation on length at a_{min} that is unique for fish of each birth year. The median estimate of either the annual or inter-cohort variation for each species was taken from Stawitz et al. (2015a) and analyzed using an AR model fit via the forecast package in R (Hyndman and Khandakar 2007). We then used the estimated autocorrelation (ρ_g) and standard deviation (σ_g^2) of these time series to simulate a time series of growth deviations, δ_t, which we then added to the mean growth curve as described below.

We calculated length of a fish at each age in each simulation year ($L_{a,t}$) as the sum of the fish's mean size at the previous age in the previous year, the mean growth increment, and added variation (Equation 2.6).

$$L_{a,t} = L_{a-1,t-1} + \overline{\Delta L_{a,a+1}}(1 + I_a \delta_t r_a m_a); \;\; t > 1 \qquad (2.6)$$

where I_a is an indicator variable denoting if variation is present for age a, and δ_t is the deviation from average growth in year t (annual variation) or birth year (inter-cohort variation) t. The mean growth increment $\overline{\Delta L_{a,a+1}}$ is calculated by rearranging Equation 2.4. The values m_a and r_a denote the scaled CV of length and magnitude of the growth effect on fish of age a, respectively, which were introduced to scale variation by age and ensure deviations are plausible, as described in supplementary methods. For annual variation scenarios, variation was added to length at all ages ($I_a = 1, \forall a$). For inter-cohort variation scenarios, variation was only added at age a_{min} ($I_{amin} = 1, \forall a \neq a_{min}, I_a = 0$) and subsequent ages' length was calculated using Equation 2.6; this allows for the inter-cohort effect to persist throughout the fish's life.

2.2.5 *Scaling of growth deviations*

A number of additional corrections were made to ensure the variation was scaled by age and was realistic. The relative variation by age was scaled by the estimated true variability by age. For

example, in cases where variability in growth increases with age, m_a was scaled to linearly increase with age proportionally to the estimates of variability at age L_A and age L_{amin}, and when growth variability decreases with age, m_a was scaled to decrease with age. The r_a parameter scaled the impact of deviations by the relative growth rate of each age according to Equation 2.6.

To ensure animals did not shrink due to added growth deviations, negative growth deviations were constrained to be no smaller than the mean growth increment at that age ($\delta_{a,t} \geq \frac{-1}{\Delta L_{a,a+1}}, \forall a$). This has the effect of allowing animals to not increase in size in a given year. If any deviations (δ_t) violated this constraint, the entire time series was scaled down proportionally such that the maximum deviation satisfied the constraint.

2.2.6 *Simulation*

Each species was simulated for ten lifespans (Figure 2.1), where lifespan length was equivalent to the maximum population age (A_{max}). A total of nine scenarios per species were simulated: three alternative variation scenarios (i.e. recruitment variation only, growth variation only, recruitment and growth variation), and three age truncation rates. We hypothesized that age-truncation, i.e. due to selective fishing, would increase the importance of recruitment and decrease the importance of somatic growth. To test this, we introduced three fishing rates. The first was the fishing rate (fraction of vulnerable fish removed annually) producing maximum sustainable yield (F_{msy}), which was calculated numerically for each species (strong age-truncation). The second (0.5 F_{msy}) and third (1.5 F_{msy}) fishing rates were intended to explore a range of age-truncation. Each variation scenario across each species was simulated 500 times, and simulations began at equilibrium at the respective harvest rate. We measured population response as the coefficient of variation (CV) of annual mature fish biomass and production.

Though annual production is a ratio value, harvest ensures the mean of this metric is positive in our scenarios. All simulations were conducted in R version 3.2.1.

Comparison to alternative population models

To ensure output estimates of spawning stock biomass CV were in line with empirical estimates, we compared the output of alternative population dynamics models constructed for management purposes for Pacific halibut (Stewart et al. 2016) and hake (Berger et al. 2017). These species were chosen as these management models encompassed species captured in our analysis which employ empirical weight-at-age data. This empirical data provides a quantitative estimate of somatic growth variation obtained in a different method from the method used in this manuscript to simulate length-at-age variation. Alternative models were run using Bayesian Markov Chain Monte Carlo estimation within the Stock Synthesis 3 package (Methot and Wetzel 2013). Three alternative scenarios were run for each species: 1) without growth variation only (no empirical weight-at-age data), 2) without recruitment variation only (including empirical weight-at-age data but not estimating recruitment error), and 3) with both growth and recruitment variation. Each scenario was run for $12x10^6$ iterations, thinning every $2.4x10^3$ iteration.

2.3 RESULTS

2.3.1 *Empirical and simulated demographic variability*

The magnitude of deviations from mean recruitment and somatic growth rates varied across species. Pacific hake (Figure 2.2a) had the largest recruitment fluctuations, while petrale sole and Pacific hake (Figure 2.2 b,d) had relatively large magnitude growth fluctuations. Petrale sole are an example of a species where the magnitude of growth variability exceeded the magnitude of

recruitment variability (Figure 2.2 a,b). For most species, the magnitude of recruitment variation exceeded that of growth variation.

Simulated recruitment deviations were consistent in magnitude and frequency with empirical recruitment deviation estimates (Figure 2.3). Model selection suggested autocorrelated recruitment deviations provided the best fit for Northern rock sole, Pacific hake, Pacific halibut, and walleye pollock. Pacific hake recruitment deviations were negatively autocorrelated between years (Table 2.1), potentially indicating negative effects of juveniles on survival of subsequent year-classes. Pacific hake, walleye pollock, and widow rockfish had the largest magnitude estimated recruitment variation, while petrale sole, Pacific halibut, and Pacific cod had the smallest magnitude recruitment variation (Table 2.1).

The variability (CV) of simulated growth trajectories either increased or decreased with age, depending on the characteristic pattern of somatic growth variation (Figure 2.4). The CV of length in species whose growth variation was cohort-based (variation in initial size across birth years) (Northern rock sole, Pacific hake, walleye pollock) decreased as species aged. However, the CV of length of species whose growth variation was annual (all ages respond to an annual signal) increased with age, due to the compounding of annual growth changes over time.

2.3.2 *Importance of growth or recruitment variability*

The relative importance of growth and early life history on biomass variation varied across simulated species (Figure 2.5). Growth variation affected the output biomass CV of all species. As measured by the ratio of CV values under growth and recruitment variation (growth scenario biomass CV:recruitment scenario biomass CV), the biomass CV of two species were more strongly driven by growth (petrale sole: 2.09; canary rockfish: 1.46). Remaining species were more strongly driven by recruitment (Pacific hake: .48; Northern rock sole: .34, walleye pollock:

.42; widow rockfish: .62; Pacific halibut: .37) or relatively equally by recruitment and growth (Pacific cod: .97).

The relative strengths of recruitment and growth on population productivity followed similar patterns as biomass, although growth variation impacted productivity more than population abundance (Figure 2.6). Growth variation induced the greatest production fluctuations (growth CV:recruitment CV) for four out of eight species (Pacific cod [3.44], petrale sole [5.96], canary rockfish [4.40], Pacific halibut [1.96]). Walleye pollock (.40), Pacific hake (.36), and Northern rock sole (.34) experienced greater median CV in production due to recruitment (Figure 2.6). Widow rockfish showed a slightly stronger response to growth variation (1.23), but simulated intervals overlapped, suggesting that both processes were important.

2.3.3 *Interaction effect with age truncation*

For all species, greater age truncation introduced through increased fishing pressure magnified the effect of recruitment variation on the estimated biomass CV, but had variable effects on growth variation scenarios (Figure 2.5). For growth variation scenarios, output biomass variability decreased as harvest increased for petrale sole and widow rockfish, increased for Pacific halibut, Northern rock sole, and canary rockfish, and had little change for Pacific hake, Pacific cod, or walleye pollock (Figure 2.5). The effect of increasing age truncation on recruitment variation scenarios was most pronounced for widow and canary rockfish, two of the longest-lived species in this analysis. The effect of age truncation was the least pronounced in recruitment scenarios for Pacific halibut (Figure 2.5). Counter to our expectation, increased age truncation either decreased (petrale sole, walleye pollock, both rockfish species, Pacific cod) or did not affect (Pacific hake, Northern rock sole) the estimated annual production CV across all variability scenarios (Figure 2.6).

2.3.4 *Comparison to alternative population models*

We found the ratio of the coefficient of variation of mature biomass under growth variation compared to the CV of mature biomass under recruitment variation was 1.670 for Pacific halibut and .183 for Pacific hake. When compared with the simulation model, the alternative population model yielded a higher estimate of mature biomass CV under both scenarios for halibut (growth only: 0.532; recruitment only: 0.318), and a lower estimate of mature biomass CV under both scenarios for hake (growth only: 0.065; recruitment only: 0.355).

2.3.5 *Relation to life history characteristics*

The relative importance of growth and recruitment depended more on growth and recruitment time series than life history characteristics. We express life history diversity along the two axes suggested in Charnov et al. (2013), in which A (referred to as "catabolic coefficient": a function of the consumption rate of a fish at maturation) is plotted against M, natural mortality. This scheme collapses a number of correlated life history traits into two dimensions. Based on this life history characterization, we found no clear pattern between life history strategy and relative importance of growth vs. recruitment (Figure 2.7a). Contrary to our hypothesis, species with larger terminal body size were not more sensitive to growth variation across both output CV metrics. Instead, species with low or zero growth autocorrelation (ρ_g) were more strongly influenced by growth variation, while increased sensitivity to early life history variation corresponded with inter-cohort effects in growth and high recruitment variance (σ_r^2) (Figure 2.7b). Growth variation was not consistently more important in species with larger growth variance (σ_g^2). However, some species with large growth variance, such as Pacific hake, also had very large recruitment variation (Figure 2.2).

2.4 DISCUSSION

Here we explored which types of demographic variation govern population variability in marine teleosts, a taxon exhibiting a variety of life history strategies. We found that somatic growth variability has at least as much influence as reproductive variability on population dynamics for some species. This finding is counter to the commonly-held paradigm that marine population variability is caused primarily by reproductive variability (Hjort 1914). Our results suggest that the relative effect of different types of demographic variation on population variability differs across species. Unexpectedly, we did not find strong correlations between life history parameter values and the importance of growth or recruitment. Rather the magnitude and autocorrelation of variation time series were more influential towards how each process drives productivity. Age truncation did not alter which process was more influential; however, increased age truncation made population variability track recruitment time series more closely, while not increasing the effect of growth variation.

We demonstrate here a direct effect of somatic growth variation on population production, but note that somatic growth variation can have other indirect effects on populations. In mammals, the effect of size and growth on population is usually manifest through changes in fecundity related to reduced female body condition (Solberg et al. 1999). In marine fish, biomass can also lead to enhanced egg production, but in general egg production is not highly correlated to reproductive success (Szuwalski et al. 2015). However, high growth rates can promote maternal effects (i.e. larger maternal size) that enhance offspring survival (Hendry et al. 2001, Hixon et al. 2014), though effects at the population scale are not clear (O'Farrell and Botsford 2006). Therefore, it may be important to consider interaction effects between somatic growth and reproductive variability.

Contrary to our hypotheses, and findings of other studies (Sæther and Bakke 2000, Williams et al. 2010), we did not see a clear relationship between life history traits and which type of variation was more influential. A large body of theory suggests the level of environmental disturbance a population experiences shapes the evolution of life history traits (Winemiller and Rose 1992), which then influence how populations respond to disturbance (Denney et al. 2002). However, we saw that time-series characteristics (autocorrelation between growth deviations, variance of recruitment deviations) also determined which process was more influential in production dynamics. As an example, as classified in Charnov et al. (2013), if natural mortality rate is assumed to be inversely proportional to lifespan, species with higher mortality rates would also have higher lifetime reproductive output. Two species within the same family, Pacific cod and walleye pollock, share relatively low survivorship, and therefore, we might expect both species to exhibit more sensitivity to recruitment variation, due to this increased lifetime reproductive output. However, while walleye pollock responded more strongly to recruitment variation, Pacific cod was most strongly affected by growth variation. Examination of a species selection spanning a larger range of life history trait values could provide further insight on if which type of variation is more influential correlates with life history traits.

We expect the finding that somatic growth variation can affect production as much as recruitment variation to be generalizable to across marine teleosts in marine and freshwater environments. Although our analysis was restricted to eight populations, we chose species spanning life history trait values and magnitudes of growth and recruitment variation. Moreover, we did not explicitly consider density-dependent growth, which would likely dampen the effect of recruitment variation. For example, if density-dependence in growth was included, we would

expect the effect of years of high reproductive success to be lessened, since increased competition between these juveniles would reduce growth rates. Lorenzen (2008) showed that density-dependent growth may regulate some teleost species more than density-dependence in recruitment. Here, our results suggest that growth and recruitment rates which fluctuate independently of population biomass can have similar effects on population biomass and production: i.e. that some species are more sensitive to changes in growth while others are more sensitive to recruitment. Finally, we confirmed that somatic growth can influence biomass and production variability as much as recruitment variability through sensitivity tests to alternative harvest rates and comparison with alternative population dynamics model output.

Our finding, that age structure truncation consistently increased biomass variation but not production variation, is consistent with our hypothesis. The storage effect theory, that complete age structure buffers a population's resilience to recruitment variation (Warner and Chesson 1985), is supported by our observation that the impact of recruitment variability increased with age truncation. This is also consistent with our observation that the impact of growth variation did not consistently increase with age truncation. The impacts of growth variation on populations might be mediated by harvest-induced age structure truncation in different ways. For example, the effect of growth variation could be reduced the more age structure is truncated, because the individuals who would be subject to the largest variation in somatic growth rate are removed from the population. Conversely, since harvest targets larger individuals, changes in size impact mortality rates, and therefore age truncation induced by harvest might exacerbate the effect of growth rate variation.

The finding that somatic growth variation can induce population fluctuations supports the recent focus on incorporating ecosystem considerations into studies of the population ecology,

including population models and management, of both marine (Gaichas et al. 2010) and terrestrial environments (DeFries et al. 2004). That is, ecosystem models predict production dynamics largely based on fluctuations on prey and predator populations. If empirical productivity was unrelated to growth and determined solely by early life history events, then the predicted dynamics from these models would have little bearing on the real world. The empirical growth variation patterns we document in this study likely depend, in part, on changes in prey availability (Bjorndal et al. 2000, Rose and O'Driscoll 2002). Thus our finding, that growth variation may subsequently introduce corresponding fluctuations in biomass and production, confirms the underlying assumptions of ecosystem models (Fulton et al. 2011, Hartvig et al. 2011), which link somatic and/or population growth of predators to prey biomass and prey mortality rates to predator biomass.

TABLES

Table 2.1 - Species life-history parameters: female natural mortality (M), length-weight coefficient (α), length-weight exponent (β), stock-recruit model (SR) (BH denotes Beverton-Holt, R denotes Ricker, and C denotes constant mean recruitment), parameters of the S-R relationship: for Beverton-Holt: steepness (h), log of unfished recruitment ($Ln(R_0)$), a and b if Ricker or standard Beverton-Holt is used, recruitment deviation autocorrelation (ρ_r) and variance (σ_r^2) estimate for each species.

	canary rockfish	**Northern rock sole**	**Pacific cod**	**Pacific hake**	**Pacific halibut**	**petrale sole**	**walleye pollock**	**widow rockfish**
M	0.09	0.15	0.38	0.21	0.15	0.15	0.3	0.12
a_{min}-a_{max}	1-40	1-20	1-14	1-20	3-30	2-17	1-15	1-36
select.	length	age	length	age	length	length	age	length
α	$1.6x10^{-5}$	$6.2x10^{-3}$	$8.8x10^{-6}$	$6.5x10^{-6}$	$6.8x10^{-6}$	$2.1x10^{-6}$	$6.6x10^{-6}$	$5.5x10^{-6}$
β	3.03	3.12	3.07	2.99	3.11	3.47	3.02	3.29
Early life history parameters								
SR	BH	BH*	C*	BH	C*	BH	R*	BH
h	0.51	-	-	0.87	-	0.86	-	0.76
$ln(R_0)$	8.12	-	-	21.59	-	9.72	-	10.06
a	-	195.22	-	-	-	-	49.03	-
b	-	$1.59x10^{-5}$	-	-	-	-	$7.03x10^{-7}$	-
$\bar{R}$	-	-	$5.18x10^5$	-	$3.14x10^4$	-	-	-
Growth parameters								
Mode	ann.	i.s.	ann.	i.s.	ann.	ann.	i.s.	ann.
L_1(cm)	8.04	12.85	30.97	20.8	43.67	15.88	26.38	15.34
L_2(cm)	60.36	40.03	100.67	49.42	142.02	56.24	61.71	42.57
k	0.13	0.18	0.13	0.38	0.06	0.13	0.21	0.2
CV_1	0.12	0.06	0.05	0.07	0.18	0.18	0.1	0.11
CV_2	0.04	0.17	0.16	0.06	0.15	0.03	0.11	0.05
a_{min}-A_c	1-20	3-20	2-14	1-20	3-25	2-17	2-15	2-30
Early life history (r) and growth (g) time series properties								
ρ_r	0	0.67	0	-0.37	0.73	0	0.37	0
σ_r^2	0.43	0.6	0.29	1.31	0.37	0.33	0.65	0.66
ρ_g	0	0.74	0	0.86	0	0.27	0.67	0.38
σ_g^2	0.4	3.71	1.01	1.04	0.47	0.64	0.53	0.26

* denotes stock-recruit curve fit by Stachura et al. (2014)

Table 2.2 – Equations used in modeling

Number	Equation	Description
1	$R_t = \frac{.8hR_0B_t}{.2\phi_0R_0(1-h)+(h-.2)B_t}$ or $R_t = \frac{\alpha B_t}{1+\beta B_t}$	Beverton-holt stock recruit function
2	$R_t = \begin{cases} \bar{R}; & B_t > .1\bar{R} \\ 0; & B_t \leq .1\bar{R} \end{cases}$	Knife-edged stock recruit relationship
3	$R_t = f(B_t)\exp(\gamma_t)$, $\gamma_t = \rho_r\gamma_{t-1} + \sqrt{1-\rho_r^2}\epsilon_t$, $\epsilon_t \sim N(\log\left(-\frac{\sigma_r^2}{2}\right), \sigma_r^2)$	Lognormal recruitment variation
4	$L_{min} + ba, \quad a < a_{min}$	Juvenile growth ($a<a_{min}$)
5	$\overline{L_a} = L_\infty + (L_{amin} - L_\infty)\exp(-k[a - a_{min}])$ $L_\infty = L_{amin} + \frac{L_A - L_{amin}}{1-\exp(-k(A-a_3))}$	Adult growth ($a_{min}<a<A$)
6	$L_{a,t} = L_{a-1,t-1} + \overline{\Delta L_{a,a+1}}(1 + I_a\delta_t r_a m_a)$	Growth deviation
7	$r_a = 1 + (.5 - 1) * \exp\left(-k(a - a_3)\right);\ A_c > a > a_3$	Growth variation scaling
8	$N_{a+1,t+1} = N_{a,t}\exp(-M + s_{a,t} * F_t)$	Survivorship from age a to $a+1$
9	$E_t = \sum_{a>amat} mat_a N_{a,t} w_{a,t}$	Egg production
10	$w_{a,t} = aL_{a,t}^b$	Weight-length relationship

Figures

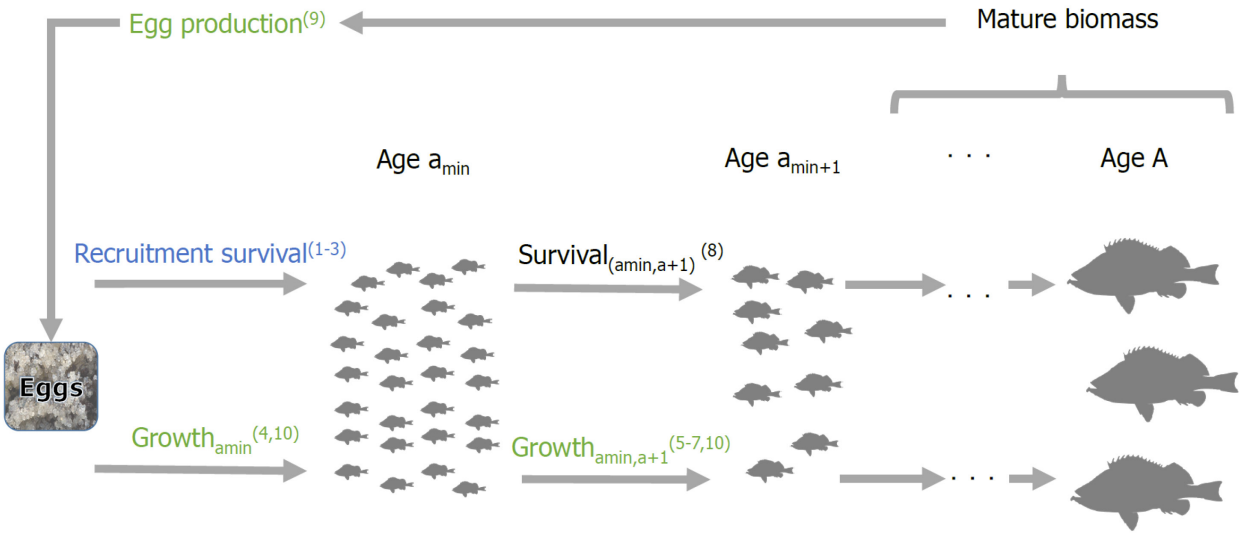

Figure 2.1 - Schematic for population model. Superscript numbers in parentheses refer to the equation used to model the associated process. Items denoted in green represent processes which become variable as a result of introduced growth variation. Items in blue represent processes which become variable as a result of introduced recruitment variation.

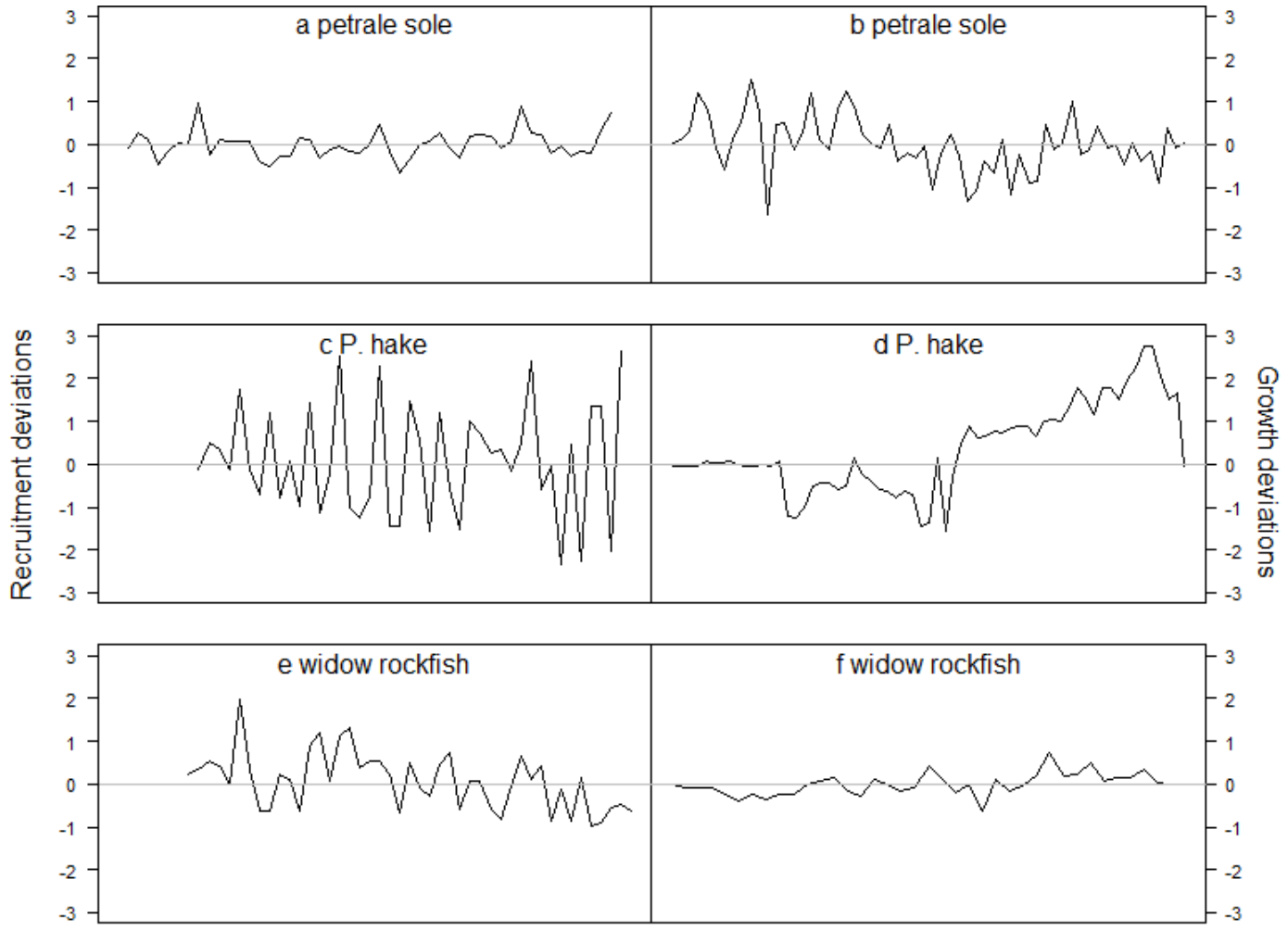

Figure 2.2 - Empirical estimates of recruitment (a,c,e) and growth (b.d.f) scenarios for petrale sole, Pacific hake, and widow rockfish.

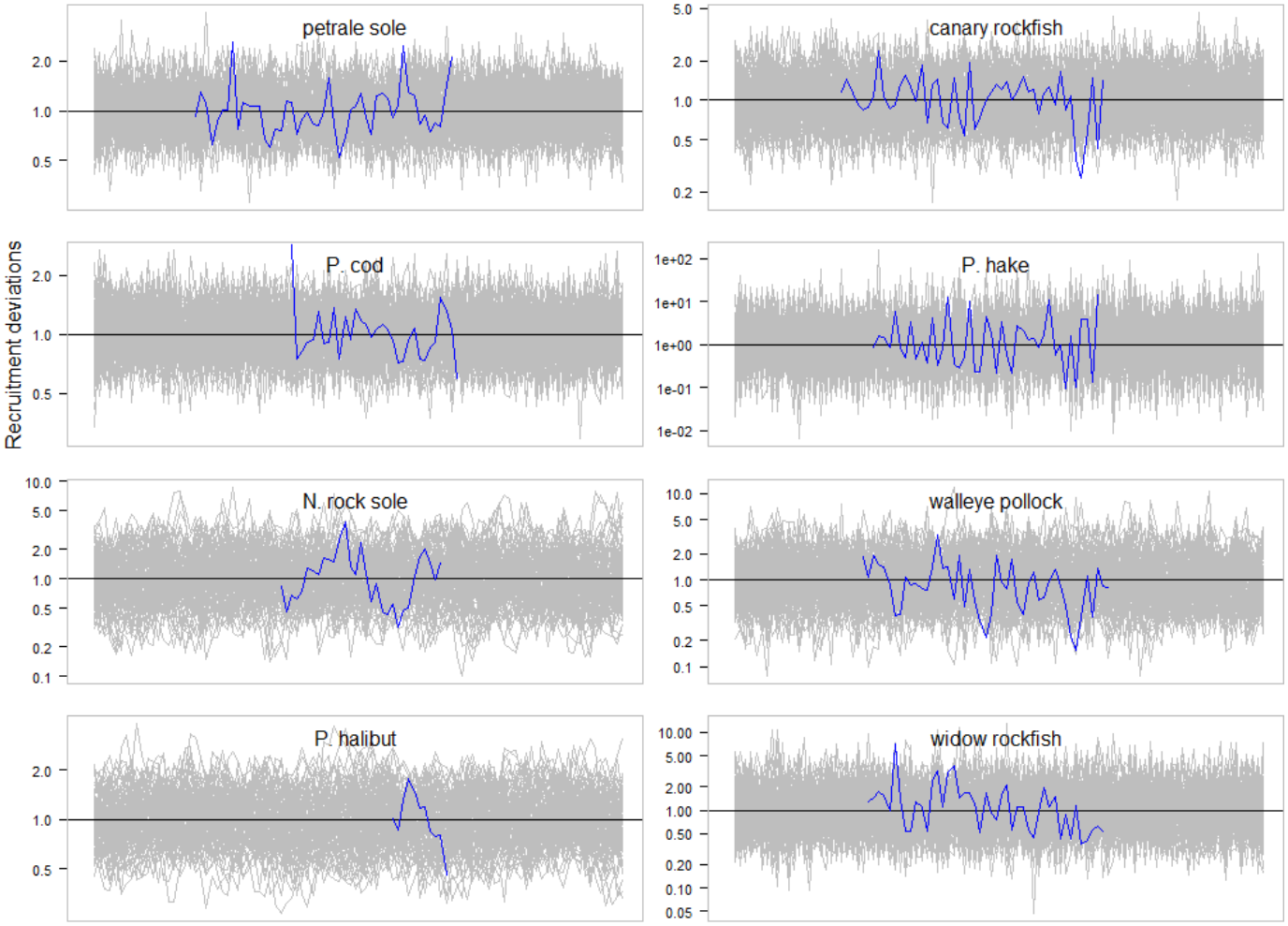

Figure 2.3 - Comparison of simulated recruitment deviations (gray) to empirical recruitment estimates (blue).

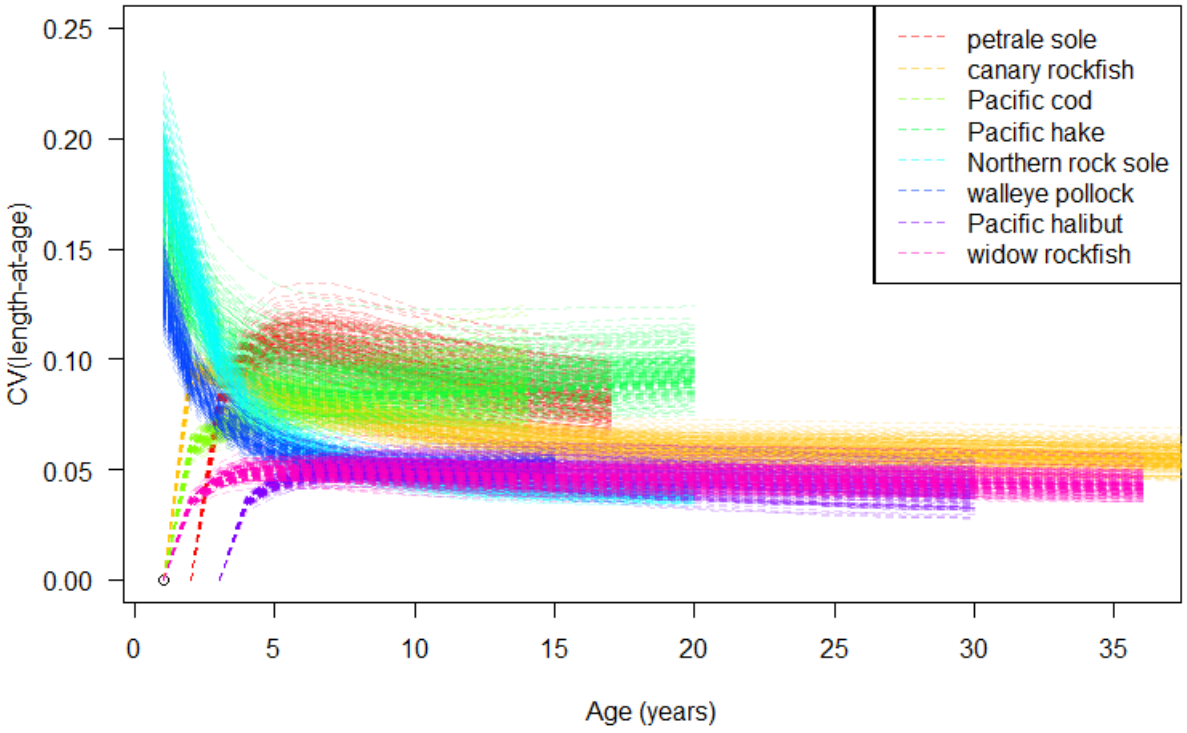

Figure 2.4 - CV of simulated length-at-age for each species modeled. Color represents species, where each line is one simulation.

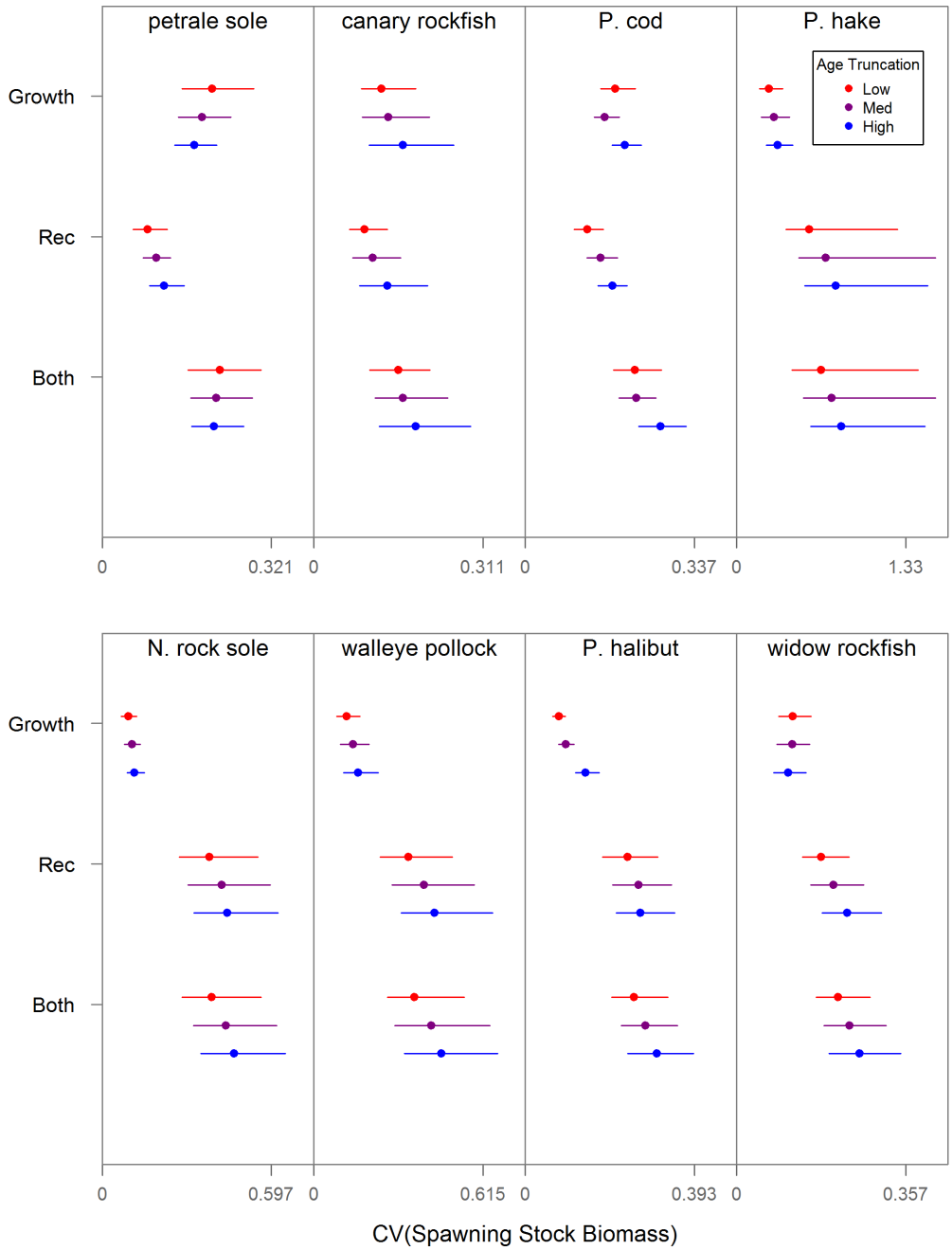

Figure 2.5 - 95% quantiles (lines) and medians (points) of mature biomass CV across three levels of age truncation. “Growth” denotes scenarios with growth variation only, “Rec” denotes scenarios with recruitment variation only, and “Both” denotes scenarios with both types of variation.

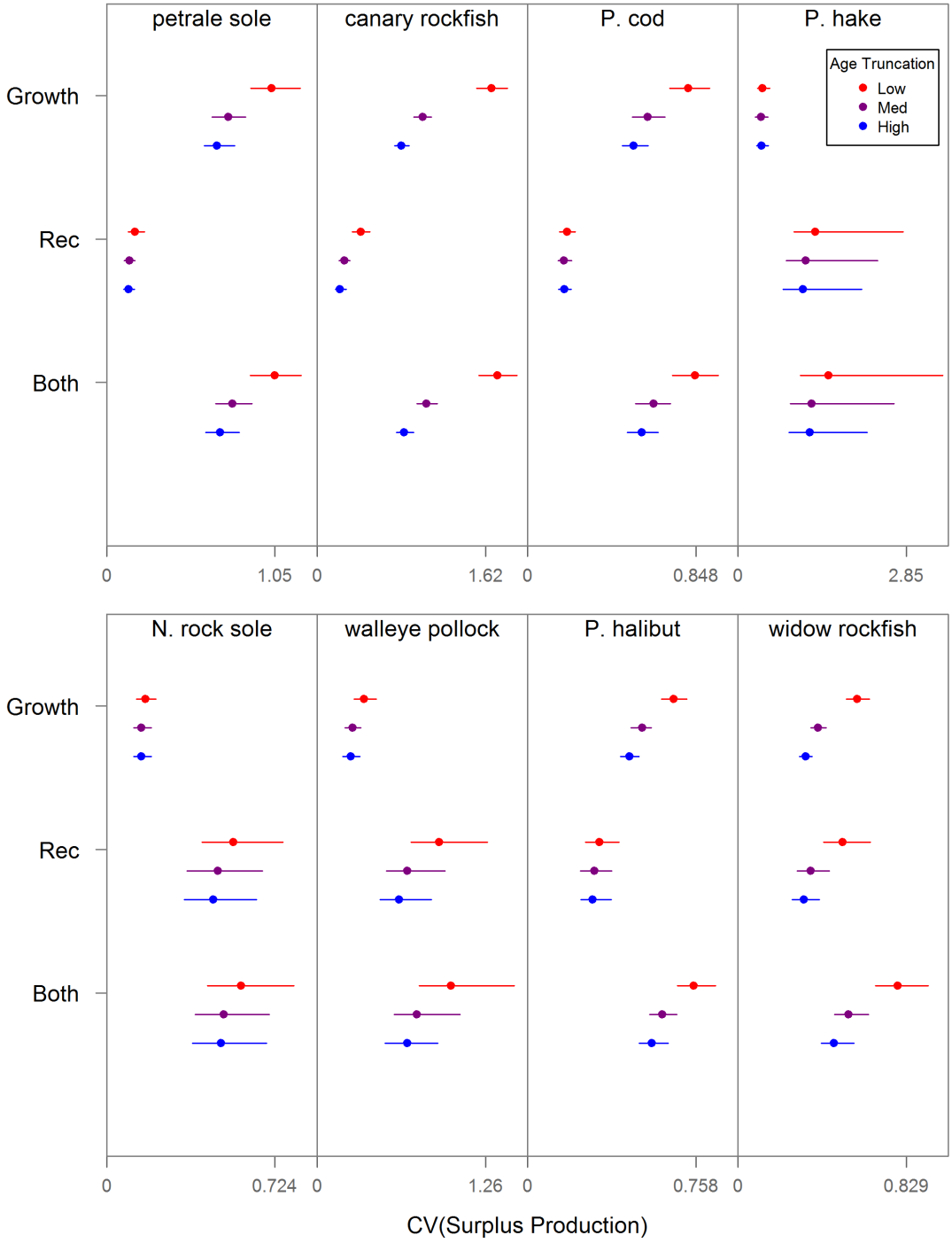

Figure 2.6 – 95% quantiles (lines) and medians (points) of the coefficient of variation of annual production from output scenarios. “Growth” denotes scenarios with growth variation only, “Rec” denotes scenarios with recruitment variation only, and “Both” denotes scenarios with both types of variation.

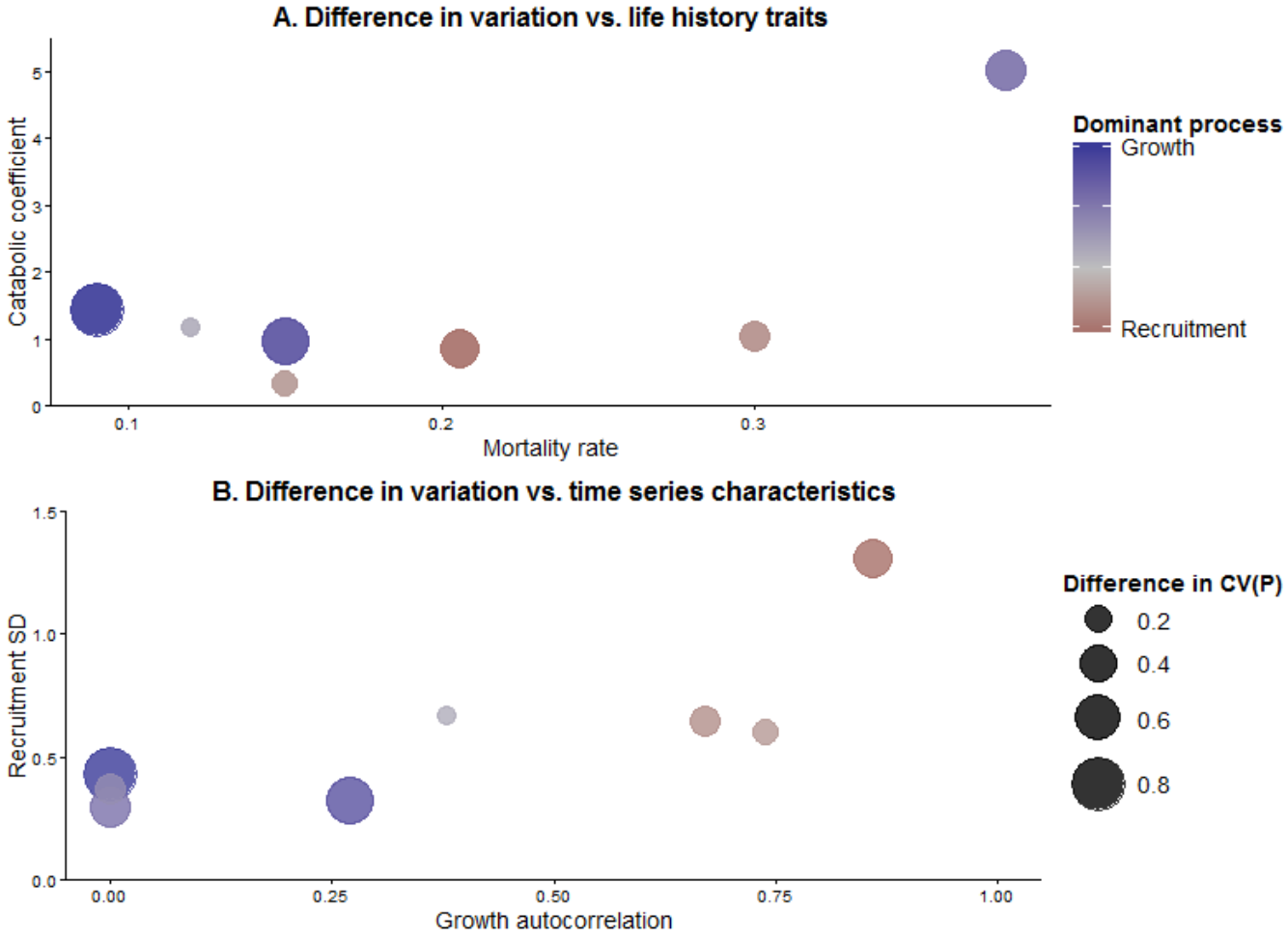

Figure 2.7 - Colors and bubble size indicate relative dominance of growth (purple) or recruitment (red) variation (as measured by the difference of the median output CVs of annual production), against (a) the catabolic coefficient (A) compared with mortality rate (M) and (b) the standard deviation of recruitment deviations compared with autocorrelation of growth deviations.

Chapter 3. How does growth misspecification affect management advice derived from integrated fisheries stock assessment models?

ABSTRACT

Analysts make many decisions regarding model specification when fitting integrated fishery stock assessment models. While variation in vital rates (i.e. recruitment, somatic growth, and natural mortality) is common, capturing this variation in stock assessment models fit to available data is often infeasible or impractical. Here we seek to determine how growth misspecification affects management advice derived from integrated stock assessment models that use the Stock Synthesis 3 (SS3) platform. We conduct a simulation-based case study on California Current petrale sole (*Eopsetta jordani*) to test how alternative patterns of somatic-growth variation may introduce bias into management reference points when estimation stock assessment models misspecify growth. Scenarios included inter-annual and block (regime-like) changes in two key parameters (k and L_2) used to model somatic growth in SS3. We find estimation models that ignore growth variation when size-at-age is decreasing can underestimate uncertainty in and overestimate stock status (i.e. depletion is positively biased). This bias may be mitigated or eliminated if the assessment model includes time varying growth. However, biases can be difficult to detect when data are limited, suggesting that attempts to estimate growth variation in stock assessment models may only be successful in relatively data-rich cases. We recommend that authors of data-rich assessments consider incorporating time-varying growth parameters into assessment models or decision tables more frequently to account for potential biases and uncertainty.

3.1 INTRODUCTION

Integrated fishery stock assessment models are the state-of-the-art tools used to generate management advice for marine fisheries (Maunder and Punt 2013). These complex models jointly estimate uncertainty in biological processes and can account for bias and measurement error in data (Methot 1990). However, although the ability to estimate large numbers of parameters simultaneously within such models is advantageous for capturing complexity, it requires stock assessment analysts to make many modeling choices based on the best scientific information available. Such choices include how to specify process variation in key biological rates (i.e. recruitment, somatic growth, and mortality). Despite evidence that vital rates vary across space, time, or age class (Clark et al. 1999, Gaichas et al. 2010, Whitten et al. 2013), in practice data are often too limited to accurately estimate variation in all three rates (Ono et al. 2014). As such, quantifying if and how misspecification of variation in vital rates increases bias and reduces precision of estimated management reference points is necessary. Historically, temporal variation in somatic growth rates has not been included in many assessment models, and consequences of this omission are not fully understood.

Population size-at-age of marine fish across time or population segment may vary for two main reasons. First, biological drivers that introduce variation into feeding and/or metabolic rates may induce growth variation; second, size selective fishing that selectively removes larger, faster-growing individuals from the sampled population, may reduce population size-at-age. Feeding and metabolic rates may increase or decrease in synchrony due to changes in temperature (Cheung et al. 2012), or feeding rates alone may vary because of changing food supply driven by density-independent (i.e. bottom-up changes in prey biomass) (Black 2009) or density-dependent causes (i.e. inter- or intra- species competition) (Rijnsdorp and van Leeuwen

1992). Beyond biological drivers of growth, sampled size-at-age may change due to removal of the largest, fastest-growing individuals from each cohort as fishing pressure increases, resulting in temporal patterns of size-at-age corresponding to fishing effort (Hilborn and Minte-Vera 2008). Either type of variation may affect size of all age classes in a temporal period, or be manifest in specific cohorts (Stawitz et al. 2015a). In this study, we focus on changes in growth occurring temporally across age classes, but do not limit our analysis to one cause of variation in population size-at-age. Although fishery selectivity may change temporally, introducing biased patterns of size-at-age variation in the data that do not reflect actual population size-at-age (Thorson and Simpfendorfer 2009), we did not examine the effect of this effect in this study.

Assuming a constant growth rate when size-at-age varies temporally can cause biased population estimates and management advice (Helser and Brodziak 1998, Walters and Wilderbuer 2000). Density-dependence induces inverse correlation between population size and somatic growth rates, and ignoring these effects leads to overestimating the population growth rate and therefore how quickly stocks can rebuild to sustainable levels (Helser and Brodziak 1998, Gårdmark et al. 2006). Kuriyama et al. (2016) demonstrated that spawning stock biomass estimated in an integrated assessment model may be significantly biased (up to 30%) in the same direction as size-at-age variation if it is not specified correctly or captured using empirical weight-at-age data. These studies imply management recommendations may be improved by incorporating growth variation in stock assessment models. However, these studies examine the impact of growth variation under simulated patterns of high contrast fishing and growth variation, making detection of such changes easier than is often the case in assessment models used for management. The question remains whether incorporating empirical estimates of growth variation into complex integrated assessment models can provide the same benefits.

Including growth variation either empirically or mechanistically in population models can improve model fits and estimation of process uncertainty. The version of the von Bertalanffy growth curve (Bertalanffy 1957) used in the Stock Synthesis 3 (SS3) program (Schnute 1981) is governed by three parameters: L_2, the mean size at maximum age, L_1, the mean size at minimum adult age, and k, the exponential rate of approach to L_2 (Ricker 1975). Growth variation may be incorporated into stock assessments by estimating different fixed or random effects on these parameters, or by using an empirical weight-at-age table to convert age to mass (Helser et al. 2004). Stock assessments for Pacific hake including growth variation have resulted in improved fits to length composition data (Berger et al. 2017). When conducting the stock assessment model for walleye pollock (*Gadus chalcogrammus*), Ianelli et al. (2016) found including annual random effects on growth increment improved model prediction performance and provided a more realistic estimate of process uncertainty to use in population projections. Though empirical weight-at-age data may reduce bias compared to fixed or random effects incorporated into the growth model (Kuriyama et al. 2016), this approach is only feasible when a very large amount of unbiased weight-at-age data can be collected. Additionally, use of sampled weight-at-age does not account for sampling bias (i.e. due to selectivity), offer insight into mechanistic causes for growth variation, or allow for forecasting future implications for growth variation on management recommendations.

Here we build upon previous theoretical work outlining the importance of including growth variation in population models to provide practical advice for stock assessment analysts on when and how to include growth variation. We explore how growth variation may affect a practical fisheries stock assessment, that of California Current Petrale sole (*Eopsetta jordani*), and explore whether realistic rates of growth variation are detectable and how they impact

management recommendations. This species represents an ideal test case, as Petrale sole have been shown to experience growth variation (Stawitz et al. 2015a) and have a large repository of size-at-age data. We determine whether several different types of empirically-derived patterns of growth variation lead to biased or imprecise management advice under historical fishing rates. We explore the effect of both regime-like (block) changes and inter-annual variation in the k and L_2 growth parameters on estimates of management reference quantities. By comparing bias and precision of management quantities across correctly and incorrectly specific growth model scenarios, we can provide guidelines for stock assessment analysts regarding the feasibility and utility of incorporating growth variation into stock assessment models.

3.2 METHODS

In this study, we used simulation analysis to explore how growth variation and misspecification of growth parameter values affects estimates of biological reference points. Our goal was to use the most realistic estimates of growth variation possible; therefore, we began by fitting simplified versions of the integrated stock assessment model used in management of California Current petrale sole to empirical data. We used the Stock Synthesis (SS3) software (Methot and Wetzel 2013), which is a program used to conduct a large number of fisheries stock assessments. Outputs from this model were used to parameterize key life history trait values and five different growth variation specifications. Data simulated from operating models were used to fit estimation models across 30 scenarios using the ss3sim R package (Anderson et al. 2014), ensuring results are highly applicable to models used in fisheries management. Finally, we compared estimated median relative errors and 95% quantiles of scalar management quantities, including spawning stock biomass at maximum sustainable yield (SSB_{msy}), stock depletion, the

estimated spawning stock biomass without fishing (unfished biomass), and time series estimates of spawning stock biomass, between simulation cases to test how misspecification of the somatic growth model affects management recommendations from an integrated stock assessment model.

3.2.1 *Model adaptation*

We started with the most recent petrale sole stock assessment model (Stawitz et al. 2015b) in order to ensure biological realism, but greatly simplified the model to ensure results could be clearly interpreted and to speed runtime to allow for many iterations. We first fixed two key biological parameters: natural mortality (M) and the steepness of the stock-recruit relationship (h), at model estimated values to reduce the number of parameters estimated in the model. This enables the estimation model to better estimate growth parameters, which can be confounded with h and M. We also fixed parameters modeling extra variance on survey catch-per-unit-effort at zero. We simplified the fishery fleet dynamics to a single winter fleet and a single summer fleet (instead of spatially-distinct North and South fleets for each season), aggregating catches across the two winter and two summer fisheries and removing length- and age-composition data for the South fleets. Next, we removed time blocks of fishery selectivity, instead specifying a single fishery selectivity curve for each fishery and scientific survey. We then fixed parameters of each of these selectivity curves at estimated values. Next, we removed data on discarded fish and fish mean weight, as these are relatively limited data sets that minimally impact the model. We also removed catch-per-unit-effort indices for the winter fishery from model fitting, fitting the model instead only to indices of abundance estimated from scientific survey data. Finally, we altered the timing of when fish were removed in scientific surveys and fisheries to occur at the midpoint of each year. At each step of simplification, we compared time series plots and

confidence intervals of biomass estimates between simplified models and full assessment models to ensure species dynamics were still captured in our simplified model (Figure 3.1).

3.2.2 *Specification of operation model growth parameters*

Estimates from the simplified model described above fit to empirical data were used as input life history parameters (i.e. growth, reproduction, growth variation). We chose to use the simplified integrated stock assessment model to obtain growth variation estimates as this integrated model simultaneously models two components that may affect estimates of growth: selectivity curves and harvest rate. Not accounting for gear selectivity can potentially bias growth curve estimates towards faster-growing young fish (Thorson and Simpfendorfer 2009). Additionally, application of consistent harvest pressure can gradually reduce the size of the oldest fish (i.e. those in the "plus group") remaining in the population (Methot and Wetzel 2013). These effects are explicitly accounted for in SS3. These outputs were estimated from empirical data from male and female fish collected during two seasonal fisheries (summer and winter) and three surveys (Alaska Fisheries Science Center early triennial survey, 1980-1992 and late triennial survey, 1995-2004; Northwest Fisheries Science Center annual groundfish trawl survey: 2003-2014). Length- and age-composition data from the North fishery and all survey data, including conditional age-at-length compositions from the annual groundfish trawl survey (Figure 3.2), were used to obtain growth variation parameter estimates. Distinct male and female growth parameters (L_1, L_2, k) of the Schnute (1981) growth curve (Equation 3.1) were estimated within the stock assessment model (Methot & Wetzel 2013) due to substantial sexual dimorphism in growth.

$$L_a = L_2 - (L_1 + L_2) + L_2(1 - \exp(-k(a_4 - a_3))) \quad (3.1)$$

L_a represents the length of a fish of age a, a_3 is the youngest age of adult fish well-sampled in the data, and a_4 is the oldest age of adult fish well-sampled in the data. This model represented the base model, from which biological parameters were estimated across ten alternative cases.

To obtain parameter values for simulation, we estimated time-varying growth in four ways within the integrated assessment model: an environmental index effect on L_2, the growth parameter representing average length at the oldest age well-sampled in the data, an additive time block effect on L_2, an environmental index effect on k, the growth parameter representing the slope of the adult growth curve, and an additive time block effect on k. We include a time block effect, because we hypothesize environmental deviates on growth alone might underestimate how much growth variation can bias model outputs. Environmental deviates are generally constrained to be centered on a mean value, while blocks can capture the potentially more influential effect of a monotonic increase or decrease in parameter values.

We hypothesized that three different processes might induce block-like changes in growth, so we used model selection within SS3 to determine which of three sets of time block periods were best supported by the data. The first two processes were the positive and negative phases of two well-known oceanographic phenomena influencing Northeastern Pacific ecosystems, the El-Niño Southern Oscillation (ENSO) (Wolter and Timlin 1993, 1998), and the Pacific Decadal Oscillation (PDO) (Mantua and Hare 2002). The final process was based on changes in harvest pressure (as measured by fishing mortality, F) that may also affect observed size-at-age by removing larger individuals disproportionately (Hilborn & Minte-Vera 2008). To estimate years for growth parameter blocks for ENSO and fishing mortality, we constructed regression trees using recursive partitioning on their respective time series (ENSO index and F) as implemented in the rpart R package (Breiman et al. 1984). Blocks for shifts in the PDO are

taken from those estimated in Field (2007), which estimated block shifts for the *k* growth parameter of chilipepper rockfish along the U.S. Pacific coast. Mean L_2 parameter values were unique to each sex, but time periods for blocks were shared, since there was no evidence for sex-specific time periods of growth variation. Methods for fitting both types of variation within SS3 are detailed in Methot and Wetzel (2013). We compared the likelihoods estimated within SS3 for each of the three chosen block time periods, for both the *k* and L_2 growth parameters. We choose the time block period based on the PDO for L_2 and the time block period based on fishing rate for *k* to use in our operating models, since these were best supported by the data (Table 3.2).

3.2.3 *Simulation framework*

Data were simulated using the ss3sim R package (Anderson et al. 2014). This software uses SS3 to generate expected values for age and length composition data, catch, and abundance, from user-supplied parameter inputs. These expected values, along with user-supplied process and observation errors, are used by ss3sim to generate replicate data. Fishing mortality rates for the two fisheries estimated in the base model are used in the operating model to ensure simulations reflect reality. When simulations were run, estimated parameters were given initial values corresponding to the "true" operating model values, except in cases where otherwise specified. Parameter values used in simulation are given in Table 3.1. The simulation begins in 1876; although the Petrale sole fishery spans 1876 to 2014, only the final 49 years of data were used to simulate and estimate results, as age composition data were not available prior to 1965.

Process error was introduced both via simulated deviations from mean recruitment and simulated block (regime-like) and random walk deviates (inter-annual variation) from mean values of the somatic growth parameters. Observation error was included both around fishery-independent indices of abundance and through limiting age- and length-composition data sample

size. We simulated variation corresponding to a CV of 0.2 for the index of abundance from triennial survey data for both data cases. For the annual trawl survey, which spanned the final 14 years of the time series (Figure 3.2), a CV of 0.1 was used for the data-rich case, and a CV of 0.2 was used for the data-poor case. Both data-rich and data-poor cases included 49 years of commercial composition data. Simulations included samples of 100 fish ages and lengths in each year from fishery data, and 500 samples of ages and lengths of fish per year in the data-rich case. In the data-poor case, 20 samples of age- and length-composition data were included for each year, from all sources. The estimation routine used SS3 to fit models; starting values were initialized at the "true" OM values.

Growth variation cases represented five levels each of "true" (i.e. operating model generated) and estimated growth variation. In the null growth variation case, male and female growth parameters were held constant over time. In the inter-annual L_2 variation case, estimated annual deviations from the expected value of L_2 in the simplified assessment model described above were used to simulate data (Figure 3.3). In the block L_2 variation case, estimated additive block offsets from the expected value of L_2, according to year blocks derived from Field (2007), were used to simulate data. A similar simulation procedure was used across time-varying scenarios for the k parameter, except the span of simulated annual blocks were based on fishing rate blocks (Figure 3.3). These same three growth variation scenarios were used within the estimation routine to estimate if simulated growth variation could be detected. Each scenario combination was run 100 times.

3.2.4 *Response metrics and convergence criteria*

To evaluate performance of models under different scenarios, we examined the relative error and uncertainty of estimated biological reference points. Biological reference points evaluated

included the spawning stock biomass at maximum sustainable yield, final year stock depletion (current spawning biomass relative to unfished spawning biomass), and unfished spawning stock biomass. Bias was calculated as the relative error (standardized difference between operating model (θ) and estimation model ($\hat{\theta}$) values, RE= $[\hat{\theta}-\theta]/\theta$) in each parameter or derived quantity θ over each scenario. We also calculated the uncertainty of estimated reference points in the estimation model as the width of the 95% quantile of the three estimated management reference points. Finally, we examined time series of bias in estimated spawning stock biomass, because the magnitude of observed bias in scalar quantities might be smaller than point estimates of bias in one year or block of years.

As in Monnahan et al. (2016), we recognize that fisheries stock assessments typically undergo multiple convergence checks, which are impractical at the scale of this simulation. Therefore, we include results derived from simulations with a maximum gradient less than 0.1 with no parameters stuck on bounds. We report the percent of simulations converged out of the 100 total simulation runs per scenario and only report summary metrics for runs that meet the convergence criteria.

3.3 Results

The accuracy and uncertainty of stock depletion and spawning stock biomass at maximum sustainable yield (SSB_{MSY}) estimates depended on if growth was correctly specified in the estimation model (EM), while estimated unfished biomass was not affected by growth misspecification. Particularly, when operating model (OM) growth parameters (k or L_2) varied in block patterns, but the estimation model assumed constant growth, positive bias of up to 11% was apparent in estimates of stock depletion and spawning stock biomass at maximum

sustainable yield. If regime-like shifts in growth parameters in the operating models were fit by estimation models containing either regime-like shifts or inter-annual variation, bias was reduced to less than 5%. If growth parameters were held constant in the operating model, but estimated as time-varying, results were very like those from an estimation model that assumed constant size-at-age. Estimates of unfished biomass were not sensitive to growth variation. Any type of introduced growth variation reduced the precision of estimated stock depletion, but only slightly reduced the precision of estimated SSB_{MSY}. Finally, regime-like changes in the k parameter could only be estimated when all other growth parameters were fixed at constant values.

3.3.1 *Bias in management quantities in data-rich case*

Biases (as measured by median absolute relative error) in estimated management quantities were largest either when k varied inter-annually or when L_2 varied in regime blocks (Figure 3.4) and a constant estimation model was used. Bias in stock depletion was highest when L_2 changed in blocks (11.11%), and this was the only scenario for which positive bias was consistent across runs (i.e. the 95% quantile of relative error did not span zero). Estimated depletion was slightly positively biased when k varied inter-annually (5.38%) in the operating model, but was estimated as constant. Estimated SSB_{MSY} was also the most biased in these two scenarios. This quantity was negatively biased when k varied in a block pattern (-9%) and positively biased when L_2 varied in blocks (8%), but was estimated with a constant operating model.

Conversely, other scenarios including operating model growth variation and a constant estimation model showed relatively little bias in estimated management quantities. When L_2 varied inter-annually, stock depletion estimates were unbiased (-2%). When k had block-like variation in the operating model, but a constant estimation model was used, estimated depletion was only slightly biased (4%). Estimated SSB_{MSY} was slightly biased when L_2 varied inter-

annually (5%), but bias in estimates across other inter-annual variation scenarios was negligible (<±5%). Although biases across these scenarios are non-zero, they are comparable to the "best case" (i.e. when a constant estimation model is fit to data simulated from a constant operating model), which showed a -4% bias in estimated depletion and -4% bias in estimated SSB_{MSY}. Including time variation within SS3 in the estimation model reduced bias when the operating model included time-varying growth, even if the pattern of estimated variation did not match the pattern of generated variation (Figure 3.4). When L_2 had block-like variation in the operating model, relative error in depletion estimates was low for both estimation scenarios where L_2 varied in blocks (-4%) and inter-annually (1%). When k varied in blocks in the operating model, depletion was generally unbiased when inter-annual k variation was estimated (-2%) and when block variation in k was estimated (-4%). Relative error in SSB_{MSY} was similarly low when L_2 varied in blocks and was estimated in blocks (-3%) or with inter-annual variation (-3%). Estimated SSB_{MSY} was also unbiased when k varied in a block pattern and was estimated as such (-4%), or was estimated with annual deviates (-4%).

Spawning stock biomass in a single year can be overestimated by up to 16% if "true" regime-like shifts in growth are not captured in a constant OM (Figure 3.5). When L_2 varied in a block pattern, spawning stock biomass was overestimated for most of the time series (2%-16%, 1974-2014) unless the estimation model matched. Modeling L_2 with block variation removed this bias (maximum bias in a single year: ±1%), and estimating L_2 with inter-annual variation reduced bias somewhat, but not entirely (bias <-5% in four years). Notably, spawning stock biomass in the year of regime shift was still biased (-8% in 1997, year of largest bias) when inter-annual variation in L_2 was estimated. Similarly, spawning stock biomass was consistently overestimated (5%-13%, 1965-2014) if k varied in blocks and time-invariant growth was

estimated. Estimates of spawning stock biomass were biased in some years (relative error quantile did not overlap zero) when *k* inter-annual variation was simulated and a constant model was fit (11 years), or when *k* varied in blocks but was estimated with inter-annual variation (2 years). However, the relative error over the length of the time series was centered on zero (mean median relative error: 0.4% and 0.8%, respectively).

3.3.2 *Increase in uncertainty in data-rich case*

When growth variation is introduced into the operating model, estimated some biological reference points were less precise, even if they were unbiased. When simulated L_2 varied with annual deviates, the corresponding estimation model estimates depletion as more uncertain (width of relative error quantile is 0.26) compared with a time-invariant estimation model (0.15). Similarly, when L_2 varied according to a block pattern, the corresponding estimation model (0.23) and an estimation model with annual L_2 variation (0.22) estimate depletion with more uncertainty when compared with a time-invariant estimation model (0.12). Estimated uncertainty of depletion did not change significantly along with estimation model configurations in scenarios where *k* varied. Estimated uncertainty of SSB_{MSY} also did not change significantly when growth variation was introduced in the operating model.

3.3.3 *Effect of data limitation*

When data were poor (sample size <50 ages/year), the effect of growth misspecification on estimated management quantities was generally masked by the increase in uncertainty. Exceptions to this in scalar quantities were observed when L_2 or *k* varied in a block pattern but was estimated as constant (Figure 3.4). In these cases, median relative error was positive (11.11% L_2, 3.80%, *k*) in the data-rich case, but negative (-1.24% L_2, 3.80%, -9.24% *k*) in the

data-poor case. Exceptions in time series of spawning stock biomass were when k or L_2 varied in block patterns but were estimated as constant; in this case, 95% quantiles of relative error did not overlap zero for some years (Figure 3.5). Finally, as expected, reducing the amount of available data increased the uncertainty; the width of the 95% quantiles of relative error in depletion in the data-poor case ranged from 207.32% - 469.72% the quantile width in the data-rich case. Estimated SSB_{MSY} uncertainty increased less with data removal (quantile width increases ranged from 120.73% - 210.28%).

3.3.4 *Convergence*

Estimation models specifying time blocks in the k parameter only converged when all other growth parameters were fixed at their true values. Some iterations did not converge when L_2 was estimated with inter-annual variation (96% when fit to simulated inter-annual variation and 98% when fit to simulated block variation patterns), and when a constant estimation model was fit to simulated block (98%) or annual (98%) variation in k. All scenarios that did not converge were data-rich. All other scenarios converged 100% of the time.

3.4 DISCUSSION

Our results suggest misspecification of growth in practical stock assessment models can introduce bias into estimated management reference quantities, but that this bias may be mitigated or eliminated by estimating time-varying growth inside the assessment model. Even if management quantities were unbiased when growth was miss-specified, ignoring time-varying growth leads to an underestimate of the uncertainty surrounding management reference points. However, in data-poor scenarios (i.e. sample sizes <50), biases in management reference points caused by growth misspecification were masked by uncertainty in these estimates. These

findings suggest stock assessment authors should consider incorporating time-variation in growth parameters to reduce bias, if there is evidence variation occurs and there are at least fifty samples per year of composition data spanning several decades.

Our analysis suggests stock assessment authors should consider incorporating inter-annual growth variation in assessment models on a case-by-case basis. This is particularly true for stocks that experience regime-like block shifts in growth, which are likely to be the most biased because of growth misspecification, and are good candidates for estimation of time-varying growth. Detecting regime shifts is difficult on ecological time scales, and therefore block-like patterns in growth may only be detected if several decades of age- and length-composition data are available (Andersen et al. 2009). In our simulation, regime-like shifts followed a "step-down" pattern, so it may be that the direction of growth variation (i.e. constant decrease) is more important in determining whether this variation introduced bias than the pattern (i.e. regime-like vs. inter-annual). Incorporating time-varying growth in estimation models when growth is constant does not significantly reduce precision, suggesting it may be prudent to include variation in cases where it is uncertain if biological growth is time-varying. Furthermore, if growth is time-varying, an estimation model that specifies constant growth may underestimate the uncertainty in estimated management quantities. This suggests that if growth is hypothesized to vary, stock assessment authors should explore providing estimates of management quantities from models with alternative growth specifications to managers in the form of model sensitivities and decision tables.

Practical considerations, namely convergence issues, run time, and data availability, limit the benefits of including time-varying growth parameters to well-behaved data-rich to data-moderate assessment models. The Petrale sole stock assessment model is relatively well-behaved, and yet

estimating time blocks in k required fixing other growth parameters at their true values to achieve convergence, similar to Field (2007). It is likely that estimates of time-varying growth would be more difficult to obtain had the key parameters of h and M not been fixed in our simulations. Estimating time-varying growth is therefore infeasible for stock assessment models that already experience poor convergence. Extremely data-rich stock assessments are also unlikely to benefit from time-varying growth estimation, for both performance and accuracy reasons. Modeling time variation increased runtime by a factor of two (for estimation of time blocks) or three (for estimation of inter-annual deviations) and is therefore impractical for base stock assessment models fit to vast quantities of composition data. However, if there is evidence supporting time-varying growth, then sensitivity model runs to such data-rich assessments should be explored. Kuriyama et al (2016) suggest in very data rich cases, the incorporation of empirical weight-at-age data reduces bias caused by time-varying growth in estimates of spawning stock biomass more than estimation of time-varying parameters. Conversely, when data are limited, we show estimates of management quantities are not adequately precise to be affected by time-varying growth. Therefore, modeling growth variation may only be practical in data-moderate (>50 age- and length-composition samples per year) to data-rich (<1000 composition samples per year) cases.

Selecting which growth parameters to model variation in, as well as what type of variation to include, also seems to depend more on practical rather than theoretical considerations. Though the Schnute (1981) reparameterization of the von Bertalanffy (1957) growth curve is more numerically stable, k and L_∞ are inherently anti-correlated (Pilling et al. 2002) and it is difficult to isolate which parameter of the growth curve varies from biological data. Thorson and Minte-Vera (2016) find changes in weight-at-age are difficult to isolate from those in growth (as

measured by k), but that 45% of the variation in their data set is explained by k variation. We found time variation in k was more difficult to estimate than that in L_2 within an integrated assessment model. Furthermore, although growth scenarios with block variation introduced greater bias to management estimates, estimating inter-annual variation in growth parameters reduced bias in estimated quantities substantially in these scenarios. Furthermore, annual deviations in growth were easier to estimate (for k) than block variation. Finally, estimation of block variation necessitates analysts to pre-specify the number and length of each time-block of variation, and this requires breakpoint analysis to be conducted external to the assessment model.

The somatic growth patterns we estimated and then used for simulation may capture or correlate with variation in other demographic processes; however, we argue these patterns are still the most realistic available. In estimation models used to derive simulation patterns for growth variation, alternative forms of demographic variation were not explored; it is therefore plausible that changes in age- and length- composition data attributed to changes in somatic growth therein are the product of time-variation in natural mortality, fishing mortality, or recruitment. However, estimating growth as time-varying did not reduce the magnitude of recruitment variation, suggesting our modeled changes in growth are not capturing recruitment variation. Finally, covariation in demographic rates is certainly non-zero (Parma and Deriso 1990, Thorson et al. 2015); however, incorporating this covariation into production assessment models is likely infeasible until these patterns of covariation are better documented in the literature.

All demographic rates (growth, recruitment, and natural mortality) as well as sampling processes (i.e. selectivity) vary over time, both independently and synergistically; here we suggest process error due to somatic growth variation should be considered more explicitly by

stock assessment analysts. Somatic growth is more (imperfectly) observable than recruitment or natural mortality, and therefore realistic estimates of variation may be easier to attain for species with many (>50) age- and length-composition samples spanning several decades. Furthermore, although incorporating time-varying natural mortality may improve accuracy in assessment models (Jiao et al. 2012), misspecifying natural mortality as time-varying may introduce bias into model estimates (Fu and Quinn 2000). Therefore, if it is unclear whether mortality or growth varies, it may be safer to incorporate time-varying growth, as the same negative effects were not observed in this study if "true" growth was constant, but was estimated as time-varying. If growth variation is not included in assessments used for management, authors should be wary that uncertainty in management quantities may be underestimated.

Tables

Table 3.1 - Scenarios tested span 15 permutations of operating and estimation model growth specifications, and each scenario is run for both the data-rich and data-poor case.

Operating model specification	Estimation model specifications
L21. Environmental deviates on L2 simulated using assessment model fit to fishery & survey data	L21, C
L22. Blocks on L2 simulated from assessment model fit to fishery & survey data	L21, L22, C
K1. Environmental deviates on k simulated using assessment model fit to fishery & survey data	K1, C
K2. Blocks on k simulated from assessment model fit to fishery & survey data	K2, K1, C
C. Constant	C, L21, L22, K1, K2

Table 3.2 – Time blocks evaluated for periods of growth variation. Negative log likelihoods are derived from the simplified assessment model fit to available data. Asterisk(*) denotes selected block time periods.

Block Name	Block Years	Negative log Likelihood (k)	Negative log Likelihood (L_2)
Fishing mortality	1965-1977, 1978-1986, 1987-2002, 2003-2014	1453.26*	1427.91
ENSO	1965-1976, 1977-1998, 1999-2014	1463.36	1442.55
PDO (Field)	1970-1979, 1980-1988, 1989-1991, 1992-1998, 1999-2006, 2007-2014	1453.31	1425.62*

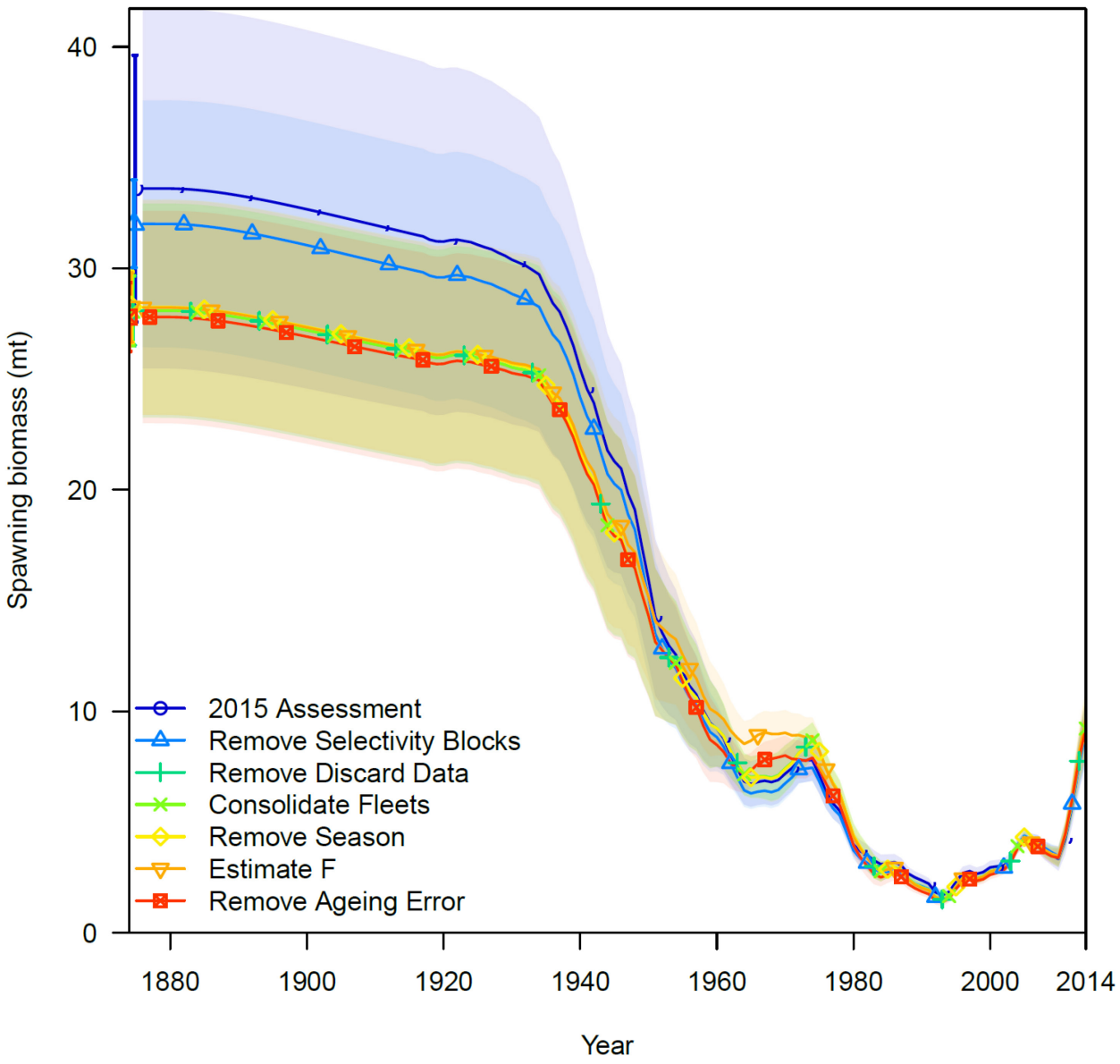

Figure 3.1 - Comparison of trajectory in spawning stock biomass as model simplification occurred (from top to bottom). Dark blue represents the assessment model used for the 2015 update assessment; red model represents the final simulation model. Shaded areas represent 95% confidence interval.

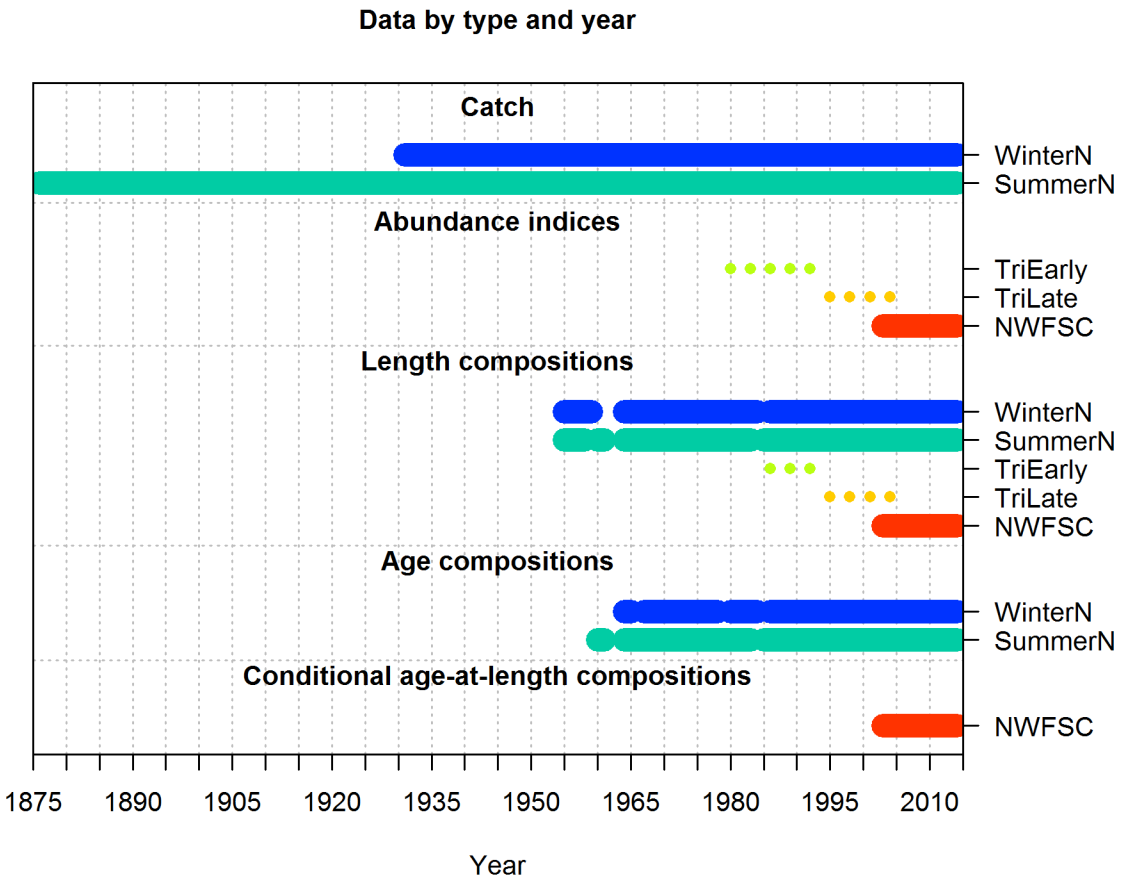

Figure 3.2 - Illustration of data used in base estimation model by year and type.

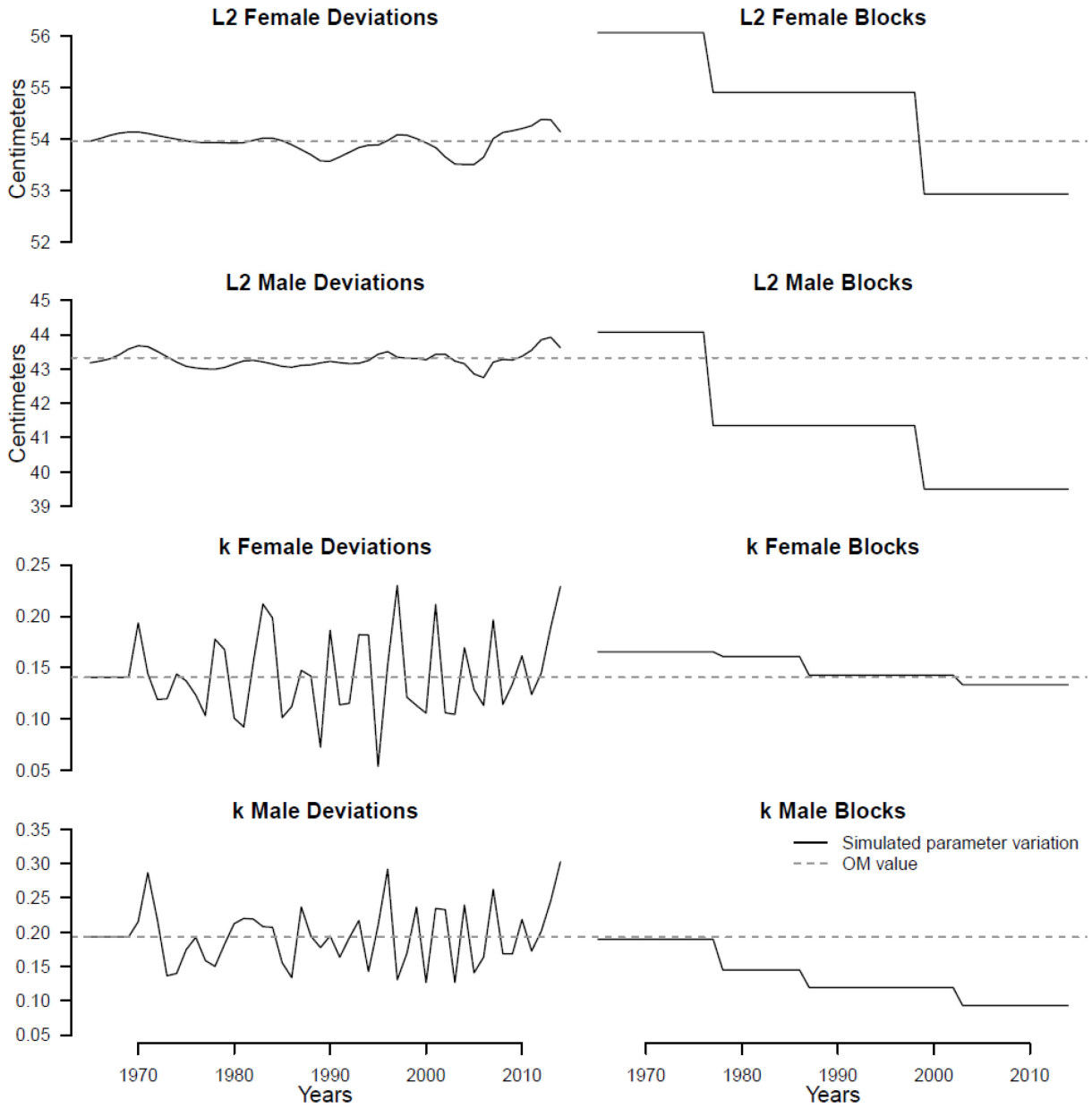

Figure 3.3 - Input growth parameter variation across four EM and OM configurations. Gray dashed line represents starting parameter value, and black line represents simulated patterns under alternative growth scenarios for male and female fish.

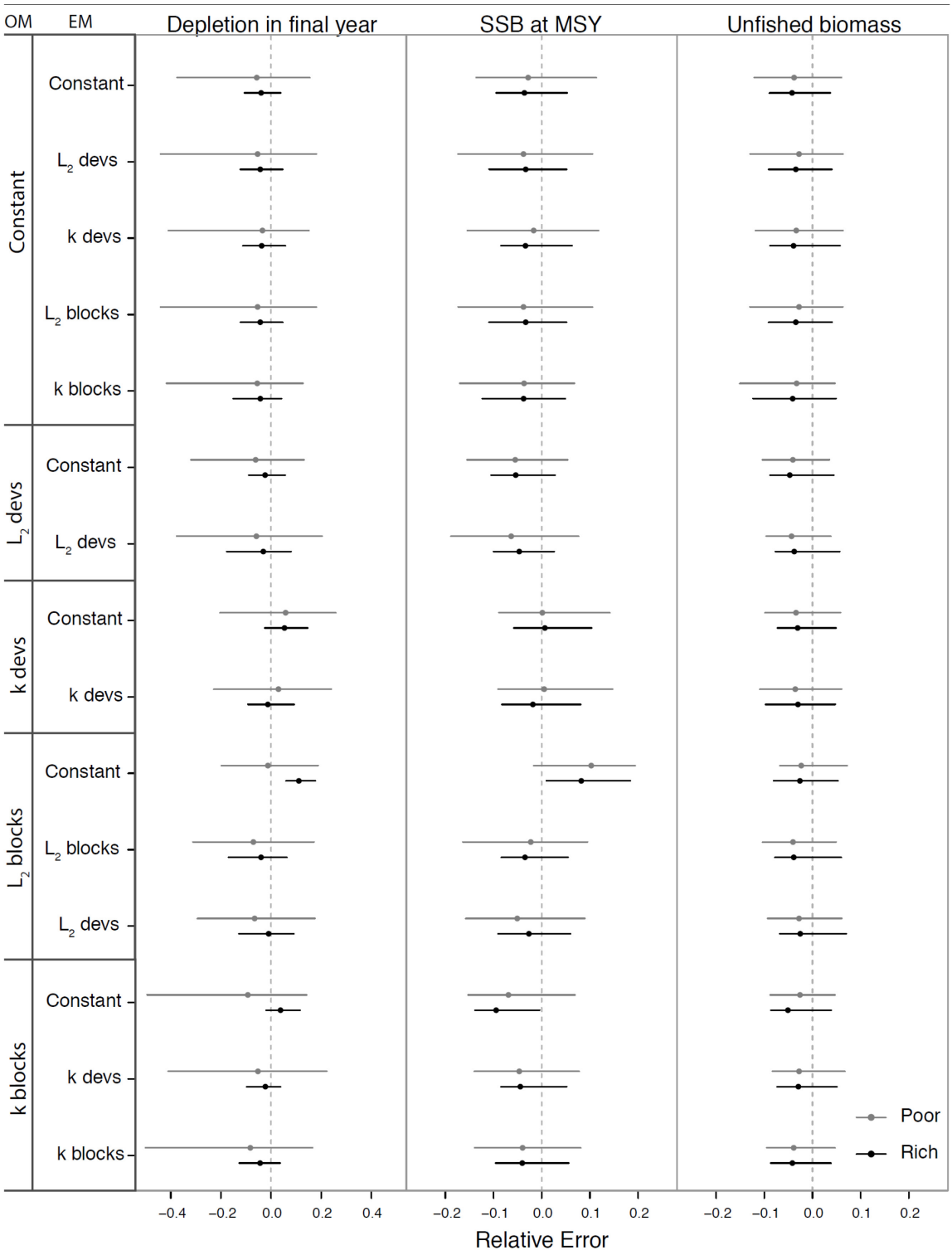

Figure 3.4 - Median (point) and 95% quantiles (lines) of relative error in estimates of depletion in the final model year (left), spawning stock biomass at maximum sustainable yield

(middle), and unfished biomass (right). Operating model configurations (OM) and estimation model configurations (EM) for each scenario are on the left.

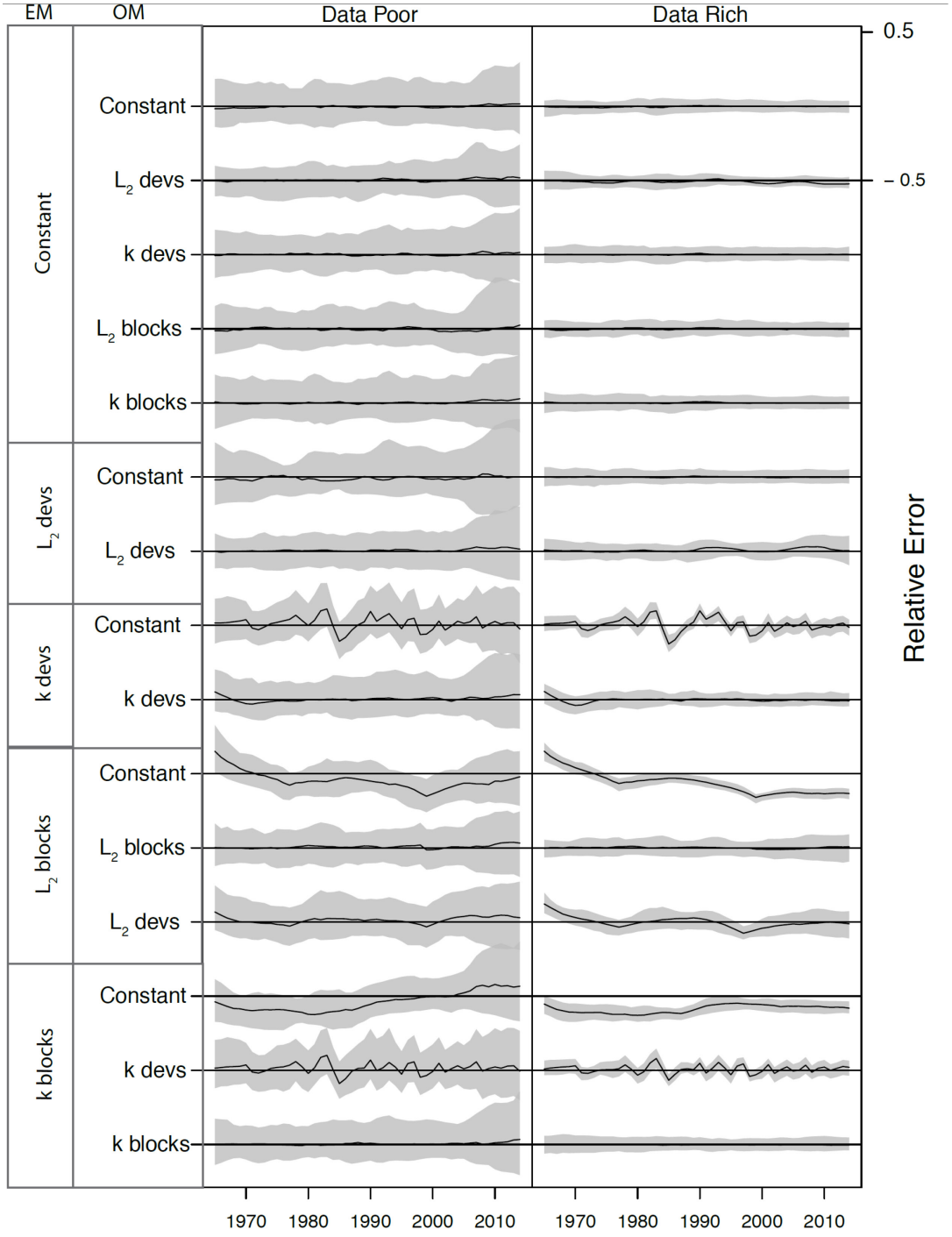

Figure 3.5 - Time series of relative error in estimated spawning stock biomass over time. Gray shaded area represents the 95% quantile, while black line represents the median. The

straight black line represents no error over the time series. Each scenario is presented on the same scale, with the maximum pictured error of +0.5 and -0.5. Operating model configurations (OM) and estimation model configurations (EM) for each scenario are on the left.

Chapter 4. Testing the applicability of size-spectrum food models to a species-rich tropical lake

ABSTRACT

Ecosystem models are commonly used to explore potential consequences of drivers and threats. Tropical freshwater ecosystems face many threats, therefore conservation decision making might be aided by models that can identify likely ecosystem responses. However, such systems often have limited data (i.e. biomass time series or ratios) that are commonly used to parameterize ecosystem models. Size-spectrum approaches are promising for low-data systems, as they require fewer species-specific parameters than typical ecosystem models. However, tropical freshwater species are often highly omnivorous and lack strong body size-trophic position relationships, violating size-spectrum model assumptions. Here we assess if size-spectrum models can adequately represent tropical freshwater systems by constructing an ecosystem model for Tonlé Sap Lake, Cambodia. We predict dynamics of five species groups across seven alternative scenarios. We test model fit by comparing metrics between model predictions and empirical data: 1. size-trophic level relationships, 2. weight distribution, and 3. relative biomass of species. We find the model's stability is highly sensitive to parameters governing trophic interactions and primary productivity. Model predictions and data agreed best for size-trophic level relationships (median average relative error: 8%-19%), although the model predicts a stronger trophic level-size relationship than stable isotope-derived estimates. Mean weight estimates were less accurate

(error: 0.13-6.94), and relative biomass predictions were off by 2-4 orders of magnitude. This mismatch has two implications for modeling such a system. Further data could improve model stability by more accurately parameterizing diet preference and utilization of food from different habitat areas. Secondly, survey data would greatly improve ability to model fishery selectivity and thereby increase agreement between empirical and model-derived metrics.

4.1 INTRODUCTION

Ecosystem models are useful to predict possible consequences of anthropogenic and physical drivers on aquatic ecosystems and food webs across a range of alternative scenarios (Rosenberg & McLeod 2005). Simulations of ecosystem dynamics using such models are governed by parameters that are generally taken directly from measurements or estimated by fitting single-species models to data (Plagányi *et al.* 2014). Therefore, the single- and multi-species processes that an ecosystem model can represent are limited by available data on rates governing these processes. The simplest mass-balance ecosystem models require estimates of total biomass, production and consumption rates, and diet information to examine potential effects of changes in biomass of one species group on others (Pauly, Christensen & Walters 2000). Adding stage-structure to each species group increases the realism of predictions by accounting for effects of processes in aquatic systems that vary by life stage (i.e. growth, mortality) (Collie *et al.* 2014). However, this additional realism typically requires additional data on species-specific life history traits to resolve species biomass and interactions by stage.

Species-rich, data-poor tropical freshwater systems require a multi-species approach, but lack biomass or life history trait estimates that can be used to parameterize a traditional ecosystem model. Therefore, size spectrum models may be useful for modeling data-poor systems, because they require only a single species-specific input parameter, an organism's asymptotic maximum size (Andersen & Beyer 2006) and can capture complex food web dynamics (Hartvig & Andersen 2013). From this trait, other quantities, including fishing effects (Shin *et al.* 2005), growth and mortality rates (Werner & Anholt 1993), predator-prey interactions (Werner & Gilliam 1984) and relative biomass (Blanchard *et al.* 2009) may be derived based on assumed allometric scaling relationships. These relationships have been

empirically validated across temperate freshwater and marine systems (Jennings & Mackinson 2003; Woodward *et al.* 2005). Because of their relative simplicity, size-spectrum models are increasingly emerging as valuable management tools to evaluate plausible future scenarios (Rochet & Benoît 2011; Barange *et al.* 2014).

However, size-spectrum models make several assumptions regarding trophic interactions that tropical freshwater systems may violate. Size-spectrum models typically assume that the dominant source of nutrients for all consumers is plankton (Hartvig, Andersen & Beyer 2010), or at most, a coupled pelagic-benthic pool (Blanchard *et al.* 2009). Conversely, tropical freshwater systems typically have a significant component of production from microbial inputs (Mann 1988). Secondly, size-spectrum models assume diet preference is dictated primarily by size, with the consequence that trophic position is highly correlated with size. While this has been shown in temperate systems (Post 2002), tropical freshwater fish often exhibit more complex feeding preferences. Tropical freshwater systems house fish species with a diversity of specialized feeding habits (McConnell & Lowe-McConnell 1987; Winemiller 1990), leading to complex food webs and species-specific diet differentiation (Jepsen & Winemiller 2002). Consequently, tropical systems include primary consumers exhibiting a broad range of body sizes, leading trophic position to be decoupled from body size (Layman *et al.* 2005).

Tonlé Sap lake (TSL) in Cambodia supports a large, multispecies fishery that is critically important to the local population yet faces many threats. Estimates of annual catch from TSL range between 177,000-252,00 tonnes (Lamberts 2001), and over 4 million people live on and base their livelihoods off of the lake (Sokhem & Sunada 2006). The lake experiences dramatic seasonal flooding, therefore proposed hydropower has the potential to threaten this system. The fishery is indiscriminate across species and size; 159 species are regularly documented in the

catch, and some estimates put fish species richness in the lake as high as 500 (Campbell *et al.* 2006). In addition to its species diversity, fish species exhibit dietary preferences highly adapted to both the immense seasonal variation and the significant amount of production derived from microbial and detrital inputs (Lamberts & Koponen 2008). Existing fisheries models for this system do not consider stage structure and may therefore miss the destabilizing effect of truncated size structure (McCann *et al.* 2016). Fishing degrades population stage structure (Jennings, Greenstreet & Reynolds 1999), which in turn modulates trophic interactions. Therefore, such a model would help in exploring potential future scenarios for the fishery under predicted anthropogenic and climate stressors. However, the species richness and trophic complexity of this system coupled with limited empirical data makes it difficult to capture the dynamics of this system.

Here, we tested whether a size-spectrum ecosystem model could be modified to capture the dynamics of a freshwater ecosystem with multiple resource pathways and complex diet differentiation. We parameterized the model for TSL by including both pelagic and littoral energy pathways and species-specific coupling strengths based on diet preference. Time series data are not available for this system, therefore we test the accuracy of this model using empirical data that is available: 1. Estimated trophic level derived from measurements of $\delta^{15}N$ from stable isotope analysis, 2. weight composition, and 3. relative biomass from catch data (Sopha & van Zalinge 2001; Hortle, K.G., Lieng, S., Valbo-Jorgensen 2004; MRC 2010). Because many system parameters are unknown, we examine whether these metrics are sensitive to several sources of uncertainty in the parameterization: 1. the diet composition of the two predator species groups, 2. the relative productivity (carrying capacity) of the two alternative resource pathways, and 3. harvest pressure.

4.2 METHODS

4.2.1 *Ecosystem model*

The size spectrum ecosystem model used here was first described in Andersen and Beyer (2006), an extension to a food web framework (referred to here as the "general model") is described in detail in Hartvig *et al.* (2010). Because this model has been detailed elsewhere (Hartvig *et al.* 2010; Jacobsen, Gislason & Andersen 2013), here we summarize the equations governing key model dynamics (Table 4.1) and detail changes to the existing food web framework to adapt it for Tonle Sap lake. In this manuscript, "resources" refer to food sources for the smallest fish; these sources are not limited to primary producers but instead capture all food items excluding the modeled "species." "Species" in this context refer to groups ($i = 1,\ldots,5$) of species that share a similar maximum asymptotic weight, $W_{\infty,i}$, (Table 4.2) and diet preferences. We chose asymptotic weight values based on five representative species represented well in catch data (Sopha & van Zalinge 2001; Hortle, K.G., Lieng, S., Valbo-Jorgensen 2004; MRC 2010) that span different ecological niches. The model was parameterized for one small pelagic specialist (*Rasbora aurotaenia*), one small generalist (*Henicorhynchus siamensis*), one large generalist predator (*Channa micropeltes*), one large pelagic predator (*Boesemania microlepis*), and one large detritivore (*Pangasius larnaudii*). Species-specific W_{∞} values were taken from Fishbase (Table 4.2). The primary model modification beyond Hartvig *et al.* (2010) concerns the addition of a second resource pathway: a littoral resource, in addition to pelagic food sources. We construct the model as described below, then run it for fifty years in 0.2 year timesteps. Equilibrium values for the abundance of each species group were calculated as in Andersen and Beyer (2006). Initial abundance was set to these equilibria.

4.2.2 *Dynamics*

The size-structured model captures the dynamics of species groups (i.e. changes in the density of each weight group m in each species group i, $N_i(m,t)$, Table 4.1, equation 1) (McKendrick 1925; von Foerster 1959) by modeling key life history processes (i.e. recruitment, somatic growth, and mortality) of a specified number of fish species. Most life history trait values were derived based on assumptions they scale allometrically with species' specified asymptotic weights, $W_{\infty,i}$ (Table 4.2), which is the only specified life history trait value in the general model. We note exceptions, where in the specific model, we specified traits directly for each species group i (Table 4.2). The resource spectra dynamics were specified according to semi-chemostatic growth (Table 4.1, equation 2). Each resource spectrum had the same growth rate but its own carrying capacity. The carrying capacity of the pelagic spectrum was estimated from Lamberts and Koponen (2008). However, because the carrying capacities of benthic resources in Tonle Sap lake are not preciesly known, we defined the carrying capacity of the benthic resource spectrum relative to the pelagic resource spectrum, κ_P. Therefore, the carrying capacity coefficient for the benthic resource spectrum was $\kappa_B = c\kappa_R$. Sensitivity to this constant c was evaluated as described in the Sensitivity analyses section below. Background size spectra range from 1e-6 gram to 1 gram (pelagic) or 10 grams (benthic). None of the model parameters nor the data used to validate the model vary over time, therefore the t index is omitted for ease of notation in the equations in Table 4.1.

4.2.3 *Consumption*

Predation was specified according to the assumption that fish eat resources and other fish smaller than themselves (Table 4.1, equation 5) (Hartvig & Andersen 2013), described by a predator-prey mass ratio (PPMR) (β_i) (Ursin 1973). The amount of resource (Table 4.1, equation 3) and fish prey (Table 4.1, equation 4) encountered by an individual of species i of mass m is given by a function of the density of prey items and species' coupling strengths to resource spectra (Θ_{R_x}) and other species (Θ). Exact diet composition of species groups was not known, therefore we used ecological information (Lim *et al.* 1999) to identify what sources of prey were likely non-zero contributions to diets for each species. We used this information as a starting point, and adjusted Θ and Θ_{PP} values to optimize model stability and ensure mutual coexistence of all five species groups. *Rasbora* was assumed to consume solely from the pelagic resource and its own larvae. *Henicorhynchus* was assumed to consume both benthic and pelagic resources and also larvae from the benthos (itself and *Pangasius*, Table 4.2). *Channa* is a piscivore, therefore its was parameterized to prey on all fish species and have a lower preference for resource spectra. *Boesemania* consumed only pelagic fish (itself and *Rasbora*), and to a smaller degree, from the pelagic resource spectrum (Table 4.2). *Pangasius* is primarily a detritivore and is assumed to prey mostly on benthic resources, but a small piscivorous diet preference was introduced for itself and *Henicorhynchus* to prevent extinction of this species group within the model. Piscivores (*Boesemania* and *Channa*) were assumed to prefer predatory feeding (i.e. $\theta_{i,j} > \theta_{i,R_x}$), while planktivores and detritivores were assumed to prefer consuming resources (i.e. $\theta_{i,R_x} > \theta_{i,j}$). Sensitivity to these values is examined as described in the Sensitivity analyses section below.

The size-based feeding kernel ($s_i(m_p, m)$, Table 4.1, equation 5) describes the food available of size m_p for a predator of species guild i of size m. We modified the general model to assign a unique preferred predator-prey mass ratio (PPMR) β_i for each species guild i, instead of assuming the same PPMR for each species. We increased the PPMR for *Pangasius larnaudii* to 1000 and the feeding kernel width σ to 7. This was necessary to prevent starvation as this species' diet is comprised primarily of base resources, which do not exceed 10 grams, but its asymptotic maximum weight is 28.88kg. The food available for a predator of size m, available from resource spectra $\phi_{i,R}(m)$ (Table 4.1, equation 6) and other fish $\phi_{i,P}$ (Table 4.1, equation 7), was calculated based on the encountered food and the size kernel. A feeding level $f_i(m)$ between 0 and 1 (Kitchell, Stewart & Weininger 1977) was used to describe satiation (Table 4.1, equation 9); this feeding level is a function of available food $\phi_{i,P}, \phi_{i,R}$ and the volumetric search rate $v(m)$ (Table 4.1, equation 8, Ware 1980). Multiplying the feeding level by the consumption rate $h_i m^n$ yields the amount of food consumed (Table 4.1, equation 9); this corresponds to a Holling type II functional response. The coefficient describing maximum food intake, h_i, is allowed to vary by species to allow predators to be more efficient consumers.

4.2.4 *Energy allocation and mortality*

Dynamics of these processes are largely unchanged from Hartvig et al. (2010) and are therefore only explained briefly. Available energy E_a remaining after catabolism is allocated to growth and reproduction according to Table 4.1, equations 10-13. Density-dependent recruitment is specified using a Beverton-Holt (Beverton & Holt 1957) function (Table 4.1, equation 15). The

parameters of this function are derived from a species' asymptotic maximum weight and a scaling parameter, κ_r. This parameter governs the relative productivity of fish species to the pelagic resource spectrum, κ_{R_p}. Natural mortality is broken into three components: 1. predation mortality (Table 4.1, equation 18), 2. background mortality (Table 4.1, equation 19), and 3. starvation mortality (Table 4.1, equation 20). Predation mortality for a prey species depends on abundance and preference of predators, as well as the search volume as it is assumed that an increased search efficiency corresponds to increased vulnerability (Werner & Anholt 1993). Background mortality captures mortality due to aging. Finally, the starvation mortality parameterization ensures that if catabolic costs exceed energy intake, fish starve rather than shrink. Fishing is imposed at a constant rate across species for all fish larger than 1 gram ($F(m>1)=F_0; F(m<1)=0$), as fish in this system are harvested at all sizes across species by several hundred different gear types (Campbell *et al.* 2006).

4.2.5 *Relative biomass comparison*

To determine if the size spectrum model captures the dynamics of Tonle Sap lake reasonably well, we compare relative percentage of the catch different species supply in our model with empirical data. Catch is not generally reported for this system, and it is impossible to scale to absolute biomass without better information about fishing efficiency. Therefore, the best estimates of relative biomass of different fish species in Tonle Sap Lake come from two reports published by the Mekong River Commission (Hortle, K.G., Lieng, S., Valbo-Jorgensen 2004; MRC 2010) and one scientific report (Sopha & van Zalinge 2001), that detail which species comprise a significant percentage of the catch of several fisheries. Reported species

corresponding to those our species guilds are modeled after include *Henicorhynchus siamensis*, *Channa micropeltes*, and *Pangasius spp.* (not resolved to species level). These reported percentages were compared to percentages these species groups comprise in output catch from the size spectrum model (i.e. individuals larger than 1 gram of weight).

4.2.6 *Trophic level comparison*

Another metric we used to assess model performance was the model predicted trophic level (TL) of each species group relative to the estimated trophic levels of sampled fish based on stable isotope analysis. Fish samples were collected from fishermen and fish markets from 2010-2015 across observed species weights. Lengths and wet weights were recorded, and $\delta^{15}N$ was measured (Pool 2017). To estimate trophic level, we set the baseline trophic level ($\delta^{15}N_{base}$, assumed to correspond to TL=2) to the calculated mean $\delta^{15}N$ value across seston and zooplankton samples ($\widehat{\delta^{15}N_{base}}$= 1.49). Scaled trophic level ($\widehat{TL_{i,z}(w_z)}$) is then predicted using a formula from a recent meta-analysis (Hussey *et al.* 2014):

$$\widehat{TL_{i,z}(w_z)} = \frac{\log(\delta 15N_{lim} - \delta^{15}N_{base}) - \log(\delta^{15}N_{lim} - \delta^{15}N_{TL})}{k} + 2 \qquad (4.1)$$

where w_z is the wet weight of the sample of species i, and $\delta^{15}N_{TP}$ is the stable isotope measurement from the sample. Estimates of $\delta^{15}N_{lim}$ (21.93, the saturating isotope limit as $\delta^{15}N$ increases) and k (0.31, the rate at which $\delta^{15}N_{TL}$ approaches $\delta^{15}N_{lim}$ per TL step) were taken from Hussey et al. (2014).

To calculate predicted trophic level from the model, it was necessary to fix a trophic level for each of the resource spectra (pelagic and benthic) (TL_{R_x}). This value may vary by weight of

prey item in each spectra; however we did not have enough information to predict how trophic level would scale with size for these resource items. We assign a base trophic level of 2 to the two different resource spectra (benthic and pelagic) to be consistent with the baseline set for the stable isotope data. In our model, diet and therefore trophic level of fish depend on both species and size, therefore the trophic level $TL_i(m)$ of individuals varies by both species guild i and mass m. Model-derived trophic level (equation 4.4, derived from Table 4.1, equations 5-7) for a fish species was therefore calculated as the weighted average of the trophic levels of items it consumes as:

$$TL_{i,R}(m) = \int \sum_{x=1}^{2} \frac{m_p \mathsf{N}_{i,R_x}(m_p) s(m_p, m) TL_{R_x}}{\phi_{i,R}(m)} dm_p \tag{4.2}$$

$$TL_{i,P}(m) = \int \frac{\sum_{k=1}^{5} m_p \mathsf{N}_{i,k}(m_p) s(m_p, m) TL_k(m_p)}{\phi_{i,P}(m)} dm_p \tag{4.3}$$

$$TL_i(m) = \frac{TL_{i,R}(m)\phi_{i,R}}{\phi_{i,R} + \phi_{i,P}(m)} + \frac{TL_{i,P}(m)\phi_{i,P}(m)}{\phi_{i,R}(m) + \phi_{i,P}(m)} \tag{4.4}$$

Where $TL_{i,R}(m)$ and $TL_{i,P}(m)$ denote the average trophic level of a. resource spectra items and b. prey fish consumed by a predator i at mass m, respectively.

4.2.7 *Weight composition*

The final metric we used to evaluate model performance is weight composition. Weight data were considered more reliable than lengths (Pool 2017). Asymptotic weights given in Table 4.2 are derived from literature. However, empirical weight data show realized weight of sampled

individuals is much smaller than predicted asymptotic weight, particularly for fish reaching larger maximum sizes (Baird, Flaherty & Phylavanh 2003). This is likely due to a long history of heavy exploitation across all size classes in the lake (Hilborn & Minte-vera 2008). Because the size spectrum ecosystem model can predict the impact of fishing on size-structure (Rochet & Benoît 2011), comparing realized growth from empirical data with model output provides another check of model accuracy.

Empirical weights from the same data used for stable isotope analysis were used to approximate the weight distribution and median weight of each of the five species. The Tonlé Sap lake fishery is thought to have uniform selectivity for individuals exceeding one gram of weight (Campbell *et al.* 2006). Though selectivity may not be uniform, without fisheries-independent data we are only able to infer selectivity from the catch weight distribution. To avoid using these data twice (to parameterize the curve and as a check of model accuracy), we assume uniform selectivity so this weight comparison is a conservative metric for model accuracy. We compared the empirical weight frequencies with the predicted weight distribution from the size-spectrum model. The mean weight is skewed by large outliers, therefore we compare the empirical median weight for each species to the mean weight predicted by the model.

4.2.8 *Sensitivity analyses*

Sensitivities were evaluated to a number of different parameters: the constant c defining the proportional relationship between the two resource spectra carrying capacities, the species coupling strengths $\theta_{i,j}$, and the fishing rate F. The benthic resource is thought to be less

productive than the pelagic, therefore $c \in [0,1]$. Values for c were set to 0.1, 0.25, and .5 (Lamberts & Koponen 2008) (Table 4.3). Testing sensitivity to all 25 values in Θ would make results difficult to interpret, therefore, we tested sensitivity to only the species coupling strengths for the primary predators in the system: species groups loosely based on *Channa micropeltes* and *Boesemania microlepis*. Coupling strengths were varied to explore a range of diet overlaps for these predators, from making each predator a piscivore of only benthic (*Channa*) or pelagic (*Boesemania*) fishes, to making both generalist predators over all fishes (Table 4.3). Finally, fishing pressure could affect our metrics for model performance by truncating the weight distribution (Berkeley *et al.* 2004) or changing the relative biomass of species (Rochet & Benoît 2011), which could then impact diets and therefore trophic level. Therefore, we explored how model dynamics changed in an unfished or heavily fished state.

4.3 RESULTS

Model outputs were relatively similar across sensitivity cases, but were sensitive to some scenarios (Figure 4.1). The base case model (Figure 4.1) predicted the highest densities for *Henicorhynchus* and *Rasbora*, followed by *Channa*, *Boesemania*, and *Pangasius*. Increasing the fishing rate to high levels (F>2.5) caused the *Pangasius* population to become extinct. The species group loosely modeled on *Pangasius* was the most sensitive to parameter changes across our sensitivity analyses. In most scenarios, *Pangasius'* size spectrum was truncated (i.e. there were no individuals larger than 0.17 kg [F=2.5] - 8.03 kg [c>0.25]). Only in the unfished scenario did large Pangasius persist to the extent seen in empirical data (up to 23.96 kg). The weight distribution of the species group based on *Boesemania* was the only other one to exhibit

noticeable sensitivity to parameterizations. The maximum size of *Boesemania* individuals ranged from 1.08 kg (F=0, F=2.5) to 3.23 kg (when both predators had specialist diets).

Many scenarios resulted in one or more species going extinct in model runs, indicating that the model was highly sensitive to parameter values and assumptions. Scenarios collapsed when c (ratio of benthic:pelagic production) was less than .25, when fishing exceeded a certain threshold (F>2.5), and under certain diet configurations (i.e. *Pangasius* was strictly a resource consumer). Beyond these sensitivity cases, models were also sensitive to the scaling of the relative production of fish vs. the resource spectra (κ_r) and the assumed primary production for each resource spectrum ($\kappa_{R_{max}}$). Scaling the relative production of fish to be close to that of the resource spectra resulted in population collapse due to predation pressure. Increasing the $\kappa_{R_{max}}$ led to more oscillatory behavior in population biomasses over time.

4.3.1 *Relative biomass comparison*

All tested model cases severely underestimated the relative biomass of *Channa* and *Pangasius* to *Henicorhynchus*. Under the base model, the ratio of *Channa*:*Henicorhynchus* was underestimated by two (if compared with the low estimate the MRC 2010 report) to four (compared to the highest estimate from (Hortle, K.G., Lieng, S., Valbo-Jorgensen 2004)) orders of magnitude (Table 4.4). The ratio of *Pangasius*:*Henicorhynchus* from model output was closer to reported data; however, in the base case model this ratio was still underestimated by one (if compared with the low estimate from Hortle, K.G., Lieng, S., Valbo-Jorgensen [2004]) or the MRC [2010]) report) to two (compared to the highest estimate from the Sopha & van Zalinge [2001] report) orders of magnitude. Increasing the carrying capacity of the benthic resource

relative to the pelagic resource (increase in c) increased these ratios closer to observed catch ratios for both species. However, higher values of c are not supported by the literature (Lamberts and Koponen, 2008), and further exploration revealed species groups also begin to go extinct if c exceeds 1. Removing fishing pressure also increased these relative biomass ratios; however this system is highly exploited, so assuming $F = 0$ is unrealistic. Reducing *Boesemania* and *Chana* diet overlap brought the *Chana*:*Henicorhynchus* ratio upwards closer to observed catch percentages, but had the effect of decreasing the *Pangasius*:*Henicorhynchus* ratio.

4.3.2 *Trophic level*

Model-derived trophic level estimates had smaller errors compared to other metrics when compared to empirical data estimates (median absolute relative error [MARE] to the base model: 0.040-0.32) (Figure 4.2). Overall, for all species groups, trophic level was predicted to correlate more with weight by the model than was estimated from trophic level estimates from stable isotope data. The largest disagreements were observed for *Channa*, a carnivore, with a MARE of 0.32 compared to the base model, and *Henicorhynchus*, a small omnivore (MARE=0.18). *Pangasius*, a detritivore (MARE=0.11), had estimates of trophic level that corresponded slightly better to model predictions. Small errors were observed for the predatory croaker *Boesemania* (MARE=0.06) and the small pelagic *Rasbora*, (MARE=0.04).

4.3.3 *Weight composition*

Size-derived metrics agreed poorly for most species (Figure 4.3). The model underestimated mean weight for *Rasbora* (relative error [RE] from median = -0.39 - -0.20) except in the unfished

scenario (RE=0.49) and underestimated mean weight for *Henicorhynchus* (RE=-0.77 - - 0.56). Weight compositions from model output across scenarios underestimated the numbers of larger individuals in the *Henicorhynchus* population and the number of medium-sized *Rasbora* individuals. Mean weight for *Channa* was overestimated (RE=0.53-7.42), and similarly, the model-derived weight composition of this species predicted many more individuals near their maximum size than are seen in empirical data (Figure 4.3). Predicted mean weight for *Boesemania* was overestimated also (RE=-0.13- -0.71); however, the sensitivity case where its diet was comprised only of pelagic fish was reasonably close to empirical estimates (-0.13). This suggests the number of larger *Boesemania* are limited because of competition with *Channa* for fish prey excluding the "specialist" scenario. Finally, the weight of *Pangasius* was much more sensitive to alternative paramerizations than other species, as shown by a large spread in relative error (RE= -0.82 - 6.94). The model-derived and empirical mean weights and weight composition for *Pangasius* were reasonably accurate when higher benthic primary production is assumed (RE=0.03, c=.75; RE=0.06, c=.5; top of shaded area, Figure 4.3).

4.4 Discussion

We constructed a size-spectrum model for Tonlé Sap Lake that incorporates multiple resource pathways and diet preference. However, the low agreement of model predictions with available data across alternative model parameterizations suggest more detailed data on diet differentiation are needed to adapt size spectrum models to a tropical lake ecosystem. Few parameterizations resulted in mutual coexistence of the five species groups, with the model being particularly sensitive to parameters governing the resource spectra. Relative biomass of *Channa* and *Pangasius* were underestimated when compared to catch data. Additionally, trophic levels

estimated from empirical stable isotope data were more variable and showed a weaker relationship to body size than model predictions. Finally, both mean weight and weight composition predicted from the model did not agree with empirical weight data, suggesting the modeling approach does not capture the effect of heavy fishing on population size structure. This suggests size-spectrum frameworks, like other ecosystem models, have difficulty achieving stability at the levels of species richness commonly observed in diverse tropical ecosystems.

The difficulty in achieving mutual coexistence of a large number of species is the primary reason the size-spectrum model failed to match empirical patterns. Although our formulation only captures five species groups out of many that live in TSL, the strong effect of interspecies predation and competition leads to a very limited range of parameterizations where modeled species do not drive one another to extinction. This is known to occur in size-spectrum models when only one trait (i.e. asymptotic weight) varies across species; in fact, the addition of an additional resource and distinct diet preferences is the only reason five species groups are able to mutually coexist in our application (Hartvig & Andersen 2013). The addition of recruitment density-dependence, in addition to these diet preferences, also facilitate coexistence (Jacobsen *et al.* 2013); without the stock-recruit function, only three species may coexist.

This mismatch between the number of species groups observed in TSL and the number that can coexist in our model suggests there are factors that facilitate coexistence by limiting the effect of competition or predation in TSL that are unmodeled. This is a common issue of multispecies models; without the effect of a stabilizing functional response (Aydin 2004), complex ecosystems that are abundant in nature are difficult to represent mathematically (May 1974). One factor conferring stability to this system is likely diet diversity. Many fish species' diets are highly omnivorous and span a mix of insects, zooplankton, algae, fish, and terrestrial

plant matter (Lim *et al.* 1999). Food webs have been shown to experience increased stability when they span distinct energy channels (Rooney *et al.* 2006). Another factor that may stabilize this system is differentiated spatial utilization. Across species and seasons, groups tend to utilize different areas of the lake (i.e. floodplain, river, inundated land, (Lim *et al.* 1999)). Therefore, the strong interactions (i.e. predation and competition) between individuals predicted by the model are likely limited in reality due to limited spatial overlap. Additionally, populations are known to migrate between habitats (Hortle, K.G., Lieng, S., Valbo-Jorgensen 2004). This utilization of alternative habitats could foster population stability, as local depletions caused by predation or fishing would be mitigated by migration of new conspecifics from other habitats (Pulliam 1988).

A further limitation of this instability was that the model could not allow for the magnitude of fishing that is known to occur in this system. Heavy fishing is a dominant structuring force in aquatic ecosystems because it erodes size-structure (Berkeley *et al.* 2004; Shin *et al.* 2005) and alters trophic interactions (Werner & Gilliam 1984; Jennings *et al.* 1999). TSL has been heavily exploited for many years, and the available data suggests fishing pressure has truncated size structure across most species. These effects aren't apparent in our modeled size structure because the model's instability limited fishing pressure to a mortality of 2.5. This could explain why the mass distributions predicted by the model show more of an impact from predation (i.e. smaller fish are outcompeted when large and eaten when small) and overestimate the size of larger individuals (i.e. *Channa* and *Boesemania*, which outcompete smaller species of the same size) who are absent at large sizes from empirical data due to fishing pressure. An additional factor that could influence the mismatch between empirical and model-derived weight distributions is fishery selectivity. If the fishery is truly indiscriminate, we’d expect to see the

weight distribution of catch data dominated by smaller individuals (i.e. a balanced harvest (Jacobsen *et al.* 2013)). Instead, catch weight distribution is approximately lognormal (Figure 4.3) and so fishers likely do prefer to capture larger individuals. However, from catch data alone it is difficult to infer the shape of the selectivity curve (Reis & Pawson 1992).

The poorest agreement between the model and empirical data was seen when comparing relative biomass; this could be due to unmodeled selectivity or because of inherent properties of the model. We found the relative biomass of *Channa* and *Pangasius* was significantly underestimated by several orders of magnitude. Although the small amount of data available indicates an indiscriminate fishery (Lamberts 2001), if fishers prefer to catch larger species like *Channa* and *Pangasius*, the catch percentages would show a larger *Channa:Henicorhynchus* and *Pangasius:Henicorhynchus* ratio than what actually exists in the lake. Another reason for the mismatch could be because the theory underlying size spectrum models predicts abundance scales negatively with body size (Jennings & Mackinson 2003) because energy is lost during each trophic transfer (Pauly & Christensen 1995) and bigger organisms are higher trophic level (Jennings *et al.* 2001; Barnes *et al.* 2010). While this is frequently true in temperate aquatic environments (Woodward *et al.* 2005), predators such as *Channa* in tropical freshwater systems tend to exploit short, productive food chains and don't show strong body size-trophic position relationships (Layman *et al.* 2005). Because *Pangasius* is a primary consumer and *Channa* exploits a short food chain, they could be more abundant than the model predicts because more energy is available for them at relatively low trophic positions for their large size.

Perhaps most importantly, Tonle Sap is a flood-pulsed ecosystem that experiences dramatic seasonal variability, and this variability is not included in our model. Seasonal flooding has the effect of increasing the extent of the lake more than five-fold and switching functionally

between a primarily aquatic and primarily terrestrial system (Holtgrieve *et al.* 2013). Our parameterization comes from wet season estimates, but the equilibrium ecosystem state represented is not representative of a system that is in reality, never in equilibrium. Specifically, this is likely why model-derived trophic level estimates do not correspond with those estimated from stable isotope data: stable isotopes were collected across wet and dry seasons and therefore represent a greater range of variability than our model is able to simulate. More broadly, the absence of this flood-pulse dynamic from our model likely contributes to the propensity of species to go extinct; flooding promotes migration, and there is evidence dispersal ability can foster stable coexistence (Tilman 1994).

TABLES

Table 4.1 - Equations governing the size-spectrum model, where i denotes species groups, R_x denotes resource spectra, m denotes predator weight, m_p denotes prey weight, and j denotes prey fish.

#	Equation	Description
Dynamics		
1	$\frac{\partial N_{R_x}}{\partial t} = r_0 m^{p-1}[\kappa_X m^{-\lambda} - N_{R_x}(m,t)] - \mu_p(m) N_{R_x}(m,t)$	Resource dynamics
2	$\frac{\partial N_i(m)}{\partial t} + \frac{\partial g_i(m) N_i(m)}{\partial m} = -\mu_i(m) N_i(m)$	Conservation equation
Consumption		
3	$\mathsf{N}_{i,R}(m) = \sum_{k=1,2} \theta_{i,R_k} N_{R_k}(m)$	Density of resource prey for species group i individuals of mass m
4	$\mathsf{N}_{i,P}(m) = \sum_j \theta_{i,j} N_j(m)$	Density of fish prey for species group i individuals of mass m
5	$s_i(m_p, m) = \exp\left[-\left(\ln\left(\frac{\beta_i m_p}{m} \right) \right)^2 / (2\sigma_i^2) \right]$	Size-dependent feeding kernel
6	$\phi_{i,R}(m) = \sum_k \int w_p \mathsf{N}_{R_k}(w_p) s_i(w_p, m) dw_p$	Available food from resource spectrum
7	$\phi_{i,P}(m) = \sum_j \int w_p \mathsf{N}_{i,j}(w_p) s_i(w_p, m) dw_p$	Available food from other fish spp.
8	$v(m) = \gamma m^q$	Volumetric search rate
9	$f_{i,l}(m) h_i m^n = \frac{v(m)\phi_{i,l}(m)}{v(m)\phi_i(m) + h_i m^n} h_i m^n$	Food consumption
Energy		
10	$E_a(m) = \alpha f_i(m) h_i m^n - k_s m^p$	Energy remaining after catabolism
11	$\psi(\frac{m}{W_{\infty,i}}) = H\left(\frac{\eta_m W_{\infty,i}}{m} \right)\left(\frac{m}{W_{\infty,i}} \right)^{1-n}$	Allocation of energy to reproduction
12	$g_i(m) = E_a(m)\left(1 - \psi\left(\frac{m}{W_{\infty,i}} \right) \right)$	Somatic growth
13	$R_i = \frac{\varepsilon}{2w_0} \int_{w_0}^{W_{\infty,i}} E_a(w) \psi\left(\frac{w}{W_{\infty,i}} \right) N_i(w) \mathrm{d}w$	Egg production
14	$R = R_{0,i} \frac{R_i}{R_i + R_{0,i}}$	Density-dependent recruitment
15	$R_{0,i} = \kappa_r (\alpha f_0 h_i w_0^n k_s w_o^p) W_{\infty,i}^{2n-q-3+a} (W_{\infty,i} - W_{\infty,i-1})$	Unfished recruitment

16	$H(z) = (1 + z^{-10})^{-1}$	Size selection function
Mortality		
17	$\mu_p(m_p) = \int_{w_0}^{W_{\infty,5}} \phi\left(\frac{m_p}{w}\right)(1 - f(w))\gamma w^q \sum_i N_i(w)\mathrm{d}w$	Predation mortality
18	$\mu_b = \mu_0 W_{\infty,i}^{n-1}$	Background mortality
19	$\mu_s(m) = \{$ $0,\ E_a(m) > 0$ $\frac{k_s m^p - \alpha f(m) h_i m^n}{\xi m},\ E_a(m) < 0$	Starvation mortality

Table 4.2 - Parameter values used in the model. General model parameters taken from Jacobsen et al. (2013), except where specified. When five values are provided, parameters are species-specific. In matrices, columns denote prey/resources and rows denote predator species groups.

Parameter name	Notation	Value(s)
Asymptotic maximum weight	$W_{\infty,i}$	$(33.75, 83.41, 4.81e^4, 1.00e^4, 2.89e^4)$
Resource feeding preference	Θ_{R_x}	$\begin{Bmatrix} 0 & 1 \\ 1 & 1 \\ 0.1 & 0.3 \\ 0 & 0.3 \\ 1 & 0 \end{Bmatrix}$
Piscivory feeding preference	Θ	$\begin{Bmatrix} 0.1 & 0 & 0 & 0 & 0 \\ 0 & 0.1 & 0 & 0 & 0.1 \\ 0.8 & 0.8 & 0.8 & 0.8 & 0.1 \\ 0.8 & 0 & 0 & 0.8 & 0 \\ 0 & 0.05 & 0 & 0 & 0.05 \end{Bmatrix}$
Predator-prey mass ratio	β_i	(100,100,100,100, 1000)
Width of feeding kernel	σ_i	(1.3,1.3,1.3,1.3,7)
Maximum consumption factor	h_i	(20,20,50,28,20)
Maximum consumption exponent	n	0.75
Anabolic coefficient	α	0.6
Catabolic coefficient	k_s	$2.4\, g^{1-p} yr^{-1}$
Size at 50% maturity relative to W_∞	η_m	0.25
Gonad efficiency	ε	0.1
Resource carrying capacity	κ_{R_x}	$0.0001 g^{\lambda-1} m^{-3}$
Relative recruitment carrying capacity	κ_r	$2e^4 g^{\lambda-1} m^{-3}$
Equilibrium feeding level	f_0	0.6
Catabolic exponent	p	0.75
Search volume exponent	q	0.8
Expected mortality/growth ratio	a	0.66
Search volume factor	γ	$29.2 g^{-q} yr^{-1}$
Background mortality coefficient	μ	$2 g^{1-n} yr^{-1}$
Fraction of energy allocated to reproduction	ξ	0.1
Resource growth rate	r_0	$4 r^{1-p} yr^{-1}$
Resource growth exponent	λ	2.05

Table 4.3 - Parameter values for evaluated sensitivity cases. Values in bold denote those used in the base model configuration.

Parameter	**Values**
c	(**.25**,0.5, 0.75)
$\Theta_{3,j}$	(0,1,1,0,0); **(0.8,0.8,0.8,0.8,0.4)**; (0.6,0.6,0.6,0.6,0.3)
$\Theta_{4,j}$	(1,0,0,1,0) ;(**0.8,0,0,0.8,0)** ;(0.6,0.6,0.6,0.6,0.3)
F	(0,**2**,2.5)

Table 4.4 - Relative biomass from each of the data sources (Sopha & van Zalinge 2001; Hortle, K.G., Lieng, S., Valbo-Jorgensen 2004; MRC 2010) and model estimates under different sources of uncertainty (κ ratio [*c*], diet composition of predators, and fishing [*F*].)

Source	*Channa*:*Henicorhynchus*	*Pangasius*:*Henicorhynchus*
Hortle et al. 2004	0.40 - 1.45	0.05 - 0.73
MRC 2010	0.095 - 0.52	0.14
Sopha and van Zalinge, 2001	N/A	0.06
Base	1.010E-04	1.131E-03
Mid *c*	1.165E-04	3.614E-03
High *c*	1.064E-04	4.473E-03
No *F*	2.018E-04	1.951E-03
High *F*	9.148E-05	2.990E-07
General diet	1.015E-04	1.279E-03
Specialist diet	1.060E-04	4.768E-04

FIGURES

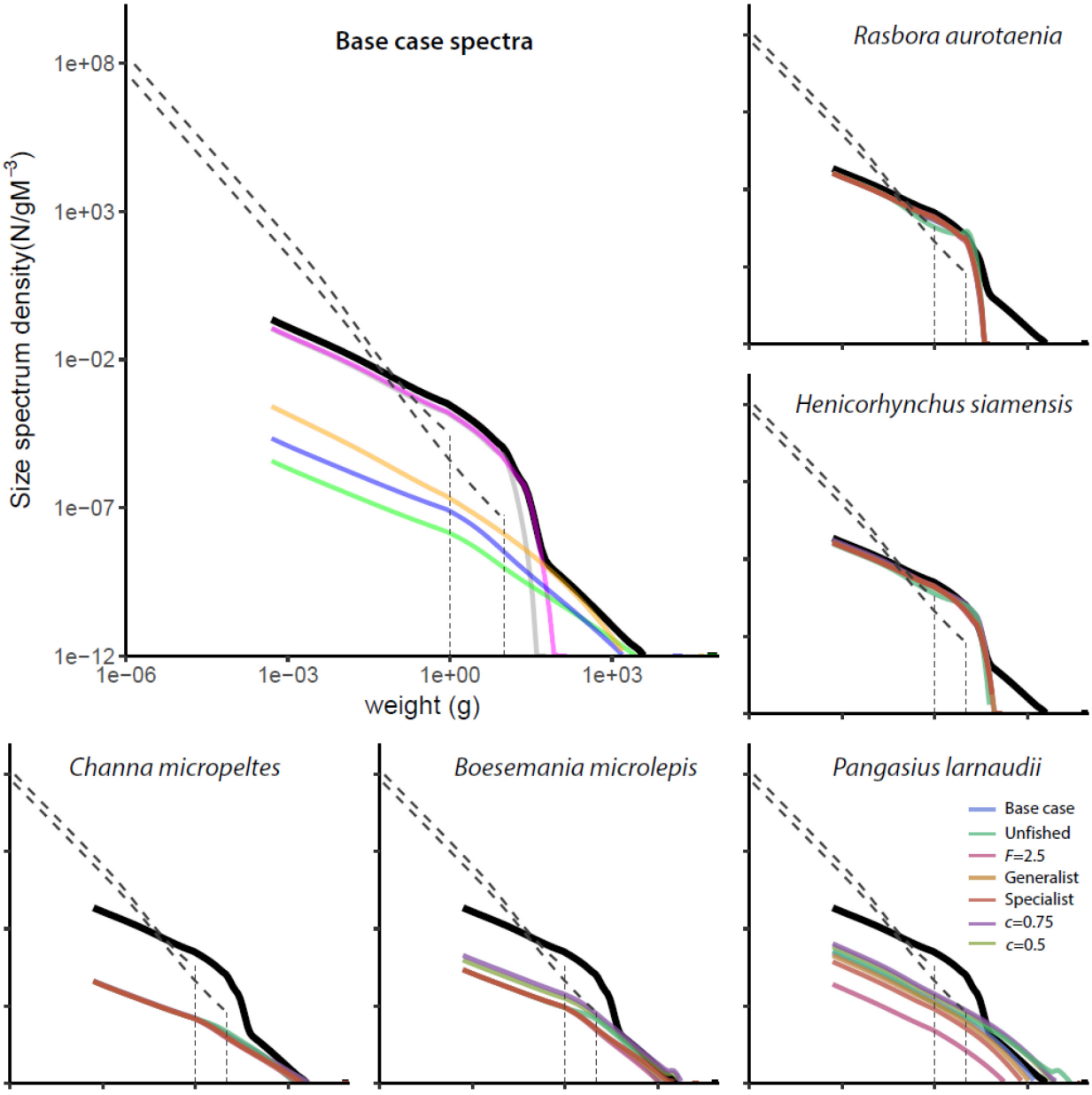

Figure 4.1 - Size spectra across scenarios. Gray dashed lines represent the two resource spectra. Gray is *Rasbora*, pink is *Henicorhynchus*, green is *Channa*, blue is *Boesemania*, and orange is *Pangasius*. Black is the community (total) size spectrum. Size spectrum and resource spectra from base case plotted on species-specific plots to facilitate comparison.

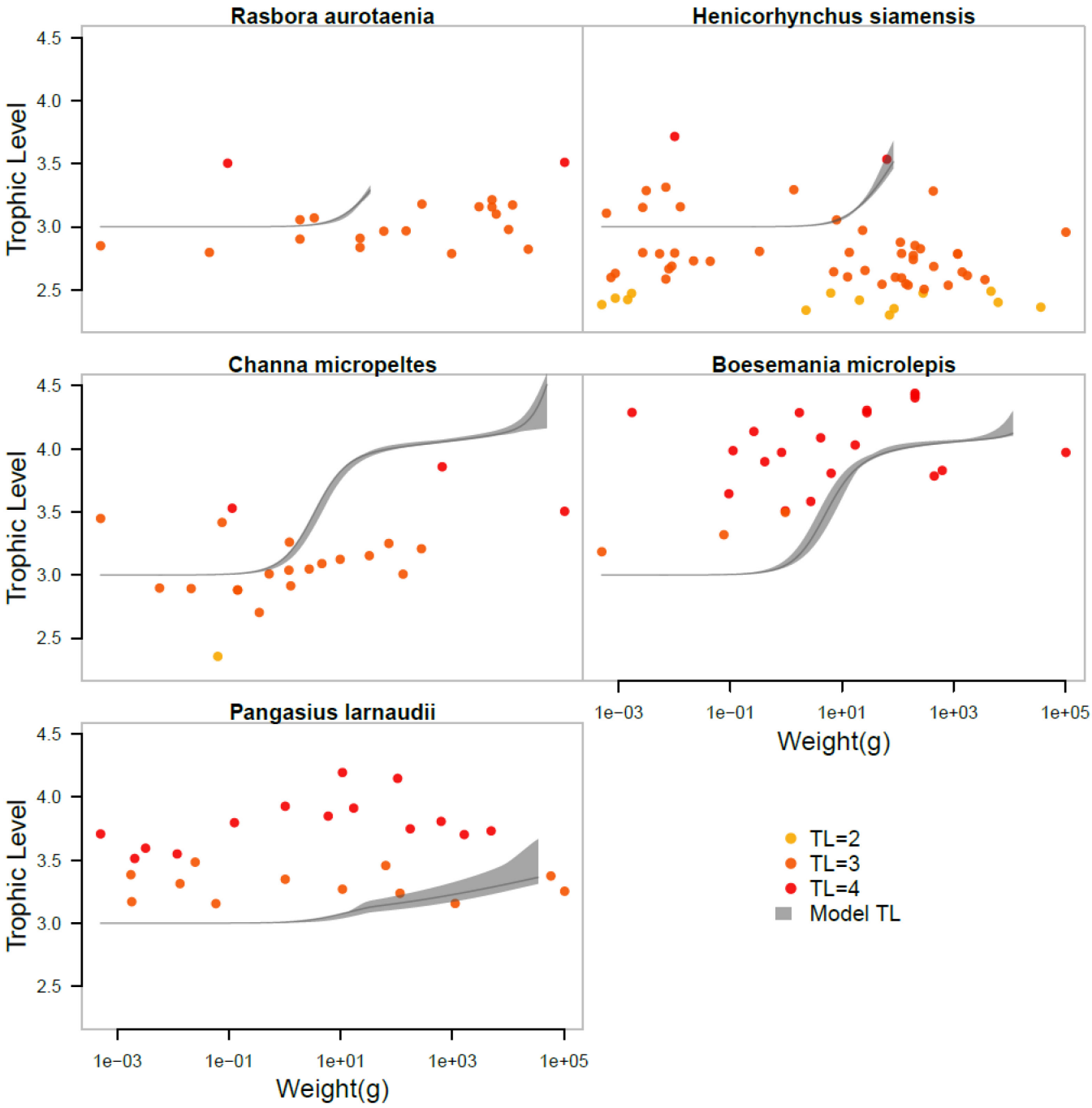

Figure 4.2 - Comparison of calculated trophic level (rounded to nearest integer value) from empirical measurements of $\delta^{15}N$ (yellow, orange, red points) and model-predicted trophic level (gray region) across sensitivity ranges.

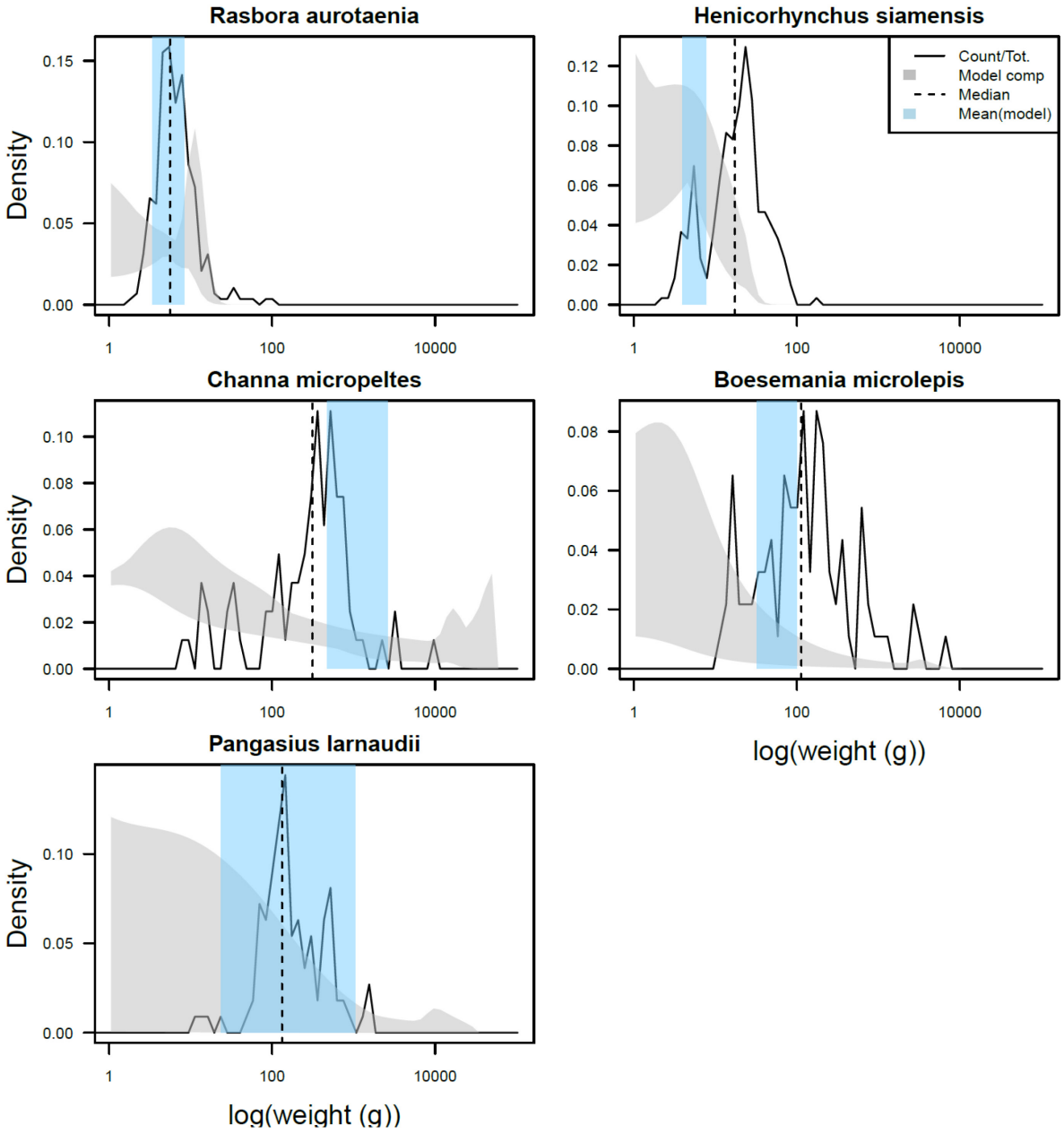

Figure 4.3 - Comparison of empirical weight distribution (black line) and median weight (black dashed line) with model output weight composition (gray) and mean weight (blue shaded area) ranges across sensitivity ranges.

Synthesis

While writing this dissertation, I've explored the benefits and drawbacks of many different approaches to specify size and growth dynamics in fish population models. By looking through a variety of models through this narrow lens, several broader considerations that are applicable to any type of population modeling and science-based population management have become apparent. The first is the importance and challenge of considering different sources of observation error and process error when analyzing ecological data. The second is the importance of considering all sources of variability, rather than assuming the most variable process is the most amenable to modeling approaches. The third theme is the value and power of mechanistic understandings of drivers of life history processes as it relates to population forecasting. Finally, some insights on bridging the gap between understanding the ecological processes that influence populations and providing the best scientific management recommendations.

Even when length-at-age data are abundant, changes in somatic growth may be difficult to quantify, but advanced statistical techniques (i.e. random effects, state-space models) are promising. Changes in annual observations of size-at-age (if not from mark-recapture data) may not reflect temporal changes in growth but rather temporal variation in fishery or survey selectivity (Thorson and Simpfendorfer 2009), the effect of removal of larger, faster-growing individuals by fishing (Hilborn and Minte-Vera 2008), ageing error (Cope and Punt 2007), effects of spatial changes in sampling (Campana et al. 1995), biases introduced by non-random subsampling of length data (Bettoli and Miranda 2001), and, of course, human error. With so many potential sources of bias, it is understandable why many population models include only observation error in the growth process. However, unmodeled process error in somatic growth

can lead to biased population estimates, or an underestimate of uncertainty. Fortunately, modern statistical techniques can account for many of these potential sources of bias. State-space models allow for simultaneous estimation of observation and process error (de Valpine and Hastings 2002) and can therefore help distinguish between biological and observation-driven changes in growth, particularly when data from multiple sources are available. Secondly, random effects on growth parameters may be used to account for variation across time and space and propagate the effects of this variation as uncertainty in population estimates (Bolker et al. 2009). As I show in Chapter 1, these tools can effectively be used to quantify variation in growth. More broadly, they are immensely useful when modeling many types of ecological data (i.e. count data, presence/absence data) and should be applied more frequently when fitting population models.

A key takeaway from this work is that it can be important from an ecological perspective to consider all sources of demographic variation influencing populations, even when some are larger in magnitude than others. Despite ample evidence recruitment is highly variable and drives much of the variation in fish populations (Cushing 1995), I found growth variation could induce as large fluctuations in several species (Chapter 2) and that population estimates of Petrale sole (*Eopsetta jordani*) were sensitive to growth variation (Chapter 3). This suggests, when data are available, it is important to account for multiple sources of variation. Current momentum towards increased ecosystem-based models (which implicitly include growth and mortality variation) suggest many fishery scientists adhere to this view (Pikitch et al. 2004). The next step along this progression is considering covariation between vital rates. Mortality scales with size (Jennings et al. 2001), so growth and mortality likely covary, and this is captured in size-structured models (Gaichas et al. 2010). It is quite possible growth and recruitment also covary, though this covariation could be positive or negative. Growth (Black et al. 2008) and recruitment

(Cushing 1982) of marine fish have both been shown to increase during times of abundance. In cannibalistic species, however, growth and recruitment may be anti-correlated (Wespestad et al. 2000), since adults predating on pre-recruits could grow faster but decrease recruitment. Further work is needed to determine if this covariation is important and/or feasible to consider when simulating or fitting population models.

It is important to continue to develop mechanistic understandings of how climate changes affect growth of marine fish. Some expect warming oceans will correlate with a unilateral decrease in size of marine fish (Cheung et al. 2012, Baudron et al. 2014) due to oxygen limitation. However, whether growth rates increase or decrease in warming oceans could be species- and ecosystem-specific, depending on whether they prefer cold or warm thermal regimes. Some species (i.e. walleye pollock) thrive on more nutritious prey associated with colder waters (Coyle et al. 2011) and therefore might have decreased growth rates as oceans warm. Conversely, yelloweye rockfish have been shown to increase growth rates during warm ocean periods (Black et al. 2008).

Since I've shown growth variation can impact populations, incorporating drivers of variation in population models could be important for forecasting to facilitate strategic management of fisheries. Incorporating empirical data on how growth varies in population models may produce accurate estimates of current population status (Kuriyama et al. 2016). However, only an approach that incorporates mechanistic relationships between growth rates and drivers may accurately project changes in fish populations in response to density-dependent and -independent processes. Incorporating density-dependent growth could yield more conservative estimates of increases and decreases in populations (Helser and Almeida 1997), since growth rates and biomass are inversely correlated. Growth rate responses to climate change could yield

either directional population change (Black et al. 2008, Baudron et al. 2014) or an increase in prediction uncertainty via propagation of uncertainty in climate forecasts. Only including mechanistic relationships for growth variability within population models can ensure population predictions account for these effects.

Finally, although it is important to understand multiple sources of demographic stochasticity influence population variability, in practice, analysts providing management advice must adapt their model scope to the situation. The problem of deciding what scale ecological models should aim to capture is well-known (Levin 1988), and adding the need to manage populations only increases the stakes of this decision. Often there is an implicit assumption that the better a model represents real-world dynamics, the better suited it is for provision of management advice. However, my findings (Chapter 3) demonstrate a model with simplified growth deviations can provide equally precise and accurate management recommendations as a model that matches "reality". Similarly, in Chapter 4, I showed that it was difficult to parameterize a size-structured model with low data. These illustrate a broader point: increasing model complexity does not necessarily increase the quality of management advice. Managers should prefer avoiding including too many untested assumptions (i.e. specifying time blocks for growth variation; scaling unknown rates with size). Though my work didn't show this, others have found there can even be detriments to specifying too much variation if it is not experienced by the population (Jiao et al. 2012). How much complexity is too much varies greatly across data availability and potentially life history: I recommend petrale sole, a slow-growing, high-data species, could be managed based on a complex integrated assessment model that incorporates both interannual growth and recruitment variation, while Tonle Sap lake, a low-data system, may

not gain much in the way of improved decision-making from adding size-structure to a population model.

In conclusion, my dissertation sums up the delicacy and thoughtfulness required of analysts, spanning theoretical ecologists to fishery stock assessment authors, who seek to model population dynamics. As data availability increases, scientists must take care to accurately adapt the model scale to the data, to consider all alternative ways stochasticity might drive population variability, and to ensure that observation error and process error are both adequately considered. The recent direction towards advanced methods of incorporating variability (random effects) and considerations of multiple population drivers (ecosystem models) is very promising. However, along this forward progression, it seems scientists may become overzealous and apply advanced statistical or modeling tools without fully understanding the drawbacks of overparameterizing population models. Learning to find "the sweet spot" of model complexity is the work of a full career, and I know throughout this dissertation I have only scratched the surface. However, my explorations into the impact of growth and size dynamics on populations in this dissertation have provided a practical "crash course" in tradeoffs associated with population modeling. Perhaps the thing I will take from my graduate experience the most is remembering to be hopeful regarding the potential modeling approaches have to aid decision-making, but humble regarding their capacity to reflect reality.

Works Cited

A'mar, T., and W. Palsson. 2014. Assessment of the Pacific cod stock in the Gulf of Alaska. North Pacific Fishery Management Council, Anchorage, AK.

Andersen, K. H., and J. E. Beyer. 2006. Asymptotic Size Determines Species Abundance in the Marine Size Spectrum. The American Naturalist **168**:54-61.

Andersen, T., J. Carstensen, E. Hernández-García, and C. M. Duarte. 2009. Ecological thresholds and regime shifts: approaches to identification. Trends in Ecology & Evolution **24**:49-57.

Anderson, S. C., C. C. Monnahan, K. F. Johnson, K. Ono, and J. L. Valero. 2014. ss3sim: an R package for fisheries stock assessment simulation with Stock Synthesis. Plos One **9**:e92725.

Ando, T. 2007. Bayesian predictive information criterion for the evaluation of hierarchical Bayesian and empirical Bayes models. Biometrika **94**:443-458.

Baudron, A. R., C. L. Needle, A. D. Rijnsdorp, and C. Tara Marshall. 2014. Warming temperatures and smaller body sizes: synchronous changes in growth of North Sea fishes. Global Change Biology **20**:1023-1031.

Baum, J. K., and B. Worm. 2009. Cascading top-down effects of changing oceanic predator abundances. Journal of Animal Ecology **78**:699-714.

Beamish, R. J. 1979a. Differences in the age of Pacific hake (*Merluccius productus*) using whole otoliths and sections of otoliths. Journal of the Fisheries Research Board of Canada **36**:141-151.

Beamish, R. J. 1979b. New information on the longevity of Pacific ocean perch (*Sebastes alutus*). Journal of the Fisheries Research Board of Canada **36**:1395-1400.

Berger, A., C. J. Grandin, I. G. Taylor, A. M. Edwards, and S. Cox. 2017. Status of the Pacific Hake (whiting) stock in U.S. and Canadian waters in 2017. Joint Technical Committee of the U.S. and Canada Pacific Hake/Whiting Agreement; National Marine Fishery Service; Canada Department of Fisheries and Oceans.

Bertalanffy, L. v. 1938. A quantitative thory of organic growth (Inquiries on growth laws. II). Human Biology **10**:181-213.

Bertalanffy, L. v. 1957. Quantitative laws in metabolism and growth. The Quarterly Review of Biology **32**:217-231.

Bettoli, P. W., and L. E. Miranda. 2001. Cautionary note about estimating mean length at age with subsampled data. North American Journal of Fisheries Management **21**:425-428.

Beverton, R. J. H. 1992. Patterns of reproductive strategy parameters in some marine teleost fishes. Journal of Fish Biology **41**:137-160.

Beverton, R. J. H., and S. J. Holt. 1957. On the Dynamics of Exploited Fish Populations. Springer.

Bjorndal, K. A., A. B. Bolten, and M. Y. Chaloupka. 2000. Green turtle somatic growth model: evidence for density dependence. Ecological Applications **10**:269-282.

Black, B. A. 2009. Climate-driven synchrony across tree, bivalve, and rockfish growth-increment chronologies of the northeast Pacific. Marine Ecology Progress Series **378**:37-46.

Black, B. A., G. W. Boehlert, and M. M. Yoklavich. 2008. Establishing climate–growth relationships for yelloweye rockfish (*Sebastes ruberrimus*) in the northeast Pacific using a dendrochronological approach. Fisheries Oceanography **17**:368-379.

Bolker, B. M., M. E. Brooks, C. J. Clark, S. W. Geange, J. R. Poulsen, M. H. H. Stevens, and J.-S. S. White. 2009. Generalized linear mixed models: a practical guide for ecology and evolution. Trends in Ecology & Evolution **24**:127-135.

Breiman, L., J. Friedman, C. J. Stone, and R. A. Olshen. 1984. Classification and Regression Trees. Chapman and Hall/CRC.

Buckland, S. T., K. B. Newman, L. Thomas, and N. B. Koesters. 2004. State-space models for the dynamics of wild animal populations. Ecological Modelling **171**:157-175.

Campana, S. E. 2001. Accuracy, precision and quality control in age determination, including a review of the use and abuse of age validation methods. Journal of Fish Biology **59**:197-242.

Campana, S. E., R. K. Mohn, S. J. Smith, and G. A. Chouinard. 1995. Spatial implications of a temperature-based growth model for Atlantic cod (*Gadus morhua*) off the eastern coast of Canada. Canadian Journal of Fisheries and Aquatic Sciences **52**:2445-2456.

Caswell, H. 1988. Theory and models in ecology: a different perspective. Ecological Modelling **43**:33-44.

Caswell, H., R. M. Nisbet, A. m. De Roos, and S. Tuljapurkar. 1997. Structured population models: many methods, a few basic concepts. . Chapman & Hall.

Chapman, D. G. 1961. Statistical Problems in Dynamics of Exploited Fisheries Populations. Pages 153-168. University of California Press.

Charnov, E. L., H. Gislason, and J. G. Pope. 2013. Evolutionary assembly rules for fish life histories. Fish and Fisheries **14**:213-224.

Cheung, W. L., L. S. Jorge, D. John, L. F. Thomas, W. Y. L. Vicky, M. L. D. Palomares, W. Reg, and D. Pauly. 2012. Shrinking of fishes exacerbates impacts of global ocean changes on marine ecosystems. Nature Climate Change **3**:254-258.

Clark, J. S. 2004. Why environmental scientists are becoming Bayesians. Ecology Letters **8**:2-14.

Clark, W. G., S. R. Hare, A. M. Parma, P. J. Sullivan, and R. J. Trumble. 1999. Decadal changes in growth and recruitment of Pacific halibut (*Hippoglossus stenolepis*). Canadian Journal of Fisheries and Aquatic Sciences **56**:242-252.

Cloern, J. E., and F. H. Nichols. 1978. A von Bertalanffy growth model with a seasonally varying coefficient. Journal of the Fisheries Research Board of Canada **35**:1479-1482.

Cope, J. M., and A. E. Punt. 2007. Admitting ageing error when fitting growth curves: an example using the von Bertalanffy growth function with random effects. Canadian Journal of Fisheries and Aquatic Sciences **64**:205-218.

Costantino, R. F., R. A. Desharnais, J. M. Cushing, and B. Dennis. 1997. Chaotic dynamics in an insect population. Science **275**:389-391.

Coyle, K. O., L. B. Eisner, F. J. Mueter, A. I. Pinchuk, M. A. Janout, K. D. Cieciel, E. V. Farley, and A. G. Andrews. 2011. Climate change in the southeastern Bering Sea: impacts on pollock stocks and implications for the oscillating control hypothesis. Fisheries Oceanography **20**:139-156.

Cushing, D. H. 1982. Climate and Fisheries. Academic Press, London; New York.

Cushing, D. H. 1995. Population production and regulation in the sea : a fisheries perspective. Cambridge University Press, Cambridge ; New York.

de Valpine, P., and A. Hastings. 2002. Fitting population models including process noise and observation error. Ecological Monographs **72**:57-76.

DeFries, R. S., J. A. Foley, and G. P. Asner. 2004. Land-use choices: balancing human needs and ecosystem function. Frontiers in Ecology and the Environment **2**:249-257.

Denney, N. H., S. Jennings, and J. D. Reynolds. 2002. Life–history correlates of maximum population growth rates in marine fishes. Proceedings of the Royal Society of London. Series B: Biological Sciences **269**:2229-2237.

Doney, S. C., and S. F. Sailley. 2013. When an ecological regime shift is really just stochastic noise. Proc Natl Acad Sci U S A **110**:2438-2439.

Durbin, J., and S. J. Koopman. 2012. Time Series Analysis by State Space Methods: Second Edition. Oxford University Press.

Field, J. C. 2007. Status of the Chilipepper rockfish, *Sebastes goodei*, in 2007. Pacific Fishery Management Council, Portland, OR.

Fry, F. E. J. 1971. The effect of environmental factors on the physiology of fish. Pages 1-98 *in* W. S. Hoar and D. J. Randall, editors. Fish Physiology: Volume 6: Environmental relations and behavior. Academic Press, Inc., New York, NY.

Fu, C., and T. J. Quinn, II. 2000. Estimability of natural mortality and other population parameters in a length-based model: *Pandalus borealis* in Kachemak Bay, Alaska. Canadian Journal of Fisheries and Aquatic Sciences **57**:2420-2432.

Fulton, E. A., J. S. Link, I. C. Kaplan, M. Savina-Rolland, P. Johnson, C. Ainsworth, P. Horne, R. Gorton, A. D. M. Smith, and D. C. Smith. 2011. Lessons in modelling and management of marine ecosystems: the Atlantis experience. Fish and Fisheries **12**:171-188.

Gaichas, S. K., K. Y. Aydin, and R. C. Francis. 2010. Using food web model results to inform stock assessment estimates of mortality and production for ecosystem-based fisheries management. Canadian Journal of Fisheries and Aquatic Sciences **67**:1490-1506.

Gårdmark, A., N. Jonzén, and M. Mangel. 2006. Density-dependent body growth reduces the potential of marine reserves to enhance yields. Journal of Applied Ecology **43**:61-69.

Gelman, A., and D. B. Rubin. 1992. Inference from iterative simulation using multiple sequences. Statistical Science **7**:457-472.

Gertseva, V. V., J. M. Cope, and S. E. Matson. 2010. Growth variability in the splitnose rockfish, *Sebastes diploproa,* of the northeast Pacific Ocean: pattern revisited. Marine Ecology Progress Series **413**:125-136.

Goodyear, C. P. 1995. Mean size at age: an evaluation of sampling strategies with simulated red grouper data. Transactions of the American Fisheries Society **124**:746-755.

Gunderson, D. R., and R. D. Vetter. 2006. Temperate rocky reef fishes. Pages 69–117 *in* J. P. Kritzer and P. F. Sale, editors. Marine Metapopulations. Elsevier Academic Press, Burlington, MA.

Hagen, P. T., and T. J. Quinn. 1991. Long-term growth dynamics of young Pacific halibut: evidence of temperature-induced variation. Fisheries Research **11**:283-306.

Hairston, N. G., F. E. Smith, and L. B. Slobodkin. 1960. Community structure, population control, and competition. The American Naturalist **94**:421-425.

Haltuch, M. A., O. S. Hamel, K. R. Piner, P. McDonald, C. R. Kastelle, and J. C. Field. 2013a. A California Current bomb radiocarbon reference chronology and petrale sole (*Eopsetta jordani*) age validation. Canadian Journal of Fisheries and Aquatic Sciences **70**:22-31.

Haltuch, M. A., K. Ono, and J. L. Valero. 2013b. Status of the U.S. petrale sole resource in 2012. Pacific Fishery Management Council, Portland, OR.

Hamel, O. S., K. R. Piner, and J. R. Wallace. 2008. A robust deterministic model describing the bomb radiocarbon signal for use in fish age validation. Transactions of the American Fisheries Society **137**:852-859.

Hansen, M. J., D. Boisclair, S. B. Brandt, S. W. Hewett, J. F. Kitchell, M. C. Lucas, and J. J. Ney. 1993. Applications of bioenergetics models to fish ecology and management: Where do we go from here? Transactions of the American Fisheries Society **122**:1019-1030.

Hare, S. R. 2010. Assessment of the Pacific halibut stock at the end of 2010. International Pacific Halibut Commission.

Hartvig, M., K. H. Andersen, and J. E. Beyer. 2011. Food web framework for size-structured populations. Journal of Theoretical Ecology **272**:113 - 122.

He, X., D. E. Pearson, E. J. Dick, J. C. Field, R. Ralston, and A. D. MacCall. 2011. Status of the widow rockfish resource in 2011. Pacific Fishery Management Council, Portalnd, OR.

Helser, T. E., and F. P. Almeida. 1997. Density-dependent growth and sexual maturity of silver hake in the north-west Atlantic. Journal of Fish Biology **51**:607-623.

Helser, T. E., and J. K. T. Brodziak. 1998. Impacts of density-dependent growth and maturation on assessment advice to rebuild depleted U.S. silver hake (*Merluccius bilinearis*) stocks. Canadian Journal of Fisheries and Aquatic Sciences **55**:882-892.

Helser, T. E., R. D. Methot Jr, and G. W. Fleischer. 2004. Stock assessment of Pacific hake (whiting) in U.S. and Canadian waters in 2003. Pacific Fishery Management Council, Portland, OR.

Hendry, A. P., T. Day, and A. B. Cooper. 2001. Optimal size and number of propagules: allowance for discrete stages and effects of maternal size on reproductive output and offspring fitness. The American Naturalist **157**:387-407.

Henson, S. M., and J. M. Cushing. 1997. The effect of periodic habitat fluctuations on a nonlinear insect population. Journal of Mathematical Biology **36**:201-226.

Hilborn, R., and M. Mangel. 1997. The Ecological Detective: Confronting Models with Data. Princeton University Press, Princeton, NJ, USA.

Hilborn, R., and C. V. Minte-Vera. 2008. Fisheries-induced changes in growth rates in marine fisheries: Are they significant? Bulletin of Marine Science **83**:95-105.

Hixon, M. A., W. J. Darren, and S. Sogard, M. 2014. BOFFFFs: On the importance of conserving old-growth age structure in fishery populations. ICES Journal of Marine Science **71**:2171-2185.

Hixon, M. A., and G. P. Jones. 2005. Competition, predation, and density-dependent mortality in demersal marine fishes. Ecology **86**:2847-2859.

Hjort, J. 1914. Fluctuations in the great fisheries of northern Europe. Rapports et procesverbaux, Conseil permanent international pour l'exploration de la mer **20**.

Hollowed, A. B., N. Bax, R. Beamish, J. Collie, M. Fogarty, P. Livingston, J. Pope, and J. C. Rice. 2000. Are multispecies models an improvement on single-species models for measuring fishing impacts on marine ecosystems? ICES Journal of Marine Science: Journal du Conseil **57**:707-719.

Hollowed, A. B., S. R. Hare, and W. S. Wooster. 2001. Pacific Basin climate variability and patterns of Northeast Pacific marine fish production. Progress in Oceanography **49**:257-282.

Hsieh, C.-h., A. Yamauchi, T. Nakazawa, and W.-F. Wang. 2009. Fishing effects on age and spatial structures undermine population stability of fishes. Aquatic Sciences **72**:165-178.

Hurst, T. P., A. A. Abookire, and B. Knoth. 2010. Quantifying thermal effects on contemporary growth variability to predict responses to climate change in northern rock sole (*Lepidopsetta polyxystra*). Canadian Journal of Fisheries and Aquatic Sciences **67**:97-107.

Hyndman, R. J., and Y. Khandakar. 2007. Automatic time series forecasting: the forecast package for R. Department of econometrics and business statistics., Monash University.

Ianelli, J. N., T. Honkalehto, S. Barbeaux, B. Fissel, and S. Kotwicki. 2016. Assessment of the walleye pollock stock in the Eastern Bering Sea. North Pacific Fishery Management Council, Anchorage, AK.

Ianelli, J. N., T. Honkalehto, S. Barbeaux, and S. Kotwicki. 2014. Assessment of the walleye pollock stock in the Eastern Bering Sea. North Pacific Fishery Management Council, Anchorage, AK.

Iles, T. D., and M. Sinclair. 1989. Population regulation and speciation in the oceans. ICES Journal of Marine Science **45**:165-175.

Jennings, S., J. K. Pinnegar, N. V. C. Polunin, and T. W. Boon. 2001. Weak cross-species relationships between body size and trophic level belie powerful size-based trophic structuring in fish communities. Journal of Animal Ecology **70**:934-944.

Jiao, Y., E. P. Smith, R. O'Reilly, and D. J. Orth. 2012. Modelling non-stationary natural mortality in catch-at-age models. ICES Journal of Marine Science **69**:105-118.

Jones, G. P. 1987. Competitive interactions among adults and juveniles in a coral reef fish. Ecology **68**:1534-1547.

Kimura, D. K., and J. J. Lyons. 1991. Between-reader bias and variability in the age-determination process. Fishery Bulletin **89**:53-60.

Kirkwood, G. P. 1983. Estimation of von Bertalanffy growth curve parameters using both length increment and age–length data. Canadian Journal of Fisheries and Aquatic Sciences **40**:1405-1411.

Kreuz, K. F., A. V. Tyler, G. H. Kruse, and R. L. Demory. 1982. Variation in growth of Dover soles and English soles as related to upwelling. Transactions of the American Fisheries Society **111**:180-192.

Kuriyama, P. T., K. Ono, F. Hurtado-Ferro, A. C. Hicks, I. G. Taylor, R. L. Licandeo, K. F. Johnson, S. C. Anderson, C. C. Monnahan, M. B. Rudd, C. C. Stawitz, and J. L. Valero. 2016. An empirical weight-at-age approach reduces estimation bias compared to modeling parametric growth in integrated, statistical stock assessment models when growth is time varying. Fisheries Research **180**:119-127.

Lasker, R. 1981. The role of a stable ocean in larval fish survival and subsequent recruitment. Pages 80-87 Marine Fish Larvae: morphology, ecology and relation to fisheries. University of Washington Press, Seattle, WA.

Levin, S. A. 1988. Pattern, scale, and variability: An ecological perspective. Pages 1-12 *in* A. Hastings, editor. Community Ecology: A Workshop held at Davis, CA, April 1986. Springer Berlin Heidelberg, Berlin, Heidelberg.

Lin Lai, H., and D. R. Gunderson. 1987. Effects of ageing errors on estimates of growth, mortality and yield per recruit for walleye pollock (*Theragra chalcogramma*). Fisheries Research **5**:287-302.

Lorenzen, K. 1996. A simple von Bertalanffy model for density-dependent growth in extensive aquaculture, with an application to common carp (*Cyprinus carpio*). **142**:191–205.

Lorenzen, K. 2008. Fish Population Regulation Beyond "Stock and Recruitment": The Role of Density-Dependent Growth in the Recruited Stock. Bulletin of Marine Science **83**:181-196.

Lorenzen, K., and K. Enberg. 2002. Density-dependent growth as a key mechanism in the regulation of fish populations: evidence from among-population comparisons. Proceedings of the Royal Society of London. Series B: Biological Sciences **269**:49-54.

Mace, P. M., and I. J. Doonan. 1988. A generalized bioeconomic simulation model for fish population dynamics.

Mantua, N. J., and S. R. Hare. 2002. The Pacific decadal oscillation. Journal of Oceanography **58**:35-44.

Maunder, M. N., and A. E. Punt. 2013. A review of integrated analysis in fisheries stock assessment. Fisheries Research **142**:61-74.

McGowan, J. A., D. R. Cayan, and L. M. Dorman. 1998. Climate-ocean variability and ecosystem response in the Northeast Pacific. Science **281**:210-217.

Melnychuk, M. C., J. A. Banobi, and R. Hilborn. 2013. Effects of management tactics on meeting conservation objectives for Western North American groundfish fisheries. Plos One **8**:15.

Methot, R. D., Jr. 1990. Synthesis model: an adaptable framework for analysis of diverse stock assessment data. Int. N. Pac. Fish. Comm. Bull **50**:259-277.

Methot, R. D., Jr., and C. R. Wetzel. 2013. Stock synthesis: A biological and statistical framework for fish stock assessment and fishery management. Fisheries Research **142**:86-99.

Millar, R. B., B. H. McArdle, and S. J. Harley. 1999. Modeling the size of snapper (*Pagrus auratus*) using temperature-modified growth curves. Canadian Journal of Fisheries and Aquatic Sciences **56**:1278-1284.

Millar, R. B., and R. Meyer. 2000. Bayesian state-space modeling of age-structured data: fitting a model is just the beginning. Canadian Journal of Fisheries and Aquatic Sciences **57**:43-50.

Miller, R. R., J. C. Field, J. A. Santora, I. D. Schroeder, D. D. Huff, M. Key, D. E. Pearson, and A. D. MacCall. 2014. A spatially distinct history of the development of California groundfish fisheries. Plos One **9**.

Mitchell, J. C. 1988. Population ecology and life histories of the freshwater turtles *Chrysemys picta* and *Sternotherus odoratus* in an urban lake. Herpetological Monographs **2**:40-61.

Monnahan, C. C., K. Ono, S. C. Anderson, M. B. Rudd, A. C. Hicks, F. Hurtado-Ferro, K. F. Johnson, P. T. Kuriyama, R. R. Licandeo, C. C. Stawitz, I. G. Taylor, and J. L. Valero. 2016. The effect of length bin width on growth estimation in integrated age-structured stock assessments. Fisheries Research **180**:103-112.

Mueter, F. J., L. B. Jennifer, A. M. Bernard, and R. Peterman, M. 2007. Recruitment and survival of Northeast Pacific Ocean fish stocks: temporal trends, covariation, and regime shifts. Canadian Journal of Fisheries and Aquatic Sciences **64**:911-927.

Myers, R. A., and J. M. Hoenig. 1997. Direct estimates of gear selectivity from multiple tagging experiments. Canadian Journal of Fisheries and Aquatic Sciences **54**:1-9.

O'Farrell, M. R., and L. W. Botsford. 2006. The fisheries management implications of maternal-age-dependent larval survival. Canadian Journal of Fisheries and Aquatic Sciences **63**:2249-2258.

Olsen, E. M., G. R. Lilly, M. Heino, M. J. Morgan, J. Brattey, and U. Dieckmann. 2005. Assessing changes in age and size at maturation in collapsing populations of Atlantic cod (*Gadus morhua*). Canadian Journal of Fisheries and Aquatic Sciences **62**:811-823.

Ono, K., R. Licandeo, M. L. Muradian, C. J. Cunningham, S. C. Anderson, F. Hurtado-Ferro, K. F. Johnson, C. R. McGilliard, C. C. Monnahan, C. S. Szuwalski, J. L. Valero, K. A. Vert-Pre, A. R. Whitten, and A. E. Punt. 2014. The importance of length and age composition data in statistical age-structured models for marine species. ICES Journal of Marine Science: Journal du Conseil **72**:31-43.

Parma, A. M., and R. B. Deriso. 1990. Dynamics of age and size composition in a population subject to size-selective mortality: Effects of phenotypic variability in growth. Canadian Journal of Fishery and Aquatic Sciences **47**:274-289.

Pikitch, E. K., E. A. Santora, A. Babcock, A. Bakun, R. Bonfil, D. O. Conover, P. Dayton, P. Doukakis, D. Fluharty, B. Heheman, E. D. Houde, J. Link, P. A. Livingston, M. Mangel, M. K. McAllister, J. Pope, and K. Sainsbury. 2004. Ecosystem-based fishery management. Science **305**:346-347.

Pilling, G. M., G. P. Kirkwood, and S. G. Walker. 2002. An improved method for estimating individual growth variability in fish, and the correlation between von Bertalanffy growth parameters. Canadian Journal of Fisheries and Aquatic Sciences **59**:424-432.

Plummer, M. 2013. rjags: Bayesian graphical models using MCMC. R package.

Plummer, M., N. G. Best, K. Cowles, and K. Vines. 2006. CODA: Convergence diagnosis and output analysis for MCMC. Pages 7-11 R News.

Pool, T. 2017.

Quinn, T. J., and R. B. Deriso. 1999. Quantitative Fish Dynamics. Oxford University Press.

Ricker, W. E. 1954. Stock and recruitment. Journal of the Fisheries Research Board of Canada **11**:559-623.

Ricker, W. E. 1969. Effects of size-selective mortality and sampling bias on estimates of growth, mortality, production, and yield. Journal of the Fisheries Research Board of Canada **26**:479-541.

Ricker, W. E. 1975. Computation and interpretation of biological statistics of fish populations. Fisheries Research Board of Canada Bulletin **191**:382.

Rideout, M. J. M., P. A. Shelton, and M. R. 2014. An evaluation of fishing mortality reference points under varying levels of population productivity in three Atlantic cod (*Gadus morhua*) stocks. ICES Journal of Marine Science **71**:1407-1416.

Rijnsdorp, A. D., and P. I. van Leeuwen. 1992. Changes in growth of North Sea plaice since 1950 in relation to density, eutrophication, beam-trawl effort, and temperature. ICES Journal of Marine Science **3**:1199-1213.

Rogers, L. A., L. C. Stige, E. M. Olsen, H. Knutsen, K.-S. Chan, and N. C. Stenseth. 2011. Climate and population density drive changes in cod body size throughout a century on the Norwegian coast. Proceedings of the National Academy of Sciences **108**:1961-1966.

Rose, G. A., and R. L. O'Driscoll. 2002. Capelin are good for cod: can the northern stock rebuild without them? ICES Journal of Marine Science **59**:1018-1026.

Sæther, B.-E. 1997. Environmental stochasticity and population dynamics of large herbivores: a search for mechanisms. Trends in Ecology & Evolution **12**:143-149.

Sæther, B.-E., and Ø. Bakke. 2000. Avian life history variation and contribution of demographic traits to the population growth rate. Ecology **81**:642-653.

Sainsbury, K. J. 1980. Effect of individual variability on the von Bertalanffy growth equation. Canadian Journal of Fisheries and Aquatic Sciences **37**:241-247.

Schnute, J. 1981. A versatile growth model with statistically stable parameters. Canadian Journal of Fisheries and Aquatic Sciences **38**:1128-1140.

Schnute, J., and D. Fournier. 1980. A New Approach to Length–Frequency Analysis: Growth Structure. Canadian Journal of Fisheries and Aquatic Sciences **37**:1337-1351.

Shibata, R. 1976. Selection of the order of an autoregressive model by Akaike's information criterion. Biometrika **63**:117-126.

Sinclair, M. 1987. Marine populations: an essay on population regulation and speciation., Washington Sea Grant, Seattle, WA.

Solberg, E. J., B.-E. Sæther, O. Strand, and A. Loison. 1999. Dynamics of a harvested moose population in a variable environment. Journal of Animal Ecology **68**:186-204.

Spiegelhalter, D. J., N. G. Best, and B. P. Carlin. 1998. Bayesian deviance, the effective number of parameters, and the comparison of arbitratily complex models.

Stachura, M. M., T. E. Essington, N. J. Mantua, A. B. Hollowed, M. A. Haltuch, P. D. Spencer, T. A. Branch, and M. J. Doyle. 2014. Linking Northeast Pacific recruitment synchrony to environmental variability. Fisheries Oceanography **23**:389-408.

Stawitz, C. C., T. E. Essington, T. A. Branch, M. A. Haltuch, A. B. Hollowed, and P. D. Spencer. 2015a. A state-space approach for detecting growth variation and application to North Pacific groundfish. Canadian Journal of Aquatic and Fishery Sciences **72**:1316-1328.

Stawitz, C. C., F. Hurtado-Ferro, P. T. Kuriyama, J. T. Trochta, K. F. Johnson, M. A. Haltuch, and O. S. Hamel. 2015b. Stock assessment update: Status of the U.S. Petrale sole resource in 2014., Pacific Fishery Management Council, Portland, OR.

Stearns, S. C., and J. C. Koella. 1986. The evolution of phenotypic plasticity in life-history traits: predictions of reaction norms for age and size at maturity. Evolution **40**:893-913.

Stewart, I. J., R. E. Forrest, C. Grandin, O. S. Hamel, A. C. Hicks, S. J. D. Martell, and I. G. Taylor. 2011. Status of the Pacific Hake (Whiting) stock in U.S. and Canadian Waters in 2011. Pacific Fishery Management Committee, Portland, OR.

Stewart, I. J., C. C. Monnahan, and S. J. D. Martell. 2016. Assessment of the Pacific halibut stock at the end of 2015. International Pacific Halibit Commission, Seattle, WA.

Szuwalski, C. S., K. A. Vert-Pre, A. E. Punt, T. A. Branch, and R. Hilborn. 2015. Examining common assumptions about recruitment: a meta-analysis of recruitment dynamics for worldwide marine fisheries. Fish and Fisheries **16**:633-648.

Taylor, N. G., C. J. Walters, and S. J. D. Martell. 2005. A new likelihood for simultaneously estimating von Bertalanffy growth parameters, gear selectivity, and natural and fishing mortality. Canadian Journal of Fisheries and Aquatic Sciences **62**:215-223.

Thorson, J. T., and C. V. Minte-Vera. 2016. Relative magnitude of cohort, age, and year effects on size at age of exploited marine fishes. Fisheries Research **180**:45-53.

Thorson, J. T., C. C. Monnahan, and J. M. Cope. 2015. The potential impact of time-variation in vital rates on fisheries management targets for marine fishes. Fisheries Research **169**:8-17.

Thorson, J. T., and M. H. Prager. 2011. Better catch curves: Incorporating age-specific natural mortality and logistic selectivity. Transactions of the American Fisheries Society **140**:356-366.

Thorson, J. T., and C. A. Simpfendorfer. 2009. Gear selectivity and sample size effects on growth curve selection in shark age and growth studies. Fisheries Research **98**:75-84.

Travis, J. M. J., D. J. Murrell, and C. Dytham. 1999. The evolution of density–dependent dispersal. Proceedings of the Royal Society of London. Series B: Biological Sciences **266**:1837-1842.

Wallace, J. R., and J. M. Cope. 2013. Status update of the U.S. canary rockfish resource in 2011. Pacific Fishery Management Council, Portland, OR.

Walters, G. E., and T. K. Wilderbuer. 2000. Decreasing length at age in a rapidly expanding population of Northern rock sole in the eastern Bering Sea and its effect on management advice. Journal of Sea Research **44**:17-26.

Warner, R. R., and P. L. Chesson. 1985. Coexistence mediated by recruitment fluctuations: A field guide to the storage effect. The American Naturalist **125**:769-787.

Wespestad, V. G., L. W. Fritz, W. J. Ingraham, and B. A. Megrey. 2000. On relationships between cannibalism, climate variability, physical transport, and recruitment success of Bering Sea walleye pollock (*Theragra chalcogramma*). ICES Journal of Marine Science **57**:272-278.

Whitten, A. R., N. L. Klaer, G. N. Tuck, and R. W. Day. 2013. Accounting for cohort-specific variable growth in fisheries stock assessments: A case study from south-eastern Australia. Fisheries Research **142**:27-36.

Wilderbuer, T. K., and D. G. Nichol. 2014. Assessment of the Northern Rock Sole stock in the Bering Sea and Aleutian Islands. North Pacific Fishery Management Council, Anchorage, AK.

Williams, N. M., E. E. Crone, T. a. H. Roulston, R. L. Minckley, L. Packer, and S. G. Potts. 2010. Ecological and life-history traits predict bee species responses to environmental disturbances. Biological Conservation **143**:2280-2291.

Wilson, J. B. 2011. The twelve theories of co-existence in plant communities: the doubtful, the important and the unexplored. Journal of Vegetation Science **22**:184-195.

Winemiller, K. O., and K. A. Rose. 1992. Patterns of life-history diversification in North American fishes: Implications for population regulation. Canadian Journal of Fisheries and Aquatic Sciences **49**:2196-2218.

Wolter, K., and M. S. Timlin. 1993. Monitoring ENSO in COADS with a seasonally adjusted principal component index. Pages 52-57 *in* Proc. of the 17th Climate Diagnostics Workshop. NOAA/NMC/CAC, NSSL, Oklahoma Clim. Survey, CIMMS and the School of Meteor., Univ. of Oklahoma, Norman, OK.

Wolter, K., and M. S. Timlin. 1998. Measuring the strength of ENSO events - how does 1997/1998 rank? Weather **53**:315-324.

Zhao, B., J. C. McGovern, and P. J. Harris. 1997. Age, Growth, and Temporal Change in Size at Age of the Vermilion Snapper from the South Atlantic Bight. Transactions of the American Fisheries Society **126**:181-193.

APPENDIX A

Table A.1 - Ages and years included in our analysis for stocks in the Gulf of Alaska ecosystem.

Stock	Min age	Max age	Min year	Max year
arrowtooth flounder	5	35	1987	2009
dusky rockfish	12	99	1996	2010
flathead sole	8	29	1990	2011
Atka mackerel	2	9	1993	2009
northern rockfish	9	99	1984	2009
Pacific cod	2	6	1987	2011
Pacific halibut	3	28	1993	2011
Pacific ocean perch	7	55	1977	2010
rex sole	3	21	1984	2009
sablefish	6	13	1982	2011
walleye pollock	4	9	1977	2011

Table A.2 - Ages and years included in our analysis for stocks in the Bering Sea & Aleutian Islands ecosystem.

Stock	Min age	Max age	Min year	Max year
Atka mackerel	4	8	1989	2011
flathead sole	13	27	1992	2011
northern rockfish	12	29	1992	2011
Pacific ocean perch	8	34	1992	2011
Pacific cod	2	6	1988	2011
rock sole	11	19	1982	2011
sablefish	3	29	1999	2010
walleye pollock	6	13	1971	2011
yellowfin sole	11	24	1980	2011

Table A.3 - Ages and years included in our analysis for stocks in the California Current ecosystem.

Stock	Min age	Max age	Min year	Max year
arrowtooth flounder	7	19	1982	2013
bank rockfish	6	39	1978	2013
black rockfish	11	24	1974	2013
blackgill rockfish	41	59	1978	2013
canary rockfish	8	54	1968	2013
chilipepper	9	24	1978	2013
darkblotched rockfish	6	79	1977	2013
Dover sole	11	27	1965	2013
english sole	4	15	1961	2013
lingcod	3	15	1965	2013
Pacific hake	7	19	1965	2013
Pacific ocean perch	7	69	1966	2013
petrale sole	6	24	1955	2013
sablefish	14	49	1967	2013
widow rockfish	10	44	1971	2013
yelloweye rockfish	11	38	1978	2013
yellowtail rockfish	17	44	1968	2013

Table A.4 - Results of comparisons of estimated annual growth anomalies to estimated fishing mortality (F) from stock assessments; only stocks with estimated F values in the RAM legacy database were compared.

Stock assessment	**Pearson's correlation**
BSAI northern rockfish	-0.137
EBS Pacific cod	-0.0219
GOA dusky rockfish	-0.0214
GOA northern rockfish	0.166
GOA walleye pollock	-0.0317
GOA Pacific halibut	-0.212
GOA Pacific ocean perch	-0.354*
GOA Atka mackerel	0.0975
CC arrowtooth flounder	0.308
CC black rockfish N coast	-0.155
CC black rockfish S coast	0.346*
CC canary rockfish	0.0304
CC darkblotched rockfish	-0.007
CC dover sole	-0.469*
CC Pacific ocean perch	0.246
CC petrale sole	-0.283*
CC sablefish	0.0310
CC widow rockfish	-0.406*
CC yellowtail rockfish	-0.164

* indicates a significant correlation (p value <0.05) between fishing mortality and estimated annual trend.

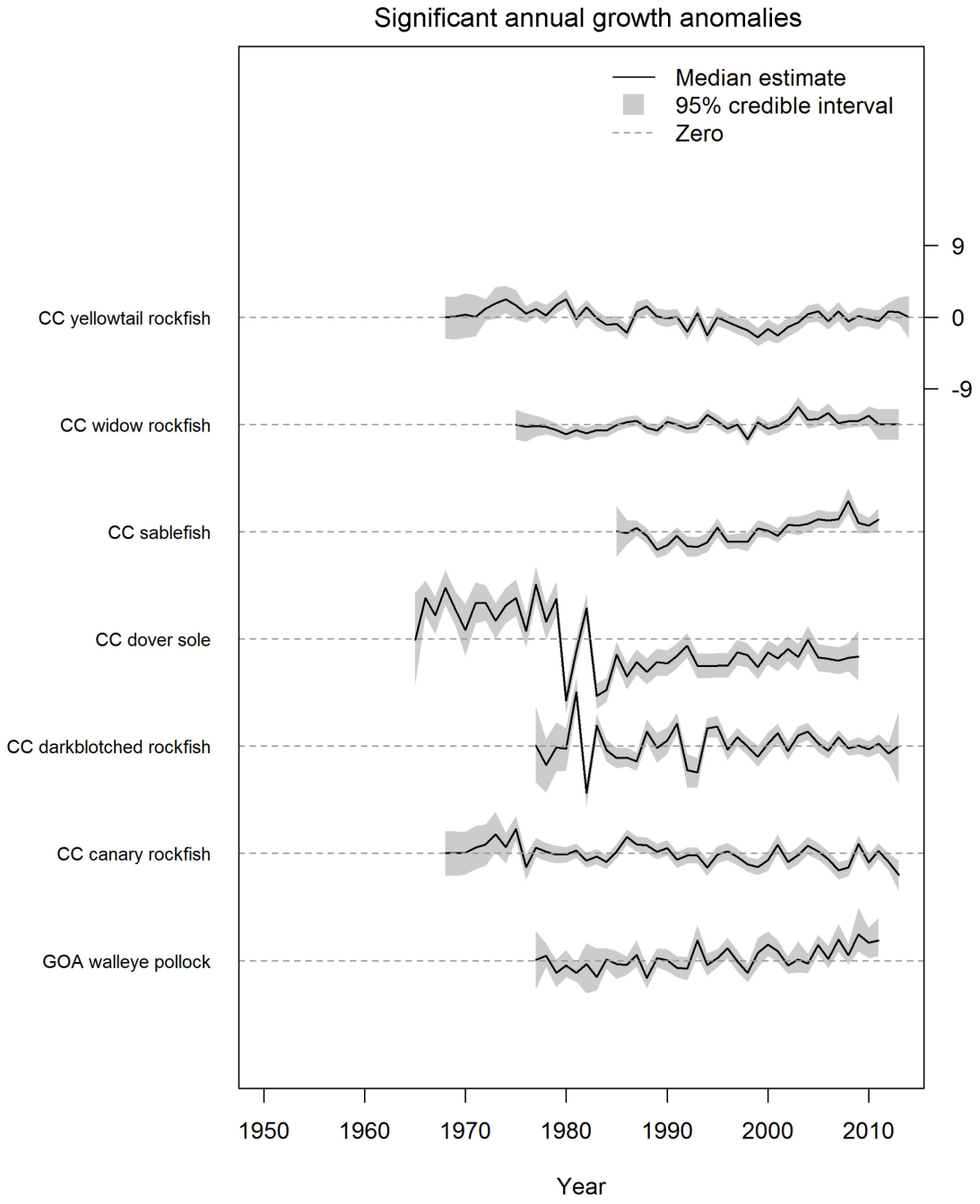

Figure A.1 - Growth anomaly estimates for stocks with significant annual growth anomalies that are not shown in Figure 1.3.

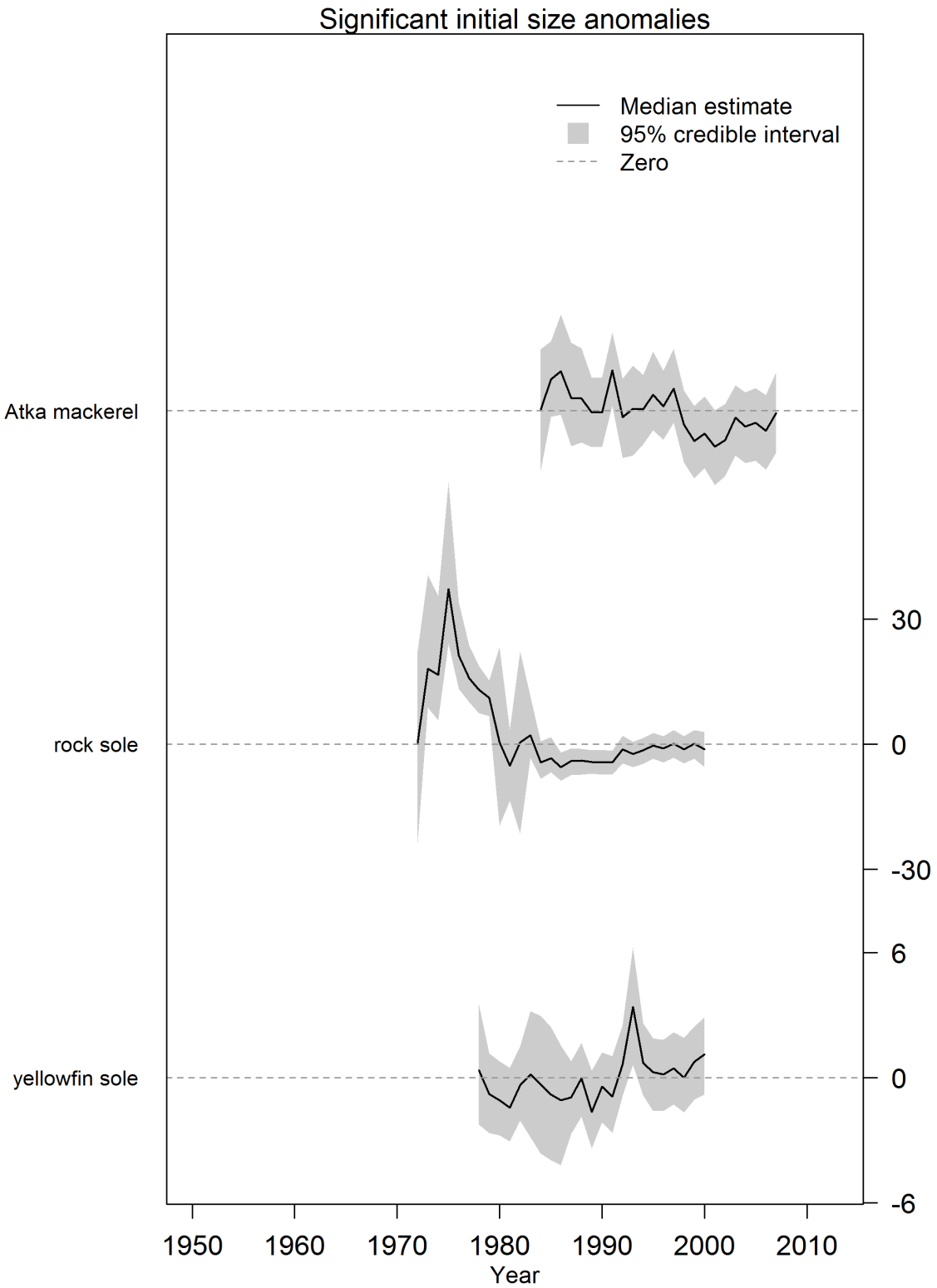

Figure A.2 - Growth anomaly estimates for stocks with significant initial size anomalies that are not shown in Figure 1.3. The x-axis represents year of birth of the cohort.

APPENDIX B

Table B.1 - Maturity (M) and selectivity (S) parameters used. Blank values at ages < Amax denote values of 1; selectivity values are not included for species with length-based selectivity.

Age	canary rockfish	Northern rock sole		Pacific cod	Pacific hake		Pacific halibut	petrale sole	walleye pollock		widow rockfish
	M	M	S	M	M	S	M	M	M	S	M
1	0	0	0	0	.08	0		0	0	0	0
2	0	0	0	0	.21	.01		0	.01	0	0
3	0	0	0	.05	.72	.49		0	.29	.05	0
4	0	0	.01	.45	.87	.66	0	.05	.64	.45	.05
5	.05	0	.02	.70	.90	.74	0	.5	.84	.65	.08
6	.10	.01	.06	.95	.91	1	0	.95	.90	.95	.26
7	.20	.01	.18	.99	.91		0	1	.95	.98	.49
8	.30	.05	.40	1	.91		0		.96	1	.75
9	.40	.20	.68		.91		.01		.97	.99	.93
10	.50	.40	.87		.91		.02		1	.99	.99
11	.60	.60	.95		.91		.06			.99	.99
12	.75	.80	.99		.91		.18			.99	1
13	.82	.95	1		.91		.40			.99	
14	.91	.99			.91		.68			.99	
15	.93	1			.91		.87			.99	
16	.95				.91		.95				
17	.97				.91		.99				
18	.98				.91		1				
19	1				.91						

VITA

Christine Stawitz was born and raised in Staten Island, New York. She graduated from the University of Virginia in 2008 with a B.S. in Systems Engineering and Computer Science minor. Her move to the Pacific Northwest was to work for a large software company, and during her three years there she met her husband Daniel, adopted Oakley the Wonder Dog, and set down firm roots in Seattle. She started the QERM program in 2011, and she is still waiting to be sent back to the tech industry at any moment because she knows nearly nothing about biology. Luckily, she picked up a fair bit of statistics while completing her dissertation, which appears to make her useful in some circles. While at UW, she also wrote the petrale stock assessment update, two papers about stock assessment modeling, and a paper on seafood mislabeling with a number of fantastic peers. She also had a baby. Her next professional adventure will be as a postdoctoral researcher with collaborators both at UW-SAFS and NOAA's Alaska Fisheries Science Center. In her free time, she bikes, hikes, and gardens.